UNIVERSIDADE FEDERAL DO RIO GRANDE DO SUL

Centro de Biotecnologia

Programa de Pós Graduação em Biologia Celular e Molecular

Urease de *Canavalia ensiformis* e peptideos derivados: Interação com a membrana lipídica e a formação de canais iônicos

Angela Regina Piovesan

Tese submetida ao Programa de Pós Graduação em Biologia Celular e Molecular da UFRGS como requisito parcial para obtenção do grau de Doutor em Ciências

Orientação:

Prof[a]. Dr[a]. Célia Regina Ribeiro da Silva Carlini

Prof. Dr. Jean-Louis Schwartz

Porto Alegre, setembro de 2013

Membros da Banca Examinadora

Dr. Luiz Anastácio Alves

Pesquisador Titular da Fundação Oswaldo Cruz e

Prof. Dr. Guido Lenz

Departamento de Biofísica e Centro de Biotecnologia, UFRGS

Dr. Fabricio Simão

Pesquisador do Instituto do Cérebro, PUCRS

Revisor: Dr. Cháristo André Dal Belo

Universidade Federal do Pampa, UNIPAMPA

Agradecimentos

Agradeço especialalmente à Célia, por ter me dado a oportunidade de começar como aluna de IC no Laprotox.

Ao meu orientador Jean-Louis Schwartz, pela pela paciência e dedicação em me ensinar o ABC sobre eletrofisiologia.

Aos membros da banca por terem aceitado a contribuir com o aprimoramento deste trabalho.

À querida Angela, minha colega desde o início da Biologia e que até hoje é minha super parceira e amiga.

À Marina, minha colega também desde o tempo da graduação e que me fez companhia aqui e lá no Canadá. Foram muitas visitas Toronto ↔ Montréal!!

À Fernanda, que foi com quem eu começei a trabalhar dentro do laboratório e me incentivou a viajar logo no início do Mestrado. Aprendi muito com ela e até hoje é meu exemplo de profissional.

À Anne, que por muitas e muitas tardes ficou esperando comigo os "channels" aparecerem!

Agradeço à todos os outros colegas laprotoxianos pelo aprendizado e companhia ao longo desses 9 anos de convívio. Karine, Val, Vanessa e Rodrigo obrigada pela amizade!

Aos amigos de Montréal: Helaine, Maysam e Sebástien. Ao Marc Juteau, pelo suporte nos experimentos iniciais. À Hélène e Mouzi pelo ótimo convívio de meses!!

Ao Tinoko pela disposição em ajudar sempre que preciso.

À Silvia e Luciano por sempre resolverem prontamente os problemas burocráticos.

Ao Matheus, que me ajudou a manter o equilíbrio nos momentos difíceis. Sem tua companhia as coisas seriam sempre mais difíceis.

À minha família, é indescritível saber que posso contar com ela sempre, pra qualquer coisa. Especialmente ao meu pai e minha mãe.

Às agências de fomento do Brasil e Canadá, sem elas nada disso teria sido feito.

A primeira parte do trabalho foi realizada no Laboratório de Proteínas Tóxicas (Laprotox), do Centro de Biotecnologia da Universidade Federal do Rio Grande do Sul, sob orientação da Prof[a]. Dr[a]. Célia Regina Ribeiro da Silva Carlini, com financiamento das agências CAPES, CNPq e FAPERGS.

A segunda parte deste trabalho foi desenvolvida no Laboratório do Prof. Dr. Jean-Louis Schwartz, membro do Centre SÈVE e Groupe d'Étude des Protéines Membranaires, Departamento de Fisiologia, na Université de Montréal – Canadá, em duas etapas de 6 meses cada, através do Programa de Intercâmbio para alunos estrangeiros financiado pelo "Fonds de recherche du Québec – Nature et Technologies (FQRNT)"

Índice

Resumo

Ureases (EC 3.5.1.5) são enzimas dependentes de níquel que catalisam a hidrólise da uréia para formar amônia e dióxido de carbono. Elas têm sido isoladas de uma ampla variedade de organismos incluindo plantas, fungos e bactérias, porém não são sintetizadas por animais. As sementes de *Canavalia ensiformis* são ricas em isoformas de urease, tal como a Canatoxina (CNTX) e JBU (jackbean urease, do inglês). A CNTX é uma proteína neurotóxica, causando diversos efeitos biológicos após injeção por via intraperitoneal em ratos e camundongos, entre eles, atividades pró- inflamatórias e indutora de agregação plaquetária, convulsões, e finalmente, morte dos animais. A CNTX também apresenta efeitos inseticida e antifúngico, potencialmente relevantes para a defesa da planta de origem. Após anos de estudos com a CNTX, verificou-se que JBU também compartilha essas atividades biológicas, como efeitos inseticida e fungitóxico, ativação de plaquetas e de células inflamatórias, incluindo letalidade em ratos e camundongos (por via intravenosa).

Na busca pelo mecanismo de ação inseticida, identificou-se um fragmento da urease com efeito letal em insetos, denominado Jaburetox (Jbtx). Indícios da interação desses polipeptídeos com membranas lipídicas nos levou a estudar de que forma esse fenômeno ocorre. Fragmentos do Jbtx originados de mutações sítio-dirigidas foram testados a fim de investigar a relação estrutura X função. Foram usados neste estudo, além de JBU e Jbtx, a porção amino-terminal do Jbtx isolada, chamada de Jbtx N-ter, a sua região carboxi-terminal, ou Jbtx C-ter, e ainda o peptídeo com a região do grampo beta removida, ou Jbtx Δ-β. Por meio de ensaios com lipossomos, foi possível certificar-se que todas as proteínas ligam-se e interagem com as vesículas de maneira muito similar. A capacidade das moléculas de inserção em bicamadas lipídicas foi confirmada através da técnica de *planar lipid bilayer*, determinando-se as propriedades biofísicas dos canais formados, e sugerindo que o peptídeo Jbtx representa a principal região da JBU capaz de interagir com membranas biológica. Os resultados contribuem para a compreensão mais aprofundada dos mecanismos de ação de ureases e peptídeos derivados, assim como das relações estrutura x função implicadas nesses mecanismos.

Abstract

Ureases (EC 3.5.1.5) are niquel dependent enzymes that hydrolyse urea into ammonium and carbon dioxide. They have been isolated from many organisms, including plants, fungi and bacteria, but are not synthesized by animals. *Canavalia ensiformis* seeds are source of urease isoforms, like Canatoxin (CNTX) and jackbean urease (JBU). CNTX is a neurotoxic protein, displaying several biological effects after intraperitoneal injection in rats or mice, including pro-inflammatory and platelet aggregation activity, and convulsions followed by death of the animals. CNTX also presents insecticidal and fungitoxic effects, which are probably relevant for defense mechanisms of the source plant. After some years of studies, it was found that JBU also share these biological activities, such as entomotoxic and antifungal effects, activation of platelets and inflammatory cells, including lethality in rats and mice (intravenously).

In the search for the insecticidal mode of action, an urease fragment lethal to insects was identified and named Jaburetox (Jbtx). Evidence of the interaction of these polypeptides with lipid membranes led us to investigate how this phenomenom takes place. Site-directed mutagenesis to obtain Jbtx fragments was applied in the search for structure X function relationships. Besides JBU and Jbtx, a peptide corresponding to Jbtx's amino-terminal half (Jbtx N-ter), a peptide corresponding to Jbtx's carboxi-terminal half (Jbtx C-ter) and a mutant with deletion of a beta hairpin motif (Jbtx Δ-β) were used in the present study. Working with liposomes it was possible to verify that all proteins bind and interact with vesicles, in a similar way. The ability of these molecules to insert into lipid bilayers was confirmed through the planar lipid bilayer technique. The biophysical properties of the ion channels formed by each polypeptide were characterized, suggesting that Jbtx is the main region from JBU able to interact with lipid membranes. The results contribute to deepen our understanding of the modes of action of JBU and derived peptides, as well as of the structure X function relationships involved in these mechanisms.

Lista de Abreviaturas

A: absorbância

CF: carboxifluoresceína

Ch: colesterol

DOPG: 1,2-di-(9Z-octadecenoyl)-sn-glycero-3-phospho-(1'-rac-glycerol)

EDTA: ácido etilendiaminotetraacético

g: força *g*

HEPES: 4-(2-hydroxyethyl)-1-piperazineethanesulfonic acid

HBS: HEPES buffer saline

I: corrente iônica

IPTG: Isopropyl β-D-1-thiogalactopyranoside

JBU: Jack bean urease

kDa: quilodaltons

mV: milivolt

MW: marcador de massa molecular

NaPB: do inglês, *sodium phosphate buffer*

OD: densidade óptica

pA: picoampere

pF: picofarad

PC: fosfatidilcolina

PE: fosfatidiletanolamina

PLB: planar lipid bilayer

pS: picosiemens

SBU: soybean urease

SDS: dodecil-sulfato de sódio

SDS-Page: gel de poliacrilamida para eletroforese com dodecil-sulfato de sódio

U: unidade

V: volt

1. Introdução

1.1. Ureases

Ureases (EC 3.5.1.5) são enzimas dependentes de níquel que catalisam a hidrólise da uréia para formar amônia e dióxido de carbono (Dixon et al, 1975) e desde o século passado, vêm fornecendo marcos importantes para a biologia moderna. Em 1926, Sumner descobriu a natureza protéica das enzimas ao cristalizar a urease das sementes do feijão de porco, a *Canavalia ensiformis* popularmente conhecida como *Jack bean urease* (JBU) (Sumner, 1926). Em 1975, Zerner e colaboradores identificaram que o íon níquel (Ni) era um importante componente do sítio ativo da enzima, o que gerou a primeira demonstração de um papel biológico para o Ni (Dixon et al, 1975).

As ureases aumentam em 8×10^{17} vezes a taxa de hidrólise da uréia (Callahan et al, 2005) e têm sido isoladas de uma ampla variedade de organismos incluindo plantas, fungos e bactérias (Mobley & Housinger, 1989; Sirko & Brodzik, 2000; Follmer, 2008), porém não são sintetizadas por animais. O papel primário e mais conhecido das ureases nesses organismos é a disponibilização de nitrogênio para o crescimento de microrganismos (Mobley and Hausinger, 1989; Follmer, 2008). Enquanto ureases de fungos e de plantas (ex. feijão de porco e soja) são proteínas que se arranjam em trímeros (α3) ou hexâmeros (α6) de subunidades de ~ 90 kDa, ureases bacterianas são multímeros complexos formados de duas ou três subunidades (geralmente [α,β,γ]3 (Mobley et al, 1995; Sirko & Brodzik, 2000). Ureases são evolutivamente conservadas. A subunidade única das ureases vegetais ou fúngicas alinha-se com a sequência primária das subunidades menores das ureases bacterianas. Por exemplo, a porção amino-terminal de ureases de planta ou fungo possui domínios muito parecidos com as cadeias β e γ da urease de *Klebsiella aerogenes,* ou a subunidade α da urease de *Helicobacter pylori*, enquanto que a porção carboxi-terminal das ureases de plantas ou fungos, onde está localizado o sítio ativo, se assemelha às subunidades maiores das ureases bacterianas (por exemplo, a cadeia α da urease de *K. aerogenes* ou *H. pylori*) (Fig. 1).

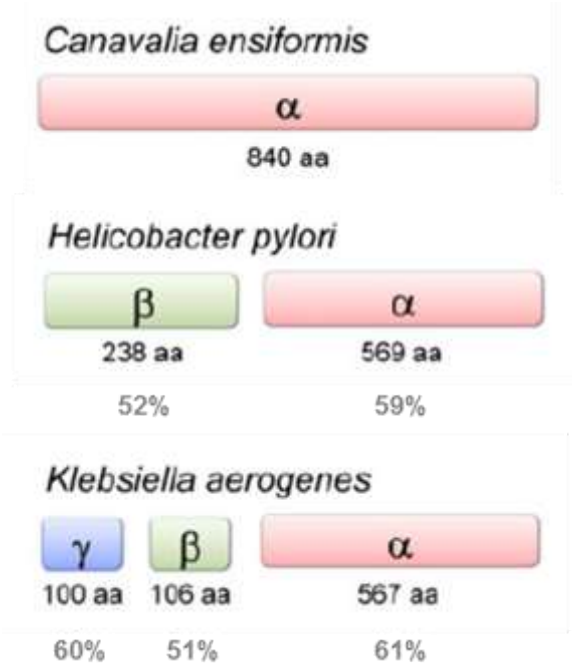

Figura 1: Estrutura esquemática de três ureases. Ureases vegetais, como a de *C. ensiformis*, possuem uma única subunidade enquanto que ureases bacterianas possuem duas (*H. pylori*) ou três subunidades (*K. aerogenes*). A porcentagem de identidade ao fragmento correspondente da urease de *C. ensiformis* é indicada em cinza. Modificado de Ligabue-Braun et al, 2013.

A estrutura 3D das ureases bacterianas de *K. aerogenes*, *Bacillus pasteurii*, e *H. pylori* já são conhecidas há mais de uma década (Mobley et al, 1995, Sirko et al, 2000; Benini et al, 1999). Somente em 2010 foi publicada a estrutura cristalográfica da JBU, com resolução de 2.05 Å (Balasubramanian & Ponnuraj, 2010), a primeira urease vegetal a ter sua estrutura determinada (Fig. 2).

A alta similaridade de seqüência de todas ureases indica que elas são variantes de uma mesma proteína ancestral, e provavelmente possuem similaridades em suas estruturas terciárias e mecanismo catalítico (Mobley et al, 1995, Sirko et al, 2000). Estudos recentes do nosso grupo revelaram que a organização ancestral das ureases é aquela de três cadeias. Assim, as ureases vegetais e fúngicas com apenas uma cadeia teriam derivado de um processo de fusão dos três genes que codificam as ureases bacterianas. As variantes de duas cadeias, no entanto, não são intermediários evolutivos do processo de fusão que levou a essa transição estrutural das ureases (Ligabue-Braun et al, 2013).

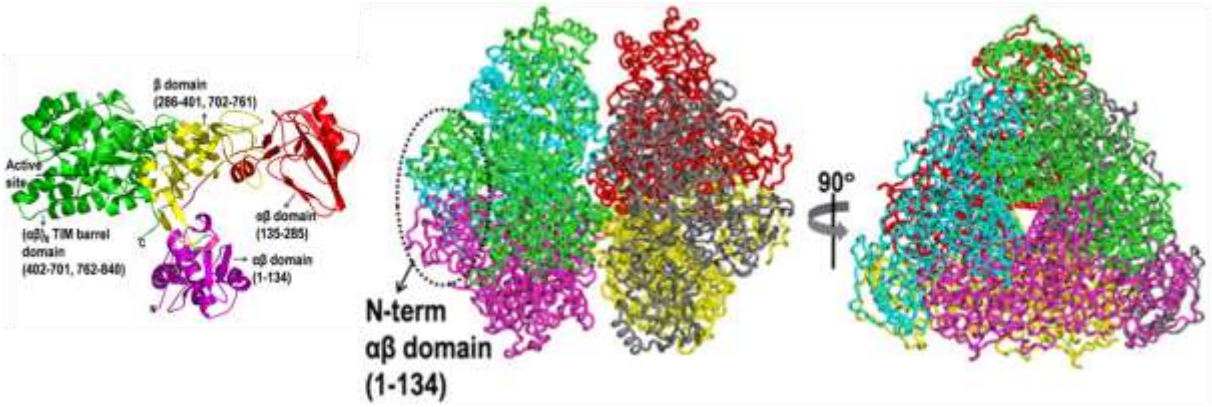

Figura 2: Estrutura do monômero e hexâmero da JBU. O formato em T do monômero está ilustrado à esquerda, indicando quatro regiões: em rosa, o domínio αβ que contém a região N terminal; em vermelho, outra parte do domínio αβ; em amarelo, domínio β; em verde, o domínio αβ, com o TIM Barril $(\alpha\beta)_8$, no qual se encontra o sítio ativo e a região carboxi-terminal. A holoenzima é composta pela interação frontal de dois trímeros (meio), que vistos de cima tem o formato de um triângulo, com uma pequena abertura central (à direita). Extraído de Balasubramanian et al, 2010.

Apesar de suas estruturas e ação enzimática altamente conservadas, pouco se sabe sobre o papel fisiológico de ureases nos organismos onde são encontradas, particularmente em plantas e em fungos. As ureases de uma maneira geral apresentam diversas atividades biológicas não relacionadas com sua atividade enzimática, o que adiciona mais complexidade ao quadro dos prováveis papéis biológicos dessas proteínas (Carlini e Polacco, 2008).

A Canatoxina (CNTX), uma proteína neurotóxica isolada de *C. ensiformis* por Carlini & Guimarães, 1981, e, vinte anos mais tarde, identificada como uma isoforma da urease clássica - JBU (Follmer et al, 2001), é letal para ratos e camundongos quando administrada por via intraperitoenal ou endovenosa, mas inativa por via oral. Consiste de subunidades de ~ 95 kDa formando um homodímero ligado não covalentemente. Esta proteína apresenta uma potente atividade secretagoga *in vitro*, sobre vários sistemas celulares isolados de mamíferos, induzindo secreção de grânulos densos de plaquetas (Carlini et al, 1985, Barja-Fidalgo et al, 1991a), secreção de dopamina e serotonina em sinaptossomas de cérebro de rato (Barja-Fidalgo et al, 1991a), liberação de histamina de mastócitos (Grassi-Kassisse et al, 1992) e secreção de insulina de ilhotas pancreáticas isoladas (Barja-Fidalgo et al, 1991a e 1991b). A maioria desses efeitos, tanto *in vivo* como *in vitro*, envolve a ativação do metabolismo do ácido araquidônico, principalmente pela rota da lipoxigenase, já que estes são bloqueados por inibidores desta via, tais como esculetina e ácido nordihidroguaiarético.

A JBU, a isoforma mais abundante de urease da *C. ensiformis*, assim como a CNTX também é capaz de ativar plaquetas, mas no entanto, somente induz efeito convulsivante e letal em camundongos quando administrada por via intravenosa, provavelmente devido ao seu maior tamanho: 540 kDa contra 185 kDa apresentado pela CNTX (Follmer et al, 2001). Tanto a CNTX como a JBU interagem com polisialogangliosídeos (GD1b e GT1b) e sialoproteínas (mucina, tireoglobulina, fetuína), na superfície de eritrócitos e em microplacas de ELISA (Carlini & Guimarães, 1991, Follmer et al, 2001). Essa propriedade de ligação a carboidratos provavelmente "direciona" as proteínas para as superfícies de células ricas com esses tipos de glicoconjugados e pode ser a explicação para a seletividade tecido-específica dessas proteínas. Além da CNTX e JBU, ureases bacterianas de *H. pylori* e *B. pasteurii* também apresentam atividades biológicas independente de suas atividades ureolíticas, como por exemplo, ativação de plaquetas, e de neutrófilos. Todas as ureases já estudadas, nesse aspecto, induzem agregação plaquetária pela via da lipoxigenase (Carlini et al, 1985, Olivera-Severo et al, 2006, Wassermann et al, 2010; Uberti et al., 2013).

Evidências vem se acumulando sobre a toxicidade de ureases vegetais para insetos e fungos, por mecanismos que são independentes da atividade enzimática (Carlini et al., 1997; Oliveira et al, 1999; Menegassi et al, 2008; Becker-Ritt et al, 2007; Defferrari et al., 2011; Postal et al, 2012). Por isso, ureases vegetais são consideradas membros do arsenal de proteínas de defesa de plantas, juntamente com as lectinas, proteínas inativadoras de ribosomo, inibidores de proteases, inibidores de amílase, entre outras (Carlini e Grossi-de-Sa, 2002; Carlini e Polacco, 2008; Becker-Ritt e Carlini, 2012).

1.2. Efeito inseticida

Ambas isoformas de urease de *C. ensiformis*, CNTX e JBU, bem como a urease da semente de soja, SBU, são tóxicas por via oral em insetos que apresentam enzimas digestivas do tipo catepsinas. Essa toxicidade é, em parte, mediada pela liberação de um peptídeo interno de 10 kDa, quando a proteína é hidrolisada por essas enzimas acídicas (Carlini et al, 1997; Ferreira-DaSilva et al, 2000; Piovesan et al, 2008; Defferrari et al, 2011; Real-Guerra et al, 2013). Algumas pragas importantes da agricultura são sensíveis a essas proteínas, como por ex.: o caruncho do feijão de corda (*Callosobruchus maculatus*), o percevejo verde da soja (*Nezara viridula*) e o percevejo manchador do algodão (*Dysdercus peruvianus*) (Carlini & Grossi de Sá, 2002, Stanisçuaski et al, 2005). O barbeiro *Rhodnius prolixus*, vetor da doença de Chagas também é sensível aos efeitos das ureases (Carlini et al, 1997; Stanisçuaski et al, 2009). Outros tipos de insetos, como as lagartas *Manduca sexta* e *Anticarsia gemmatalis*, o gafanhoto *Schistocerca americana*, moscas e mosquitos, não são afetados quando ingerem a proteína (Carlini et al, 1997).

O peptídeo tóxico produzido por hidrólise da CNTX *in vitro* por enzimas da larva de *C. maculatus*, foi purificado, caracterizado e denominado Pepcanatox (Ferreira-DaSilva et al, 2000). A partir deste, foi obtido por expressão heteróloga um peptídeo recombinante equivalente, denominado Jaburetox-2Ec (Mulinari et al, 2007). Assim como o Pepcanatox, o recombinante também tem potente atividade inseticida. Após a ingestão do Jaburetox-2Ec, os insetos são momentaneamente paralisados e mostram movimentos descoordenados de antenas que precede a morte, sugerindo que o peptídeo possa agir como uma neurotoxina (Mulinari et al, 2007; Stanisçuaski e Carlini, 2012). Esse peptídeo tem um espectro de ação mais amplo, atuando sobre insetos que são insensíveis à urease intacta, age mais rápido do que as proteínas de origem, e não é tóxico quando administrado por via oral ou injetado em ratos e camunudongos (Mulinari et al, 2007). Uma versão otimizada do peptídeo, denominado simplesmente Jaburetox (Jbtx), sem o epítopo de reconhecimento V5, e que mantém a mesma atividade inseticida, foi construído por Postal et al (2012).

O mecanismo de ação inseticida das ureases ou peptídeos derivados ainda não está completamente elucidado. Já foi demonstrado que JBU e o Jaburetox-2Ec reduzem a diurese de *R. prolixus* após alimentação, sugerindo um efeito no balanço de água e íons na célula. Enquanto a JBU age alterando canais de cálcio, o Jaburetox-2Ec altera o potencial transmembrana das células dos túbulos de Malpighi (Stanisçuaski et al, 2009). Real-Guerra e

colaboradores, 2013, demonstraram recentemente a importância de resíduos acídicos e de lisina na atividade entomotóxica da JBU, sendo que a modificação química destes aminoácidos reduz a mortalidade dos insetos. A modificação dos resíduos acídicos reduziu a toxicidade por alterar a liberação do fragmento tóxico quando a proteína é ingerida pelo inseto, pois existem dois ácidos aspárticos na JBU que flanqueiam a região do peptídeo, e quando modificados, impedem a hidrólise pelas enzimas digestivas que liberam o peptídeo. Provavelmente, a atividade inseticida residual observada nesse caso, se deve à ação da urease intacta, que sabidamente atravessa o epitélio do intestino e circula pela hemolinfa (Stanisçuaski et al, 2009). Por outro lado, somente a JBU com lisinas modificadas perdeu seu efeito antidiurético em *R. prolixus*, talvez porque esses resíduos sejam importantes na etapa de interação com membranas, levando consequentemente a uma abolição do efeito (Real-Guerra et al, 2013).

Inicialmente, foi proposto que uma região do peptídeo que forma um grampo beta era a responsável pelas atividades biológicas (Mulinari et al., 2007), pois estruturas semelhantes são vistas em algumas proteínas formadoras de poro, tal como protegrina e caribdotoxina (Bontems et al, 1992, Fahrner et al, 1996). Em 2010, com a estrutura cristalográfica da JBU resolvida, Balasubramanian e Ponnuraj reforçaram essa hipótese. A estrutura do peptídeo é mostrada em detalhes, com destaque para o grampo beta (Fig 3).

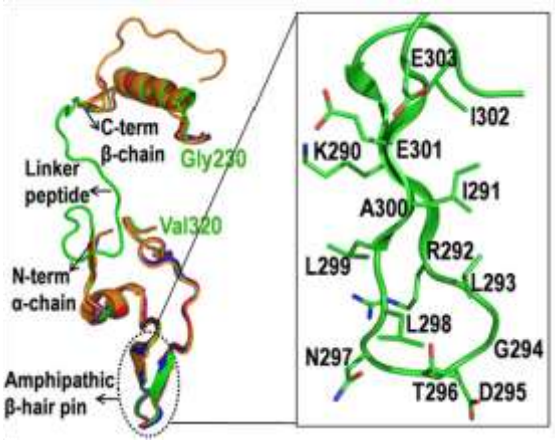

Figura 3: Estrutura do Jaburetox . À esquerda, o peptídeo entomotóxico, como encontrado na estrutura cristalográfica da JBU. À direita, em destaque a região do peptídeo que contém um grampo beta com características anfipáticas. Extraido de Balasubramanian e Ponnuraj, 2010.

Em 2012, o mesmo grupo publicou outro trabalho mostrando, através de simulações e dinâmica molecular, a região do grampo beta do peptídeo inseticida se oligomerizaria formando um barril β, quando em uma interface polar/apolar. Os autores sugereriam ainda que essa estrutura atravessaria a membrana lipídica formando um poro, propondo que esse fenômeno fosse a base molecular do efeito inseticida do Jbtx (Balasubramanian et al, 2012).

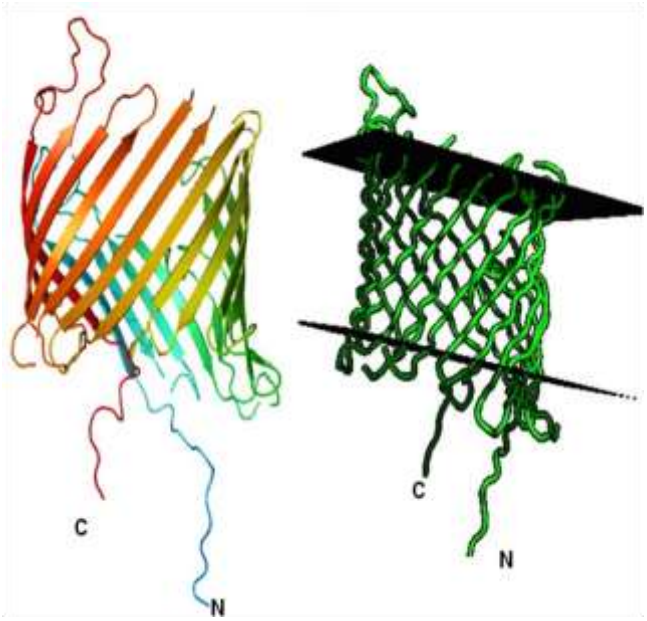

Figura 4: Modelagem molecular do Jaburetox inserido numa interface apolar. À esquerda está ilustrada a estrutura de um β-barril formado pela oligomerização de dez grampos beta do Jbtx. À direita, é mostrado um modelo deste β-barril inserido numa membrana; em preto está representada a membrana. Extraído de Balasubramanian et al, 2012.

Com o intuito de estudar as relações estrutura-função do Jbtx e identificar as regiões responsáveis por suas diferentes atividades biológicas, Martinelli e colaboradores realizaram mutações sítio-dirigidas deletando porções relevantes da molécula: a região N-terminal, a região C-terminal e a região do grampo beta, conforme ilustrado no esquema a seguir (Fig. 5):

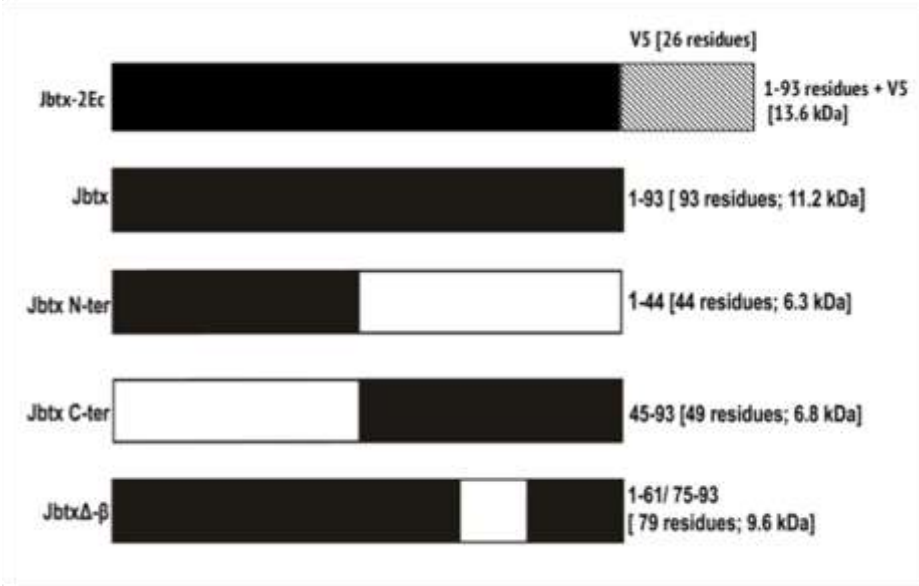

Figura 5: Representação esquemática das sequências de Jbtx e seus mutantes. O número de resíduos de aminoácidos de cada peptídeo, representado em preto, está indicado no lado direito. A parte que falta em cada peptídeo, em relação ao Jbtx, é representada como "caixa vazia". Extraído de Martinelli et al, 2013 (anexo 1).

No entanto, Martinelli et al, 2013 (anexo 1) mostraram que, apesar das especulações a respeito do grampo beta, essa região não está envolvida no efeito inseticida. Assim, o peptídeo sem a região do grampo beta possui todas as atividades descritas para o Jbtx em diferentes modelos biológicos, tanto em fungos e insetos, sendo ativo nas mesmas concentrações que o peptídeo original. Enquanto que o peptídeo que contém o grampo beta, correspondendo à porção C-terminal do Jbtx (Jbtx C-ter) não foi letal para insetos, o peptídeo contendo somente o N-terminal (Jbtx N-ter) apresentou atividade inseticida, indicando ser esta região o domínio entomotóxico do Jbtx (Martinelli et al, 2013) (anexo 1). No entanto, considerando que o peptídeo Jbtx C-ter foi ativo em outros ensaios biológicos, como inibição de diurese em túbulos de Malpighi e bloqueio da junção neuromuscular de baratas, não se pode descartar uma contribuição desta região da molécula no efeito entomotóxico geral do Jbtx, em processos que antecedem a morte do inseto (Martinelli et al, 2013) (anexo 1).

1.3. Interação da JBU e do Jbtx com membranas

O grande interesse em se estudar os efeitos que JBU e o Jbtx possam exercer em membranas celulares, reside na compreensão da toxicidade dessas moléculas tanto em insetos como em mamíferos. Sabe-se que Jaburetox-2Ec tem a capacidade de romper membranas em bicamadas lipídicas aniônicas (PG), produzindo permeabilização de lipossomos, e esse efeito é

fortemente influenciado pelo estado de agregação do peptídeo. Assim, Barros et al, 2009, mostraram que a atividade de extravasamento de CF do Jbtx-2Ec é reduzida, ou mesmo completamente abolida, em lipossomos compostos de fosfolipídeos neutros, como PC, ou uma mistura equimolar de PC/PA. Uma curva dose-resposta mostrou que 0,17 μM de Jaburetox-2Ec gera ~ 30 % de extravasamento, enquanto que 0,71 μM produz ~ 100 %. Simulações do Jbtx-2Ec em uma interface polar/apolar também foram feitas e revelaram que a molécula é capaz de assumir uma configuração transmembrana.

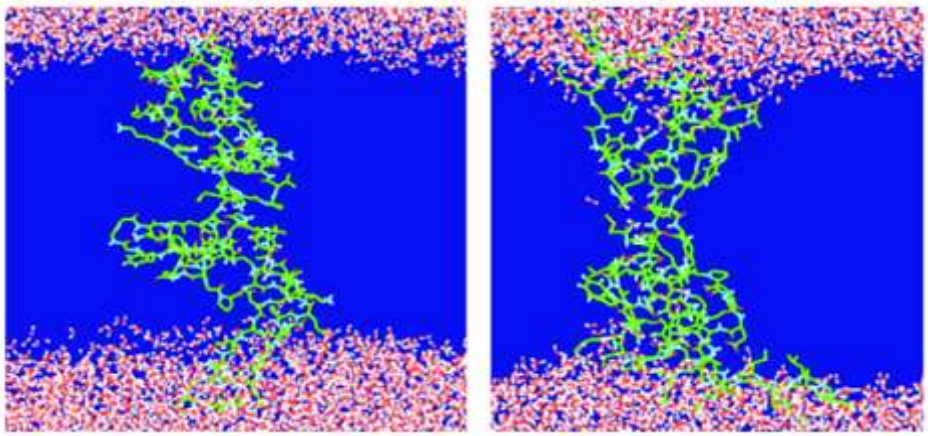

Figura 6: Simulação do Jaburetox-2Ec em configuração transmembrana em ambiente polar/apolar. O painel da direita mostra a posição inicial e o painel da esquerda mostra a posição final do peptídeo após 5 ns. Durante a simulação observa-se que o peptídeo permanece dentro da fase apolar modificando apenas alguns resíduos em contato com as camadas de água. Moléculas de água estão exemplificadas por esferas brancas e rosas. O ambiente apolar (região azul) é composto por moléculas de tetracloreto de carbono (CCl_4). Modificado de Barros et al, 2009.

Com relação à JBU, dados anteriores do grupo (não publicados) mostraram que a urease também tem efeitos sobre lipossomos miméticos de plaquetas humanas (34,1% PC, 24,3% PE, 6,1% PS, 2% PI, 7,7% EM e 25.8% Ch). Resultados de espalhamento de luz dinâmica (DLS) indicaram que 0,5 μM de JBU reduz significativamente o diâmetro das vesículas, efeito também observado em presença do Triton X-100. Em contrapartida, a análise por espalhamento de raios-x à baixo ângulo (SAXS) dos lipossomos em presença do Jbtx-2Ec mostraram que essa interação de fato leva à diminuição do diâmetro da vesícula, mas não a um aumento do número de partículas, que indicaria a lise dos lipossomos, efeito este observado somente para o Triton X-100 (Micheletto, 2011)

1.4. Proteínas formadoras de poro (PFPs)

As membranas e suas proteínas transmembranas desempenham papel crucial em diversos processos celulares como sinalização, conversão de energia, eliminação de produtos tóxicos, assimilação de nutientes, mobilidade e condutância iônica (Iacovache et al, 2012). Especificamente, os canais regulam a concentração iônica permitindo seletivamente certas espécies de íons, ex. Na^+, Ca^{2+}, and K^+, a serem transportados através da membrana. Eles são ubíquos em processos envolvendo funções celulares básicas, bem como na comunicação intercelular (Nguyen et al, 2010). Em muitos casos, os canais iônicos são homo-oligoméricos com um lúmen hidrofílico, que se forma a partir de monômeros separados. Geralmente, canais têm diâmetros menores que poros e são seletivos a íons de tamanho e carga específicos (Lopez et al, 2005).

Além dos canais iônicos fisiológicos, as toxinas de plantas e microorganismos que agem formando poros nas membranas dos organismos alvo são também de grande interesse científico, causando perda da integridade e da função da membrana (Bischofberger et al, 2012). Essas proteínas são geralmente produzidas numa forma solúvel e monomérica que, de uma maneira ordenada, pode se oligomerizar e adquirir capacidade de se inserir em membranas. As toxinas formadoras de poro (PFT) são classificadas de acordo com o motivo estrutural da porção da molécula que se insere na membrana, podendo ser PFT *α*, quando o domínio transmembrana é composto por α-hélices, ou PFT *β*, quando folhas beta se organizam para formar o poro. Podem ainda ser classificadas como formadora de poros toroidais, quando α-hélices da proteína e lipídeos da membrana se organizam formando o poro.

As proteínas mais estudadas no grupo das PFT *α* compreendem as toxinas inseticidas Cry de *Bacillus thuringiensis*, que são encontradas na bactéria como corpos de inclusão ou cristais, juntamente com outras toxinas, sendo estes dissolvidos no ambiente alcalino da digestão dos insetos suscetíveis. As toxinas Cry são produzidas como pro-toxinas e necessitam de clivagem proteolítica para adquirir sua forma ativa (Vachon et al, 2012). Essas toxinas possuem α-hélices anfipáticas que, após oligomerização, formam um barril de α-hélices que atravessa a membrana plasmática de células no intestino dos insetos.

A família das PFT *β* é composta por um número maior de toxinas mais bem caracterizadas, como a de *Bacillus anthracis* e a hemolisina de *Staphylococcus aureus.* Todas as toxinas atravessam a membrana na forma de um barril de folhas beta, porém estes podem

variar enormemente de tamanho, desde 15 Å em algumas hemolisinas até 200 Å em citolisinas (Iacovache et al, 2012).

Poros toroidais possuem característica singular, pois a bicamada lipídica se dobra de tal forma que as camadas interna e externa se unem continuamente, na presença da concentração apropriada de proteína. Quando em concentração baixa, a proteína só interage paralelamente com os fosfolipídeos de membrana. Quando atinge altas concentrações, a proteína induz uma curvatura da membrana e permanece interagindo com os grupamentos polares dos lipídeos. Dessa forma, o lúmen do poro é feito parcialmente pela proteína e parcialmente pelas cabeças polares dos fosfolipídeos (Ludtke et al, 1996; Tang and Hong 2009).

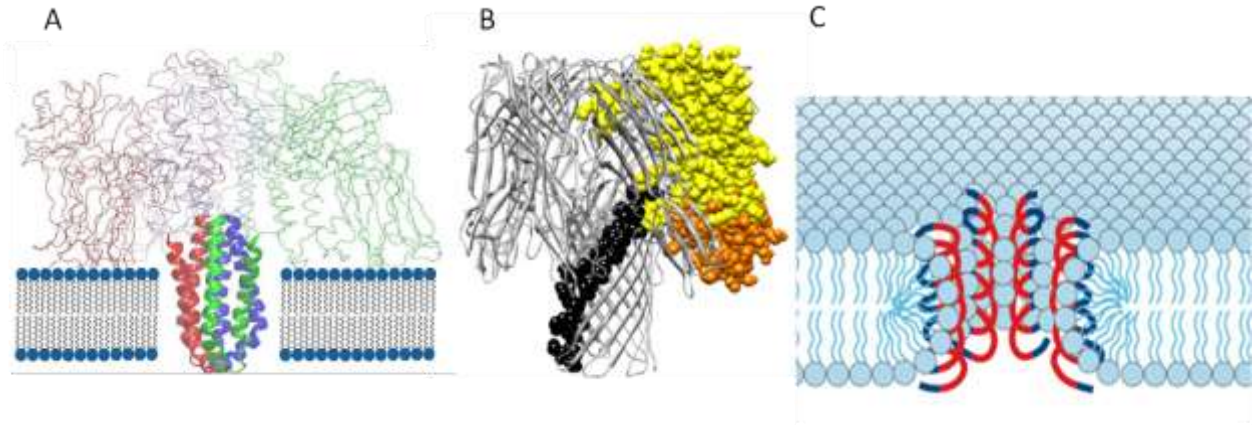

Figura 7: Tipos de PFPs. (A) Proteína Cry4Aa com seus domínios transmembranas compostos de α-hélices, modificado de Taveecharoenkool et al, 2010. (B) α-hemolisina de *Staphylococcus aureus*, mostrando que o poro adquire formato de um cogumelo. Em preto está destacado a região do grampo beta que forma a região transmembrana, modificado de Iacovache et al, 2012. (C) Modelo de poro toroidal, onde as estruturas em α-hélices interagem com o lúmen do poro composto pelas cabeças polares dos fosfolipídeos; em vermelho mostra as regiões hidrofílicas e em azul as regiões hidrofóbicas, modificado de Mueller et al, 2009.

1.5. Peptídeos antimicrobianos (AMPs)

São moléculas evolutivamente conservadas presentes em plantas, bactérias, insetos e vertebrados e que tem como papel principal atuar na defesa dos organismos. Segundo *The Antimicrobial Peptide Database* (http://aps.unmc.edu/AP/main.php) existem diversas formas para classificar estes peptídeos, as principais estão listadas à seguir.

1) **Origem biológica:** como mencionado acima, AMPs são produzidos por organismos de diversos reinos, como plantas, bactérias e animais. Entre os animais, existe uma classificação própria, que distingue os AMPs produzidos por artrópodes (escorpiões e insetoss) dos AMPs produzidos por vertebrados, tais como peixes, répteis, anfíbios, primatas, roedores, bovinos etc.
2) **Função biológica:** como o nome mesmo diz, estas moléculas têm como função biológica principal contribuir para o arsenal de defesa dos organismos que as sintetizam. Portanto, possuem papel antibacteriano, antiviral, antifúngico, antiparasita, inseticida, quimiotático, cicatrizante e promotor de crescimento.
3) **Propriedades Moleculares:** nesta categoria os peptídeos antimicrobianos são classificados de acordo com a carga da molécula, hidrofobicidade, tamanho, motivo, etc. Assim sendo, existem peptídeos catiônicos, neutros ou aniônicos quando a carga líquida da molécula é analizada. Além disso, os peptídeos podem ser classificados como hidrofóbicos, anfipáticos ou hidrofílicos, quanto à hidrofobicidade; muito pequenos, pequenos, médios e grandes, relativo ao tamanho (variando de 6 a 100 aminoácidos). No que se refere à topologia molecular, AMPs são classificados como lineares, circulares e contendo *loops*. *Loops* contêm normalmente pontes dissulfetos formadas entre as cadeias laterais dos aminoácidos. Peptídeos circulares são aqueles cujas extremidades N e C terminal são ligadas por ligação covalente.
4) **Estrutura 3D:** esta categoria se baseia no tipo de estrutura secundária existente na molécula do peptídeo, que podem ser unicamente *(a)* alfa-hélices ou *(b)* folhas-beta, a junção dos dois tipos chamada de *(c)* alfa-beta ou ainda peptídeos contendo estruturas diferente destas, chamadas de *(d)* não-alfa-beta
5) **Alvo molecular:** AMPs são também classificados de acordo o local onde eles primeiramente atuam na célula, podendo o alvo ser intracelular ou a superfície celular. Intracelularmente, os AMPs podem agir sobre proteínas, DNA ou RNA. Na superfície, os peptídeos podem atuar diretamente sobre lipídeos de membrana ou em receptorer.

1.6. Eletrofisiologia

É o estudo das propriedades elétricas de células e tecidos. Envolve medidas de mudanças de voltagem e corrente iônica em ampla variedade de escalas, de canais iônicos únicos até órgãos inteiros, como o coração. Em neurociência, inclui medidas da atividade elétrica de neurônios, particularmente a atividade de potencial elétrico.

O estudo de eletrofisiologia de um canal iônico implica, pelo menos, caracterizar o estímulo que abre ou fecha o canal (probabilidade de abertura do canal *versus* voltagem, concentração de ligante ou tensão da membrana), a condutância do canal sob condições iônicas específicas e a especificidade de um canal (quais íons podem passar).

No geral, as atividades de canais iônicos podem ser estudadas na membrana plasmática nativa de células pela técnica de *patch-clamp* ou por técnicas de microeletrodos, ou, após purificação da proteína e reconstituição, em bicamada lipídica planar (planar lipid bilayer ou PLB).

Técnicas de eletrofisiologia:

a) *Patch-clamp*: permite o estudo de múltiplos ou únicos canais iônicos em células. Foi desenvolvida por Erwin Neher e Bert Sakmann no final da década de 1970 o que lhes rendeu em 1991 o Prêmio Nobel em Fisiologia ou Medicina. A técnica é baseada numa simples idéia: uma pipeta de vidro com uma micro abertura (~ 1 μm) é usada para fazer um estreito contato em uma minúscula área, ou "patch", de uma membrana celular. Após aplicação de uma leve sucção na pipeta, o selo entre a pipeta e a membrana se torna tão firme que nenhum íon pode fluir no espaço entre a pipeta e a membrana. Então, todos os íons que fluem quando um canal iônico está aberto devem fluir pela pipeta. A corrente iônica resultante, apesar de pequena, pode ser medida com um amplificador eletrônico ultrasensível conectado à pipeta, onde estará anexado o eletrodo. Existem diversas variações da técnica mas o princípio básico é este descrito acima.

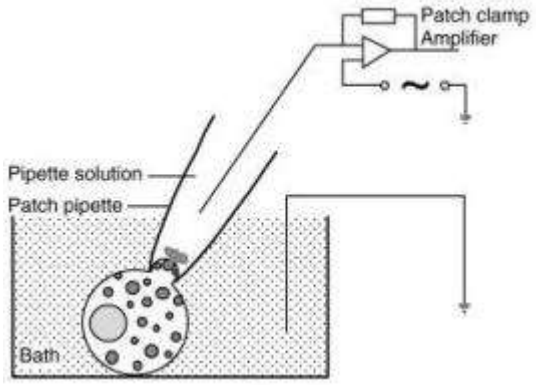

Figura 8: Técnica de Patch-Clamp convencional, em que uma micropipeta de vidro é selada através de leve sucção na membrana celular permitindo assim medir a corrente de um único canal iônico. Adaptado de Dernick et al., 2007.

b) *Planar Lipid Bilayer*: Esta técnica permite demonstrar a capacidade de uma proteína em permeabilisar membranas lipídicas através da medida da atividade de canais iônicos em membranas lipídicas artificiais. Consiste em formar uma membrana bilipídica planar numa abertura que conecta dois compartimentos aquosos, *cis* e *trans*. Após, a molécula a ser testada é adicionada no lado *cis* e pode se incorporar na membrana. O sistema está sob voltagem e a corrente que flui pelo canal inserido na membrana é monitorada. Maiores detalhes da técnica serão descritos na seção "Material e Métodos".

c) Registro Intracelular: é a medida de corrente e/ou voltagem através da membrana de uma célula. Para realizar este registro intracelular a ponta de um fino e afiado microeletrodo deve estar inserido dentro da célula de forma que o potencial de membrana possa ser medido. Tipicamente, o potencial de repouso de uma célula saudável estará entre -60 e -80 mV, e durante um potencial de ação o potencial de membrana poderá atingir +40 mV. Geralmente a pipeta é feita de vidro, a ponta tem um diâmetro menor que 1 μm e uma resistência de vários megaohms. As micropipetas são preenchidas com uma solução de composição iônica semelhante ao fluido intracelular. A voltagem medida pelo eletrodo é comparada à voltagem do eletrodo de referência, normalmente um fio de prata cloretado em contato com o fluido extracelular ao redor da célula.

Assinaturas de um canal

Canais iônicos têm assinaturas que precisam ser determinadas para bem caracterizar suas propriedades biofísicas em estudos relacionados com estrutura-função.

a) *Condutância:* é a habilidade que um canal tem em conduzir ions através da membrana; é medida em siemens (S). Até o momento sabe-se que canais fisiológicos seletivos à íons apresentam condutância que variam de 2 pS até 300 pS. Em contrapartida, canais não fisiológicos, tais como aqueles provenientes de toxinas, podem apresentar condutância tão grande quanto 2 nS (Hille, 2001).

b) *Retificação:* essa característica é observada quando a condutância de ions através do canal muda de acordo com a voltagem de tal forma que flui melhor em uma direção em relação a outra.

c) *Seletividade:* se refere à habilidade que os canais têm em discriminar espécies iônicas, permitindo alguns passar e restringindo outros. O movimento de íons através de um canal depende do gradiente eletroquímico ao longo da membrana e a seletividade do poro.

d) *Voltagem-dependência:* expressa a dependência do comportamento do canal ao potencial de membrana (voltagem aplicada). É principalmente observada pela probabilidade de abertura de um canal.

e) *Cinética (atividade):* a cinética usualmente contém o estudo da taxa de mudança que um canal sofre durante a modulação, passagem de íons, etc. A cinética é frequentemente usada para descobrir os mecanismos específicos dos canais iônicos ilustrados pela mudança de um estado para outro e para explicar o fenômeno de gatilho (gating), “jumps”, “bursts”, tempo de transição, modos de sub-condutâncias, interação de ligantes, etc.

Objetivo Geral desta tese:

Estudar a interação de JBU e Jbtx com membranas lipídicas

Objetivo Capítulo I

Descrever os efeitos produzidos por JBU e Jbtx em lipossomas.

Objetivo Capítulo II

Analisar as características biofísicas dos canais formados por JBU e Jbtx.

Organização da tese

A parte experimental desta tese é composta de dois capítulos.

O **Capítulo I** consiste em dados que compuseram parte do manuscrito entitulado **"Structure-function studies on Jaburetox, a recombinant insecticidal and antifungal peptide derived from jack bean (*Canavalia ensiformis*) urease"** (Anexo 1), estudando a interação do Jbtx e mutantes derivados com lipossomos unilamelares, através da quantificação do extravasamento de sonda fluorescente. Adicionalmente, a interação da JBU com os mesmos lipossomos também foi estudada.

O **Capitúlo II** consiste na íntegra do manuscrito entitulado "***Canavalia ensiformis* urease, Jaburetox and derived peptides form ion channels in planar lipid bilayers"**, submetido ao periódico *International Journal of Biochemistry & Cell Biology*

Cada capítulo apresenta uma seção de materiais e métodos, resultados e discussão específica. Após a Discussão Geral e Conclusão, segue a relação de todas as referências citadas na tese.

Um Anexo 2 é apresentado ao final, contendo dados preliminares pertinentes ao escopo desta tese.

Capítulo I

JBU, Jaburetox e peptídeos derivados: efeito em lipossomos

2. Objetivo

Investigar, utilizando a técnica de extravasamento de carboxifluoresceína, a capacidade de interação da JBU, Jbtx e peptídeos derivados com membranas lipídicas

2.1. Objetivos específicos

Avaliar a porcentagem de extravasamento de carboxifluoresceína contida dentro de lipossomos, quando estes são incubados com JBU ou Jaburetox.

Estudar os efeitos causados por mutantes do Jbtx, visando estabelecer relações estrutura X função implicadas na atividade de interação com membrana do peptídeo.

3. Metodologia

3.1. Expressão e purificação dos peptídeos recombinantes de Jbtx

As técnicas de clonagem, expressão e purificação foram feitas de acordo com Martinelli et al, 2013 (Anexo 1). Para expressão dos cDNAs das diferentes versões do Jbtx, plasmídeos recombinantes pET23a foram transformados em células de *E. coli* BL21-CodonPlus (DE3)-RIL (Stratagene), seguindo as intruções do fornecedor. Para a purificação do peptídeo Jbtx original e seus mutantes derivados, 200 mL de meio LB contendo 100 μg/mL de ampicilina e 40 μg/mL de cloranfenicol foram inoculados separadamente com 2 mL de cultura *overnight* de cada cepa de *E. coli*. As células foram crescidas sob agitação por aproximadamente 2 horas, à 37 °C, até que a OD de 0.7 fosse atingida. Nesse momento, IPTG foi adicionado às culturas numa concentração final de 0.5 mM. Após 3 horas de crescimento adicional, as células foram sedimentadas por centrifugação (4.000 x *g*, 15 min) e resuspendidas em 10 mL de tampão de lise (50 mM Tris, 500 mM NaCl, 5 mM imidazol, pH 7.5). Após, as células foram sonicadas e centrifugadas novamente (14.000 x *g*, 30 min). O sobrenadante foi aplicado numa coluna de 5 mL Chelating Sepharose (GE Healthcare) enriquecida com Ni^{2+} e previamente equilibrada com o tampão de lise. Após 30 minutos, a coluna foi lavada com 50 mL do mesmo tampão contendo 50 mM de imidazol. As proteínas ligadas foram eluídas com o tampão de lise contendo 200 mM de imidazol. As amostras foram dializadas contra um tampão contendo 50 mM de fosfato de sódio, 1 mM EDTA, 5 mM β-mercaptoetanol para remover o imidazol. O concentração das proteínas foi determinada pelo método de Bradford (Bradford, 1976) .

3.2. Ensaio de extravasamento de lipossomos

Vesículas unilamelares grandes (LUV) foram preparadas pelo métodos de extrusão de acordo com Hope et al, 1985. Todas as preparações foram feitas em Tris 25 mM, pH 7.5. Interações inespecíficas de carga foram reduzidas acrescentando-se NaCl 100 mM nas soluções, quando desejado. Um mini-extrusor de duas seringas (Avanti Lipids) foi usado, equipado com um filtro (Nuclepore ®, Whatman) com poro de 80 ou 200 nm. A extrusão foi feita através de 20 passagens para cada lado da seringa. Foram usados dois tipos de fosfolipídeos: ácido fosfatídico, PA, (L-α-phosphatidic acid) e DOPG (1,2-di-(9Z-octadecenoyl)-*sn*-glycero-3-phospho-(1'-*rac*-glycerol). Os lipídeos (10 mg) foram solubilizados em 500 μL de clorofórmio e o solvente foi completamente evaporado, utilizando jato de

nitrogênio, de maneira a formar um filme lipídico uniforme dentro de um tubo de vidro com fundo arredondado. A solução de carboxifluoresceína (CF) a 100 mM (massa molar = 376.32 $g.mol^{-1}$ ([2′,7′-bis-(2-carboxyethyl)-5-(and-6)-carboxyfluorescein; Molecular Probes, USA) e solubilizada em Tris 25 mM, pH 7.5, foi encapsulada dentro das vesículas, misturando-se vigorosamente 500 μL da solução adicionada ao filme lipídico previamente formado, utilizando-se vortex. As moléculas de CF livres, não contidas dentro das vesículas, foram separadas por cromatografia de gel-filtração, utilizando coluna Sephacryl® S-100 (GE Healthcare). Após essa etapa, realizou-se a extrusão conforme descrito acima. As suspensões contendo as LUVs foram padronizadas baseando-se na fluorescência da sonda fluorescente (490 nm), ajustada para uma concentração final de 0.1 A_{490} nos experimentos. Para a medida do extravasamento das LUVs, a intensidade de fluorescência da mistura reacional foi registrada ao longo do tempo. As amostras foram excitadas à 490 nm e a fluorescência foi detectada a 518 nm. Todos os experimentos foram executados no espectrofotômetro de fluorescência Cary Eclipse (Varian, USA). A ausência de extravasamento (0%) foi estabelecida como sendo a fluorescência das vesículas no tempo zero, enquanto que 100 % de extravasamento foi considerado como a intensidade de fluorescência obtida após adição de 1 % (vv) de Triton X-100.

O grau de permeabilização das LUVs foi inferido através da relação:

$$\% \text{ leakage} = [(F - F0)/(Ft - F0)] \times 100,$$

onde F é a intensidade de fluorescência após adição da proteína teste; F0 é a fluorescência inicial da suspensão inicial de vesículas e Ft é a fluorescência após adição de Triton X-100.

A figura 9 ilustra esquematicamente o princípio da técnica.

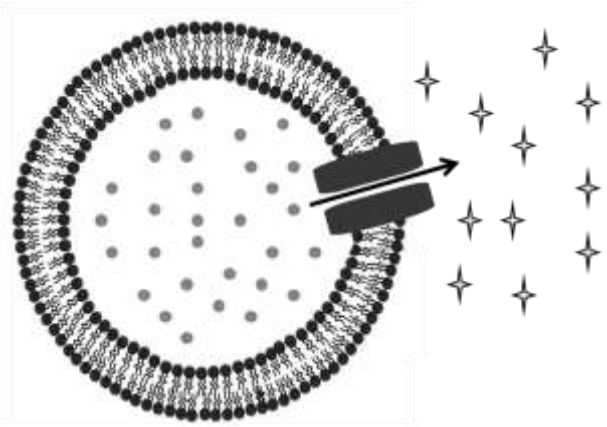

Figura 9: Princípio do ensaio de extravasamento de CF. As esferas verdes representam a sonda fluorescente contida dentro dos lipossomos, onde sua fluorescência é extinguida, efeito mais conhecido como "concentration quenching" (Chen & Knutson, 1988). Ao serem liberadas para o meio reacional, devido à um poro ou ao rompimento da bicamada, ocorre a diluição dessas moléculas no meio aquoso e, como consequência, elas emitem fluorescência.

Foram testados JBU, Jbtx, Jbtx N-ter, Jbtx C-ter e Jbtx Δ-β nas concentrações indicadas na tabela 1.

A JBU foi ensaiada com lipossomos feitos de DOPG enquanto que, para Jbtx e mutantes, foram utilizados lipossomos compostos de PA; ambos fosfolipídeos possuem caráter aniônico. Nos experimentos com JBU foi usado um tampão de reação contendo 100 mM de NaCl para minimizar as interações inespecíficas; já nos experimentos com Jbtx e mutantes foram exploradas mais condições, como ausência de NaCl e desnaturação por fervura prévia por 10 minutos. Após fervura, as amostras foram mantidas à temperatura ambiente.

4. Resultados e discussão

4.1. Permeabilização de lipossomos causada por Jbtx

Proteínas que interagem com membranas de forma a rompê-las, ou formar canais iônicos, podem ser estudadas com a técnica que quantifica o extravasamento de sonda fluorescente contida dentro de vesículas. JBU, Jbtx e seus mutantes derivados foram testados nas concentrações de 5 μg/mL, 15 μg/mL ou 50 μg/mL. A tabela 1 apresenta a massa molecular das moléculas, e as doses molares utilizadas.

Tabela 1: Comparação das doses usadas nos ensaios

	kDa	**5 μg/mL**	**15 μg/mL**	**50 μg/mL**
JBU	90	0.009 μM	0.027 μM	0.090 μM
Jbtx	11	0.45 μM	1.36 μM	4.5 μM
Jbtx N-ter	5.8	0.85 μM	2.55 μM	8.5 μM
Jbtx C-ter	6.5	0.76 μM	2.28 μM	7.6 μM
Jbtx Δ-β	9.5	0.52 μM	1.56 μM	5.2 μM

Os experimentos com lipossomos mostraram que todas as proteínas são capazes de interagir com as membranas lipídicas das vesículas, e causar o extravasamento de carboxifluoresceína (CF).

O Jbtx e seus mutantes permeabilizaram lipossomos feitos de PA. A figura 8 mostra que, tanto na concentração de 5 μg/mL como na concentração de 50 μg/mL, o extravasamento de CF é acima de 80 % para todos os peptídeos, sendo o perfil de permeabilização muito parecido para todos. Talvez exista uma pequena diferença na atividade de Jbtx C-ter, que permeabilizaria de 5 a 10 % a mais as vesículas lipídicas, quando comparado aos outros peptídeos, mas os experimentos não foram repetidos o número de vezes necessário para a confirmação dessa hipótese. Interessantemente, mesmo o mutante com a deleção do domínio grampo beta, que se suspeitava ser o responsável pelas interações do Jbtx com membranas, causou intenso extravasamento da sonda, indicando que a ausência deste motivo estrutual não afeta a interação do peptídeo com membranas lipídicas. Essa observação está de acordo com os

resultados demonstrados por Martinelli e colaboradores, mostrando que Jbtx Δ-β ainda tem efeitos biológicos em fungos e preparações com células de insetos (anexo 1).

Conforme visto na estrutura 3D do Jbtx (fig.3), o Jbtx C-ter (metade C-terminal do Jbtx) contém uma pequena α-hélice levemente anfipática, e mais outra pequena α-hélice, contendo basicamente os resíduos de histidina adicionados ao peptídeo para o passo de purificação, além das duas folhas beta formando o grampo beta. Já no peptídeo Jbtx N-ter, que compreende somente a região amino-terminal do Jbtx original, existe uma α-hélice verdadeiramente anfipática, contendo resíduos polares e apolares intercalados. Essas hélices anfipáticas, presentes em todos os peptídeos testados, poderiam ser as regiões que conferem às moléculas a capacidade de interagir com os lipossomos.

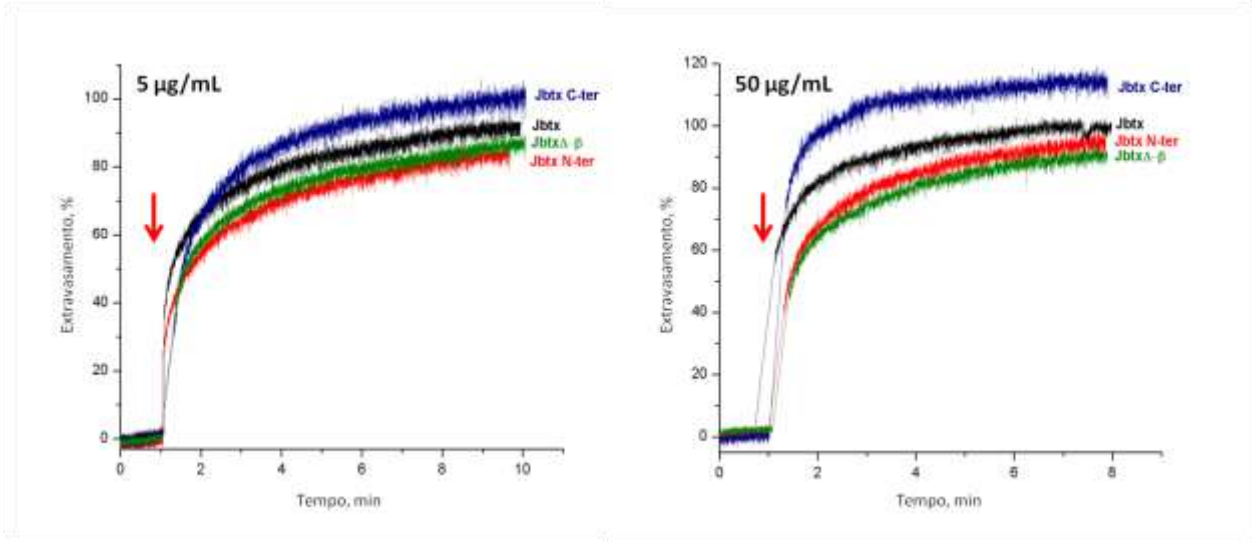

Figura 10: Permeabilização de lipossomos causado por Jbtx e mutantes derivados. A porcentagem de extravasamento de CF foi avaliada ao longo do tempo, em tampão Tris pH 7.5, à temperatura ambiente (~ 20° C). Foram testadas duas concentrações dos peptídeos, 5 e 50 µg/mL, as doses molares correspondentes estão listadas na tabela 1. As setas vermelhas indicam o momento da adição dos peptídeos na cubeta do ensaio. As curvas obtidas para cada peptídeo foram superimpostas para facilitar comparações. Resultados típicos.

As diferentes condições testadas para os peptídeos (figura 11) revelaram que mesmo na presença de sal no tampão reacional, ocorreu extravasamento, embora em menor extensão. A presença de NaCl estabiliza as vesículas e dificulta a interação das moléculas, ou seja, elimina ligações "promíscuas", pois a carga do íon proveniente do sal em solução impede o grupamento fosfato dos lipídeos de interagir com outros compostos do meio, chamado de "efeito blindagem". Já a fervura das amostras, o que teoricamente é suficiente para desnaturar as proteínas, diminuiu a interação dos peptídeos com as vesículas, mostrando que a ausência de

estrutura afeta a atividade dos peptídeos. Após fervura, as versões reduzidas do peptídeo parecem ter tido perda maior da atividade sobre membranas lipídicas, quando comparados à versão original. Observou-se que Jbtx foi o peptídeo que menos perdeu sua atividade após fervura, talvez resultado de uma renaturação parcial após a fervura.

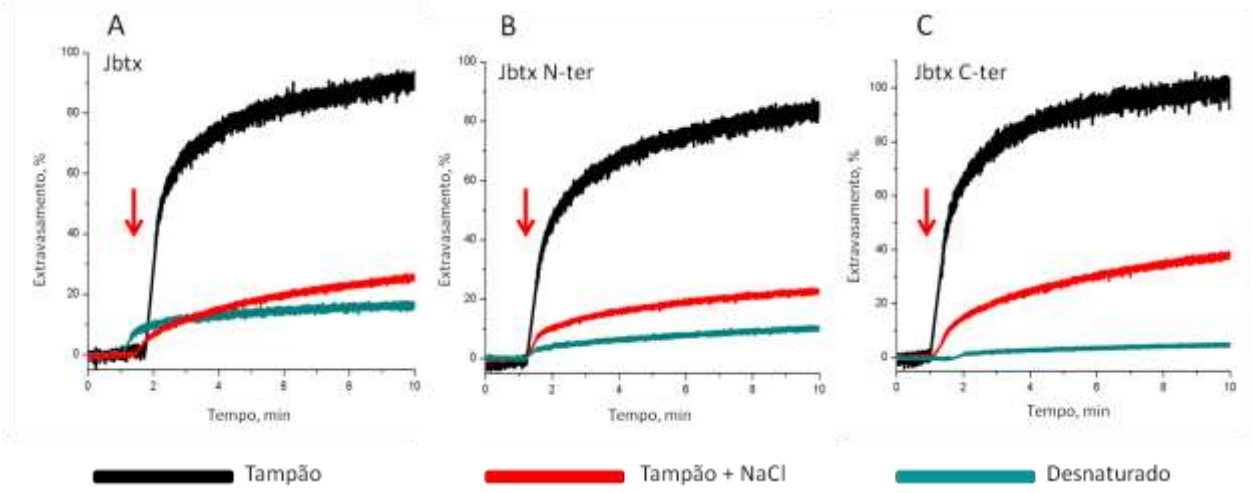

Figura 11: Permeabilização de lipossomos por Jbtx, Jbtx N-ter e Jbtx C-ter. O extravasamento de CF induzido por 5 μg/mL final de Jbtx e seus derivados foi quantificado ao longo do tempo, em diferentes condições. Os traçados mostram: em preto, extravasamento na ausência de NaCl (somente tampão Tris), à temperatura ambiente (~ 20° C); em vermelho, extravasamento na presença de NaCl; em verde, extravasamento com os peptídeos desnaturados, na presença de NaCl. As setas indicam o momento em que a solução contendo os peptídeos foi adicionada na cubeta do ensaio. As curvas para as três condições de cada peptídeo foram superimpostas para facilitar comparações. Resultados típicos.

4.2. Permeabilização de lipossomos causada por JBU

Como o Jbtx e seus peptídeos derivados, a JBU também interage com lipossomos compostos de DOPG, um lipídeo aniônico, produzindo extravasamento de CF, mesmo na presença de 100 mM NaCl. A figura 12 ilustra a porcentagem de extravasamento de CF em apenas 5 minutos de incubação, mostrando que mesmo em doses tão baixas quanto 4.8 μg/mL – 0.0086 μM, a JBU produz o extravasamento de 22 % de CF. Já a figura 13 apresenta a cinética da permeabilização ao longo de 30 minutos, na presença de 15 μg/mL – 0.027 μM de JBU, mostrando que ao final do ensaio. JBU levou a quase 40 % de extravasamento.

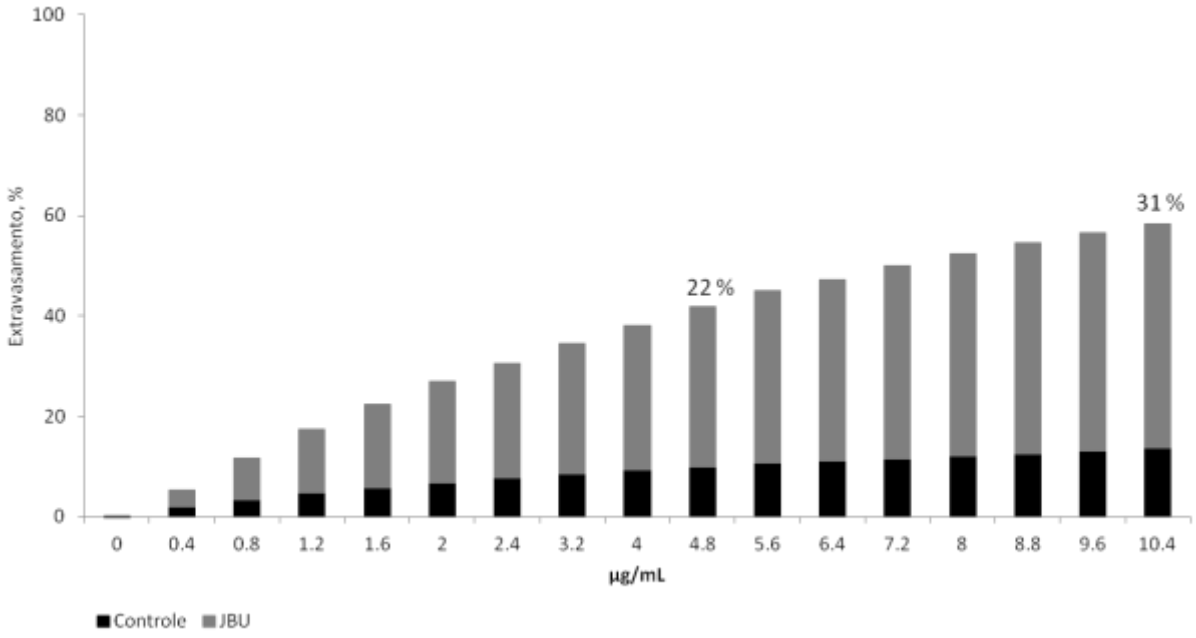

Figure 12: Extravasamento de CF causado por diferentes concentrações de JBU. Nas concentrações de 4.8 μg/mL (0.0086 μM) e 10.4 μg/mL (0.019 μM) estão indicados, acima da barra, a porcentagem de permeabilização relativa somente ao efeito da JBU. A leitura foi realizada após 5 minutos de incubação à temperatura ambiente, na presença de 100 mM de NaCl. Controle representa lipossomos incubados com o tampão de solubilização da JBU: NaPB 20 mM, EDTA 1 mM e β-mercaptoetanol 5 mM, no volume correspondente ao volume adicionado de proteína. Resultado típico de 2 repetições.

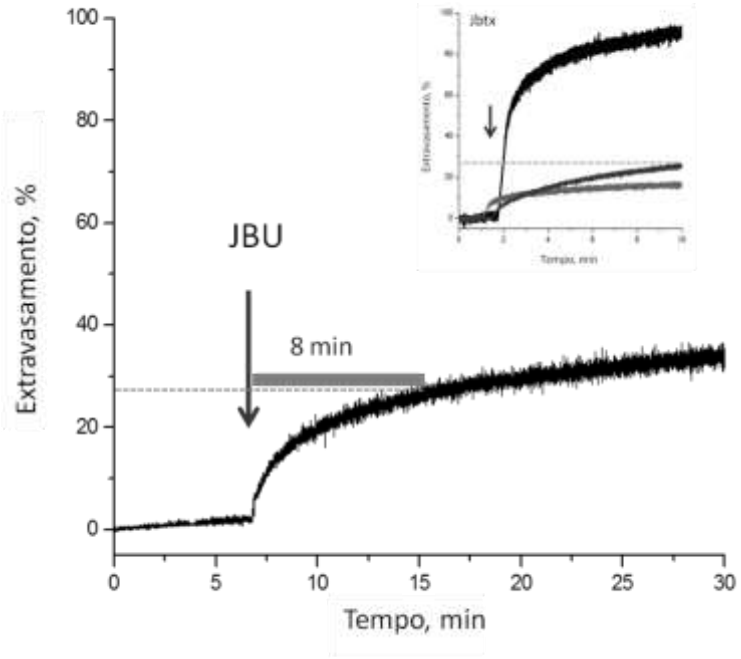

Figura 13: Cinética de extravasamento de CF induzida por 15 µg/mL - 0.027 µM de JBU, em tampão contendo 100 mM de NaCl. **A barra cinza indica o tempo comparativo ao ensaio de extravasamento com o Jbtx (*inset*).** A seta indica o momento em que a solução contendo a proteína foi adicionada na cubeta do ensaio. Traçado típico. (n=2).

O gráfico acima mostra que, em 8 minutos de atividade com 0.027 µM de JBU, o extravasamento gerado é equivalente ao extravasamento causado por 0.45 µM Jbtx, na condição experimental contendo NaCl, painel A, figura 11, traçado vermelho (em torno de 25 %), também ilustrado no detalhe do gráfico. Ou seja, a JBU é cerca de **16** vezes mais ativa que o Jbtx em promover o extravasamento de lipossomas compostos de lipídeos aniônicos.

Dados de espalhamento de luz dinâmica, em que o raio hidrodinâmico (R_h) de lipossomos multilamelares miméticos de plaqueta humana foi estimado na ausência e na presença de JBU, corroboram os resultados acima. Micheletto et al, 2011 verificou que o R_h dos lipossomos diminuiu na presença de JBU, mas sem haver lise, sugerindo que a urease interagiu com as vesículas causando a perda das camadas mais externas de lipídeos. Moro, 2010, trabalhou com os mesmos lipossomos miméticos de plaquetas humanas na presença de Jaburetox-2Ec, observando uma pequena mudança no raio hidrodinâmico das vesículas na

presença de 1.9 μM de peptídeo. Através de SAXS verificou-se ainda que 0,5 μM de Jbtx-2Ec levou à diminuição da distância interlamelar e afetou a rigidez da membrana (Moro, 2010).

O uso do modelo de lipossomos para o estudo de proteínas formadoras de poro é uma prática corrente no meio científico. Essa técnica tem sido utilizada por exemplo, para explorar as propriedades das proteínas formadoras de poros (PFPs), em resposta às alterações de pH e da composição lipídica. Fosfolipídeos aniônicos frequentemente são citados como responsáveis por aumentar a capacidade das PFPs em induzir extravasamento. Sabe-se que alguns canais de Na^+ bacterianos têm preferência por membranas carregadas negativamente (D'Avanzo et al, 2013). Da mesma forma, os fosfolipídeos aniônicos aceleram a ligação e a formação dos poros na membrana pelo peptídeo antimicrobiano lacticina Q (Yonevama et al, 2010). Outros estudos mostraram ainda que a toxina vegetal ricina A causa mudanças estruturais em vesículas feitas de POPG (Day et al, 2002).

Ensaios com a JBU ou peptídeos derivados em lipossomos compostos de diferentes fosfolipídeos não foram feitos na presente tese. A escolha em usar DOPG e PA, para os experimentos mostrados aqui, foi feita baseada nos dados de Barros e colaboradores já citados na Introdução (Barros et al, 2009), que mostraram maior atividade de Jaburetox-2Ec em membranas carregadas negativamente.

Capítulo II

Este capítulo compreende o trabalho entitulado:

Canavalia ensiformis urease, Jaburetox and derived peptides form ion channels in planar lipid bilayers

Publicado na revista Archives of Biochemistry and Biophysics

Canavalia ensiformis urease, Jaburetox and derived peptides form ion channels in planar lipid bilayers

Angela R. Piovesan [a], Anne H. S. Martinelli [a,b], Rodrigo Ligabue-Braun [a], Jean-Louis Schwartz [c,d,#], Celia R. Carlini [a,b,#,1]

[a] Graduate Program in Cellular and Molecular Biology, Center of Biotechnology, Universidade Federal do Rio Grande do Sul, Porto Alegre, RS, CEP 91501-970, Brazil

[b] Department of Biophysics, Universidade Federal do Rio Grande do Sul, Porto Alegre, RS, CEP 91501-970, Brazil

[c] Groupe d'étude des protéines membranaires (GÉPROM, FQR-S) and Department of Physiology, Faculty of Medicine, Université de Montréal, Montreal, Quebec, Canada, H3C 3J7

[d] Centre SÈVE (FQR-NT), Université de Sherbrooke, Sherbrooke, Quebec, Canada, J1K 2R

[#] Addresses for correspondence:

C. R. Carlini:

Dept. Biophysics & Center of Biotecnology

Universidade Federal do Rio Grande do Sul

Av. Bento Gonçalves, 9500.Predio 43.431.

Porto Alegre, RS, CEP 91501-970, Brazil

Tel: +55 51 3308 7606

Email: ccarlini@ufrgs.br or celia.carlini@pq.cnpq.br

J. L. Schwartz :

Département de physiologie, Faculté de médecine

Université de Montréal

C.P. 6128, succursale Centre-Ville

Montréal (Québec) Canada, H3C 3J7

Email : jean-louis.schwartz@umontreal.ca

[1] Present address

Instituto do Cérebro (InsCer), Pontifícia Universidade Católica do Rio Grande do Sul (PUCRS), Av. Ipiranga 6690, Porto Alegre, RS, 90610-000. Email: celia.carlini@pucrs.br

Abstract

Ureases catalyze the hydrolysis of urea into NH3 and CO2. They are synthesized by plants, fungi and bacteria but not by animals. Ureases display biological activities unrelated to their enzymatic activity, i.e., platelet and neutrophil activation, fungus inhibition and insecticidal effect. Urease from Canavalia ensiformis (jack bean) is toxic to several hemipteran and coleopteran insects. Jaburetox is an insecticidal fragment derived from jack bean urease. Among other effects, Jaburetox has been shown to interact with lipid vesicles. In this work, the ion channel activity of C. ensiformis urease, Jaburetox and three deletion mutants of Jaburetox (one lacking the N-terminal region, one lacking the C-terminal region and one missing the central β-hairpin) were tested on planar lipid bilayers. All proteins formed well resolved, highly cation-selective channels exhibiting two conducting states whose conductance ranges were 7-18 pS and 32-79 pS, respectively. Urease and the N-terminal mutant of Jaburetox were more active at negative potentials, while the channels of the other peptides did not display voltage-dependence. This is the first direct demonstration of the capacity of C. ensiformis urease and Jaburetox to permeabilize membranes through an ion channel-based mechanism, which may be crucial step of their diverse biological activities, including host defense.

Keywords

Canavalia ensiformis urease, insecticidal protein, ion channel, pore-forming toxin, planar lipid bilayer, membrane permeabilization

Abbreviations:

Abbreviations used: CNTX, canatoxin; JBU, jack bean urease; Jbtx, Jaburetox; Jbtx- 2Ec, Jbtx containing a V5 epitope; Jbtx N-term, C-terminal deleted version of Jbtx; Jbtx C-term, N-terminal deleted version of Jbtx; Jbtx D–b, b-hairpin deleted version of Jbtx; LUV, large unilamellar vesicles; PLBs, planar lipid bilayers; PE, Phosphatidylethanolamine; PC, phosphatidylcholine; POPG, 1-hexadecanoyl-2-(9Z-octadecenoyl)- sn-glycero-3-phospho-(10-rac-glycerol); Ch, cholesterol.

1. Introduction

Ureases are metalloenzymes (urea amidohydrolase; EC 3.5.1.5) that display many biological functions unrelated to their enzymatic activity. The primary function of these proteins is to hydrolyze urea into ammonium and carbon dioxide [1]. Plants, fungi and bacteria produce urease while animals do not [2]. The urease from Canavalia ensiformis, the so-called jack bean urease (JBU), was the first enzyme ever to be crystallized [3], thus confirming the protein nature of enzymes. JBU consists of a single polypeptide chain of 840 residues and forms either trimers or hexamers in solution [4-6]. Canatoxin (CNTX), an isoform of JBU [7], was shown to display a number of toxic properties as reviewed in [8]. CNTX and JBU, as well as the bacterial enzymes from Bacillus pasteurii and Helicobacter pylori, disrupt Ca2+ transport across membranes [9-13], bind to sialylated glycoconjugates [7] and activate blood platelets [10, 12-14] and pro-inflammatory cells [15, 16]. These various effects point to interactions of ureases with cell membranes, either directly or via receptor modulation.

Besides contributing to the bioavailability of nitrogen, plant ureases might participate in host defense against insects and fungal pathogens [8, 17, 18]. CNTX and JBU display fungicidal activity [19, 20] and insecticidal effects [21-24].

The latter is mostly due to the release of a 10 kDa internal peptide upon hydrolysis of the protein by cathepsin-like enzymes in the digestive tract of susceptible insects [23, 25]. Two recombinant His-tagged versions of this peptide were developed, Jbtx-2Ec [26] and Jbtx [19], differing from each other only by the presence of a V5 viral epitope in the first one, both displaying potent insecticidal activity [27].

The insecticidal effect of JBU and its derived peptides has been extensively studied in the cotton stainer bug Dysdercus peruvianus (Hemiptera) and in the Chagas' disease vector Rhodnius prolixus (Hemiptera) [17]. At doses ranging from 10-15 to 10-12 M, JBU and its derived peptides induce antidiuresis in isolated Malpighian tubules of R. prolixus, as part of the mechanisms which lead to the insect's death [28].

The structure of the Jbtx-2Ec peptide, predicted either ab initio [26] or by comparative molecular modeling [29], showed a prominent β-hairpin motif which is similar to the one found in a class of neurotoxic or pore-forming peptides, i.e., charybdotoxin (from the venom of the scorpion Leiurus quinquestriatus) or protegrin (from porcine leukocytes) [30, 31]. The presence of this □-hairpin was later confirmed in the 2.05 Å resolved crystallographic structure of JBU [32]. Using computational simulation and data from experiments on liposomes, Barros and co-workers provided the first evidence of the interaction of Jbtx-2Ec with lipid membranes [29]. Their simulation study predicted that the peptide could anchor at a polar/non polar lipid interface. Furthermore, when carboxyfluorescein-loaded large unilamellar vesicles (LUV) were exposed to the peptide, leakage of the fluorescent probe was observed, suggesting that the peptide interacted with LUV's membranes either by disrupting the lipid bilayer or by pore formation, or both. Preliminary experiments conducted in planar lipid bilayers (PLBs) supported the channel mechanism of membrane permeabilization by Jbtx-2Ec [33]. Later, structure-function relationships studies were performed using mutated versions of Jbtx, either

lacking the β-hairpin region (Jbtx Δ-β), or corresponding to its N-terminal (Jbtx N-ter) or C-terminal (Jbtx C-ter) domains. These studies demonstrated that only part of the membrane-disturbing activity of Jbtx could be assigned to the amphiphylic β-hairpin and that the N-terminal domain alone is responsible for the insecticidal property of the peptide [27].

Based on the evidences of lipid membrane permeabilization by Jbtx and the several cellular effects involving membrane recognition displayed by CNTX and other ureases, it was hypothesized that these proteins interact with lipid membranes through a pore-forming mechanism. The present study was designed to investigate and characterize, using an electrophysiological approach and PLBs, the membrane permeabilization process induced by JBU and Jbtx. Furthermore, by using three Jbtx deletion mutants, we aimed to explore the structure-function relationships implicated in its ability to interact with membranes. The results of this work provide critical insights into the membrane bioactivity of these molecules, contributing to the overall understanding of the mechanism of action of JBU and related peptides.

2. Materials and Methods

2.1. Chemicals

Phosphatidylethanolamine (PE), phosphatidylcholine (PC), 1-hexadecanoyl-2-(9Z-octadecenoyl)-sn-glycero-3-phospho-(1'-rac-glycerol) (POPG) and cholesterol (Ch) were obtained from Avanti Polar Lipids (Alabaster, AL, USA). Jack bean urease type C3 was purchased from Sigma Aldrich (St. Louis, MO, USA) and further purified as in [22]. It was dissolved in 20 mM sodium phosphate buffer, 1 mM EDTA, 5 mM β-mercaptoethanol, pH 7.5, and quantified by absorbance spectroscopy at 280 nm (0.604 A280 was considered equivalent to a 1.0 mg/ml protein solution). Solutions of JBU (in its 540-kDa hexameric form) at 0.5-1

mg/ml were used as stock solutions for the assays. All other chemicals used were of analytical grade.

2.2. Expression and purification of Jbtx and derived mutants

Jbtx (wild-type, 92 amino acids, 11.2 kDa) and site-directed deleted mutants of Jbtx were produced according to [19] and [27], respectively. The mutated versions of Jbtx were: Jbtx N-ter, corresponding to the first 43 amino acids of the peptide, Jbtx C-ter, corresponding to the last 49 amino acids of Jbtx (AA 44-92), and Jbtx Δ-β, a mutant without the β-hairpin central region and corresponding to the first 61 and the last 19 amino acids of the Jbtx sequence (AA 1-60 - AA 73-92) [27]. All the mutants were ligated in NdeI and XhoI restriction site of pET-23a vector, resulting in peptides carrying two remanescent aminoacids (LE) of XhoI site and six histidine tag at the carboxi end. A schematic representation of these peptides (without the residues from restriction sites) is shown in Figure 1. Solutions of the peptides (assumed to be in their monomeric form) at 1 mg/ml were used as stock solutions for the assays.

2.3. Planar lipid bilayers

The experimental technique used in this study was very similar to that described before [34, 35]. Lipid mixtures of PE:PC:Ch (7:2:1, wt/wt) or PE:POPG (4:1, wt/wt) were dissolved in decane to a final concentration of 25 mg/ml. Lipid bilayers were painted on the 250 µm circular aperture of a Delrin cup constituting the cis chamber (800 µl) of the experimental apparatus. Bilayer painting was performed with tip-occluded, pre-pulled Pasteur pipettes dipped in the lipid mixture solution. This solution was also used to pretreat the aperture of the Delrin cup. In experiments with JBU, which proved to be extremely slow to insert into membranes using the regular procedure (it took one hour or more for channel activity to be observed), the pretreatment lipid mixture was enriched with the protein (4 µg JBU/mg lipids). Thinning of the membrane was observed with a low power binocular dissecting microscope. Bilayer formation

was monitored by capacitance measurement. Typical membrane capacitance ranged between 150 and 200 pF. Once formed, the bilayers remained stable for several hours.

2.4. Electrophysiological assays

Electrical connections to the trans (1.6 ml) and cis (800 µl) compartments separating the membrane were made by Ag/AgCl2 electrodes and salt bridges made of glass pipettes filled with 1% agar and 3 M KCl to minimize liquid junction potentials. Voltage was applied to the cis compartment and the trans compartment was grounded. After bilayer formation, various levels of holding voltages were applied across the membrane for at least 30 min to ensure that there was no contaminant-induced channel activity. Incorporation of the test molecules into the lipid bilayer was performed by adding aliquots of the protein, peptide or mutants directly to the cis chamber. Channel activity was indicated by clearly resolved current jumps in response to voltage steps. Experiments were conducted either under symmetrical conditions in solutions containing 0.5 M KCl, 1 mM CaCl2, 10 mM HEPES, pH 7.5, or, for selectivity determination, under asymmetrical conditions in the above solutions in which the concentration of KCl was adjusted to 1.25 M (cis) and 0.5 M (trans). Experiments were performed at room temperature (22-25 ºC).

2.5. Data recording and analysis

Single channel currents were recorded with an Axopatch-1D patch clamp amplifier (Molecular Devices, Sunnyvale, CA). Signals were digitalized with a Digidata 1200 analogue-to-digital converter using Axoscope 10.2 software (both from Molecular Devices) at 50-kHz sampling frequency. They were low-pass filtered at 100 Hz and analyzed on a personal computer using Clampfit 10.2 software (Molecular Devices). Applied voltages are defined with respect to the trans chamber that was held at virtual ground. Positive currents (i.e., currents

flowing through the molecules inserted into the membrane (cis to trans) are shown as upward deflections in the figures.

For each applied voltage, an all-point amplitude histogram was generated and the amplitudes of the current jumps were determined by measuring the horizontal distance (in pA) between its successive peaks. The largest peak of the histogram was considered to represent the current in the main conducting state of the channels. Minor peaks were used to evaluate the amplitude of the current either in the subconducting states of the main channel or flowing through smaller channels. Current-voltage relation graphs (I/V curves) were then plotted and, when the relations were rectilinear, the channel conductances were estimated from the slopes of the linear regressions on the data points. For non-linear curves, the conductances at negative and positive voltages were obtained separately as the slopes of the linear regressions on the data points for voltages either inferior or equal to - 40 mV, or superior or equal to + 40 mV. The conductances obtained in each individual experiment were then averaged over the number of experiments performed under the same conditions. Ion selectivity was determined using the reversal potential values, VR, obtained as the voltages for which the corresponding linear regressions intersected the horizontal axis of the I/V curves. The voltage dependence of the channels was evaluated by plotting the open probability of all channels (NPo) vs the applied voltage. NPo was obtained at each voltage by calculating the ratio of the area (Aopen) under the Gaussian fit of the curve corresponding the open state of the channel over the total area under the all-point amplitude histogram, i.e., NPo = 100Aopen/(Aopen + Aclosed).

Results are expressed as means ± SEM for the number of experiments given in the text and the figure captions.

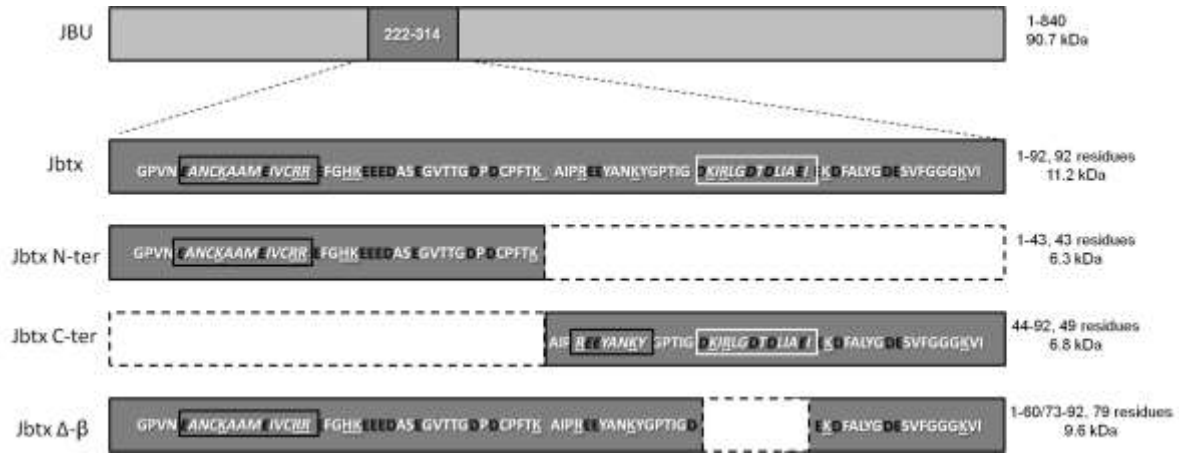

Figure 1. Schematic representation of the primary sequences of JBU, Jbtx and the Jbtx N-ter, Jbtx C-ter and Jbtx Δ-β mutants. The sequence of JBTx was derived from JBU isoform II, Genbank accession AF468788, as described in [26]. The location of Jbtx within JBU is shown as the grey area in the JBU box, starting at AA222 and ending at AA314 of the primary sequence of JBU. The AA sequences of Jbtx and its mutants are given in each of the corresponding boxes, with negatively charged residues shown in black and positively charged residues in white and underlined. The positions of the putative α-helices and β-hairpins, obtained by Swiss-Model molecular modelling [65] using JBU (3LA4) [32] as template, are indicated black or white boxes, respectively. The number of residues, and the molecular mass of each molecule are indicated on the right side of the boxes (modified from [27]). The two remanescent aminoacids (LE) of restriction enzyme (XhoI) site and the six histidine tag at the carboxi end of all Jbtx peptides were removed for clarity.

3. Results

JBU, Jbtx and its three mutants formed ion channels in PLBs. Except for JBU, they partitioned easily into the membranes. In all cases, initial insertion was facilitated by applying a negative holding voltage to the bilayers. The biophysical properties of channels are listed in Table 1 and more details are provided in the following subsections.

3.1. Channel properties of JBU

Channel activity of JBU, either in PE:PC:Ch or in PE:POPG bilayers, was extremely difficult to observe without the addition of the protein to the lipid mixtures used to pretreat the aperture of the cis chamber. As the current records obtained in either type of membrane looked very similar, here only the JBU channel activity observed in PE:PC:Ch bilayers was analyzed. The protein formed well-resolved channels at concentrations of 10-20 µg/ml (18.4-36.8 nM). Representative traces of the current flowing through the channels under symmetrical conditions (0.5 M:0.5 M KCl, cis:trans) and the corresponding current-voltage relations are illustrated in Figure 2, panels A and B, respectively. Three types of conductance were observed (n = 4), one main conductance displaying current rectification with conductance values of 79.15±8.05 pS at positive voltages and 43.95±3.10 pS at negative voltages, an intermediate non-rectifying conductance of 29.65±5.34 pS and a smaller, non-rectifying conductance of 10.52±0.22 pS. The open probability of the larger, rectifying channels is represented by the NP_o vs V plot (Figure 2, panel C) which demonstrates that the main channels formed by JBU were voltage-dependent, being open quite more often at negative voltages. Ion selectivity was determined by conducting experiments under asymmetrical 1.25 M:0.5 M KCl (cis:trans) conditions. Under these conditions, the rectifying channels were rarely observed. The channels formed by JBU displayed a conductance of 49.95±4.5 pS (n = 4) and their reversal potential, V_R, was -28.05±7.66 mV (n = 4) (Figure 2, panel D). Under the same ionic gradient conditions, the Nernst potential for K^+, V_N, calculated at 25ºC, is - 23.15 mV [36]. Therefore, the channels formed by JBU were strongly selective to cations.

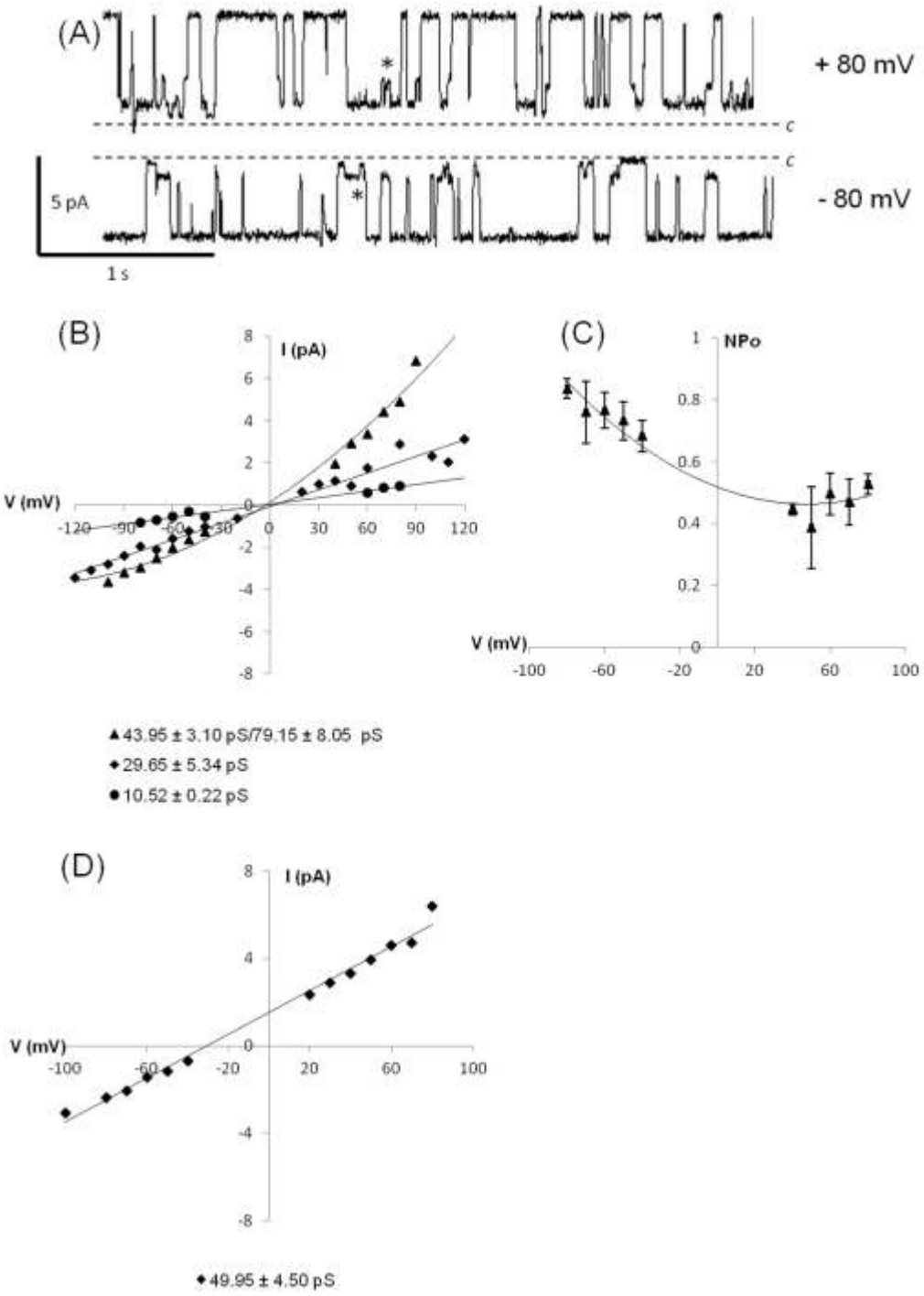

Figure 2. Channels formed by JBU, the jack bean urease. (A) Single channel currents observed at + 80 mV and - 80 mV holding voltages in a typical experiment after JBU (9.2 nM) addition to the cis side of the bilayer under symmetrical (0.5 M:0.5 M KCl, cis:trans) conditions at pH 7.5. The letter C on the right side of the traces indicates the current level at which all channels are closed. Smaller channel current jumps are marked with asterisks. (B) Current-voltage

relations of the channels formed by JBU in PLBs at pH 7.5 under symmetrical 0.5 mM KCl conditions. They show the presence of three conductances, two of them without rectification: 10.52±0.22 pS (●, conductance corresponding to the current jumps indicated by asterisks in A) and 29.65±5.34 pS (♦), and a third one (corresponding to the main channel) that rectifies the current, with conductances of 79.15±8.05 pS at positive voltages and 43.95±3.10 pS at negative voltages (▲), determined as described in section 2. Materials and Methods. The data obtained in 4 experiments was pooled together. (C) Open probability of the main channel formed by JBU. The data was derived from 4 experiments under symmetrical conditions as in A. (D) Under asymmetrical conditions (1.25 M:0.5 M KCl, cis:trans), at pH 7.5, the reversal potential was shifted to - 28.05±7.66 mV, which demonstrated the cationic selectivity of the main channel formed by JBU. The data was obtained from 4 experiments. All straight lines were fitted to the data points by linear regression (panels B and D), the rectifying line was fitted to the data points by a polynomial regression of order 3 (panel B) and the conductances (mean±SEM) are given under the corresponding graphs. The NP_o data points were fitted by a polynomial regression line of order 2 (panel C).

3.2. Channel properties of Jbtx

To test the role of the membrane charge on Jbtx channel formation and properties, two different membrane compositions were used, PE:PC:Ch, as above, which has a neutral net charge, and PE:POPG, which is negatively charged. In both cases, Jbtx formed well-resolved channels within 30 min after addition of 5-15 µg/ml (0.45 – 1.36 µM) of the recombinant peptide to the cis chamber. Channel conductance was affected by the nature of the bilayer. Under symmetrical conditions (0.5 M:0.5 M KCl, cis:trans), in neutral membranes (Figure 3, panels A and B), the main conductance of Jbtx channels was 38.63±4.48 pS (n = 8) and the

smaller one was 7.61±1.15 pS (n = 7), while in negative membranes (Figure 3, panel B), the main channel conductance was 45.52±1.91 pS (n = 4) and that of the smaller one was equal to 18.20±2.60 pS (n = 3). Neither current rectification nor voltage-dependence were observed in either type of membrane (Figure 3, panels B, C and D). Ion selectivity of Jbtx channels was tested in PE:PC:Ch bilayers and under asymmetrical 1.25 M:0.5 M KCl (cis:trans) conditions (Figure 3, panel E). The conductance of the main channel was equal to 52.62±5.92 (n = 4) and V_R was shifted to - 28.10±5.03, which demonstrated the strong cationic nature of Jbtx channels, V_N being equal to - 23.15 mV under these conditions.

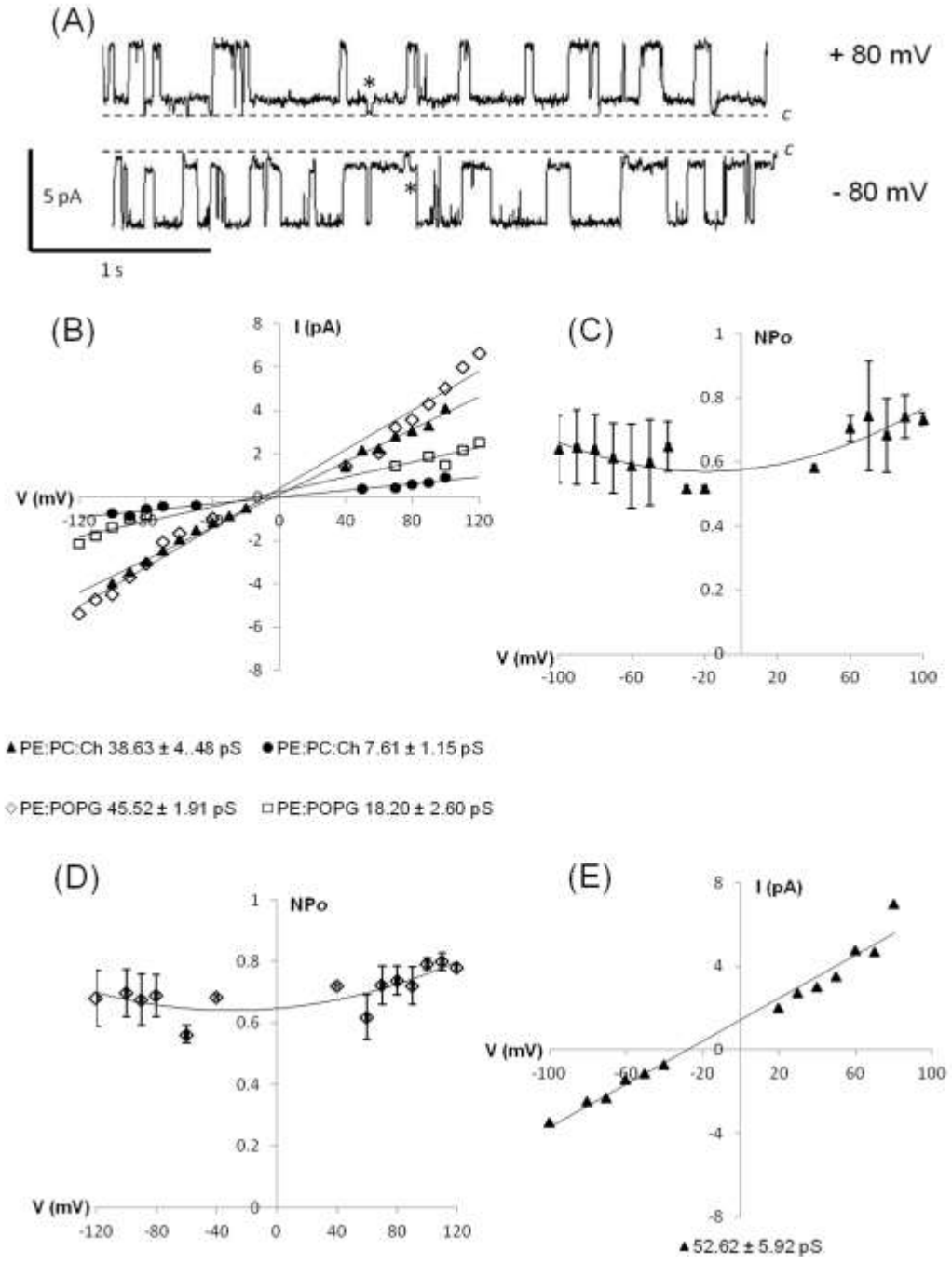

Figure 3. Channels formed by Jbtx, the 93-residue recombinant peptide derived from JBU. (A) Single channel currents observed at + 80 mV and - 80 mV in a typical experiment after Jbtx (1.32 µM) addition to the cis side of a PE:PC:Ch bilayer under symmetrical (0.5 M:0.5 M KCl, cis:trans), pH 7.5. The letter C on the right side of the traces indicates the current level at which all channels are closed. Smaller channel current jumps are marked with asterisks. (B) Current-voltage relations of the channels formed by Jbtx in PE:POPG (◊ and □) or PE:PC:Ch (▲ and ●)

PLBs, at pH 7.5 under symmetrical 0.5 M KCl conditions. They show the presence of four conductances: 45.52±1.91 pS (◊), 18.20±2.60 pS (□), 38.63±4.48 pS (▲) and 7.61±1.15 pS (●, conductance corresponding to the current jumps indicated by asterisks in A). The data was derived from 8 experiments in PE:PC:Ch bilayers and 4 experiments in PE:POPG bilayers under symmetrical 0.5 M KCl conditions in both cases, and was pooled together in each case. (C-D) Open probability of the main channel formed by Jbtx in PE:PC:Ch membrane (C) or PE:POPG membrane (D), respectively. The results were derived from 8 and 4 experiments under symmetrical conditions as in A, respectively. (E) In PE:PC:Ch membranes and under asymmetrical conditions (1.25 M:0.5 M KCl, cis:trans) at pH 7.5, the reversal potential was shifted to - 28.10±5.03 mV, demonstrating the cationic selectivity of the main channel of Jbtx. The data was obtained in 4 experiments. Straight lines were fitted to the data points by linear regression and the conductances are given under the corresponding graphs (panels B and E). The NP_o data points were fitted by polynomial regression lines of order 3 (panel C) and 2 (panel D).

3.3. Channel properties of Jbtx N-ter

Jbtx N-ter, the peptide mapping approximately the N-terminus half of Jbtx, promoted well-resolved current jumps within 30 min after addition of 5-15 µg/ml (0.85 – 2.55 µM) of the peptide to the cis chamber (Figure 4, panel A). This mutant, contrary to Jbtx, was generally poorly active at positive voltages, which made current measurements difficult at these voltages. Under symmetrical conditions (0.5 M:0.5 M KCl, cis:trans), the channel conductances of Jbtx N-ter were equal to 35.75±1.15 pS (n = 4) for the main channel, and 8.87±1.27 pS (n = 4) for the smaller channel (Figure 4, panel B). As illustrated by the NP_o plot (Figure 4, panel C), Jbtx N-ter was highly voltage-dependent, with very little activity at positive voltages, as mentioned

before. Under 1.25 M:0.5 M KCl (cis:trans) asymmetrical conditions, the channel conductance was 39.1±2.73 pS (n = 3).and V_R was shifted to - 21.8±8.77 mV (n = 3), demonstrating the strong cationic selectivity of the N-terminal peptide (Figure 4, panel D).

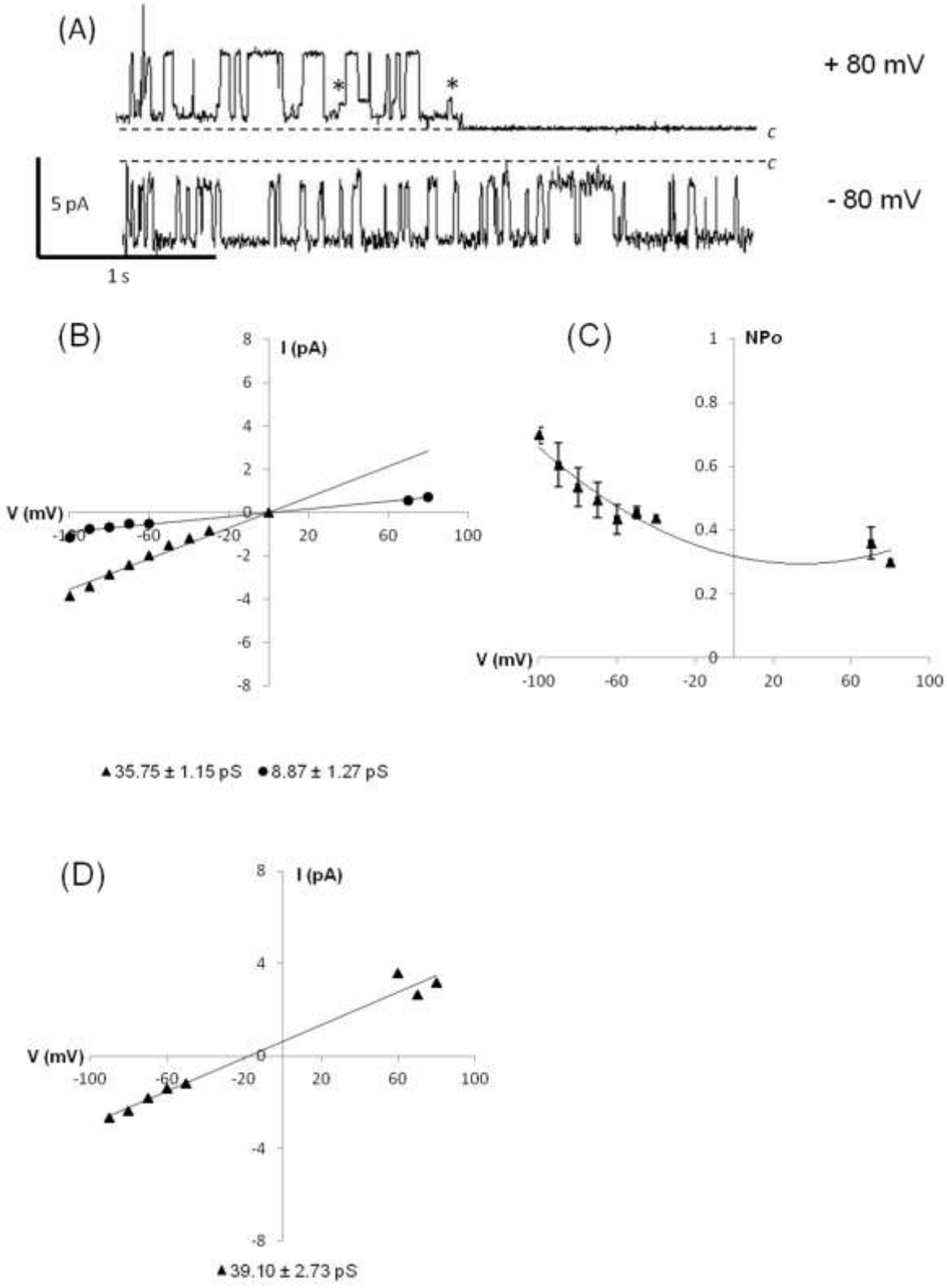

Figure 4. Channels formed by Jbtx N-ter, the 44-residue N-terminal region of Jbtx. (A) Single channel currents observed at + 80 mV and - 80 mV in a typical experiment after Jbtx N-ter (2.36 µM) addition to the cis side of the bilayer under symmetrical (0.5 M:0.5 M KCl, cis:trans) conditions at pH 7.5. The letter C on the right side of the traces indicates the current level at which all channels are closed. Smaller channel current jumps are marked with asterisks. (B) Current-voltage relations of the channel activity formed by Jbtx N-ter in PLBs at pH 7.5 under symmetrical 0.5 M KCl conditions. They reveal the presence of two conductances of 35.75±1.15 pS (♦) and 8.87±1.27 pS (●, conductance corresponding to the current jumps indicated by asterisks in A). The data obtained in 4 experiments was pooled together. (C) Open probability of the main channel formed by Jbtx N-ter. The data was derived from 4 experiments under symmetrical conditions as in A. (D) Under asymmetrical conditions (1.25 M:0.5 M KCl, cis:trans) at pH 7.5, the reversal potential was shifted to - 21.80±8.77 mV, which demonstrated the cationic selectivity of the main channel of Jbtx N-ter. The data was obtained in 3 experiments. Straight lines were fitted to the data points by linear regression and the conductances are given under the corresponding graphs (panels B and D). The NP_o data points were fitted by a polynomial regression line of order 2 (panel C).

3.4. Channel properties of Jbtx C-ter

Like Jbtx and Jbtx N-ter, Jbtx C-ter, the peptide mapping the 49 C-terminus residues of Jbtx, partitioned easily in the bilayers at 5-15 µg/ml concentrations (0.76 – 2.29 µM) and formed well-resolved channels (Figure 5, panel A). Under symmetrical conditions (0.5 M:0.5 M KCl, cis:trans), the main channel conductance was 32.1±0.5 pS (n = 5) while the smaller channel conductance was equal to 9.3±0.24 pS (n = 5). Channel activity was higher at negative voltage, but as shown on Figure 5, panel C, this voltage-dependence was not as large as it was for Jbtx N-ter. Under asymmetrical 1.25 M:0.5 M KCl (cis:trans) KCl conditions, the conductance of the main channel was 42.4±5.06 pS (n = 5) and VR was shifted to - 23.15±7.75

mV (Figure 5, panel D), not very different from VN calculated under these ionic concentration conditions (Figure 5, panel D). Thus, similar to JBU, Jbtx and Jbtx N-ter, the channels formed by Jbtx C-ter were highly cationic in nature.

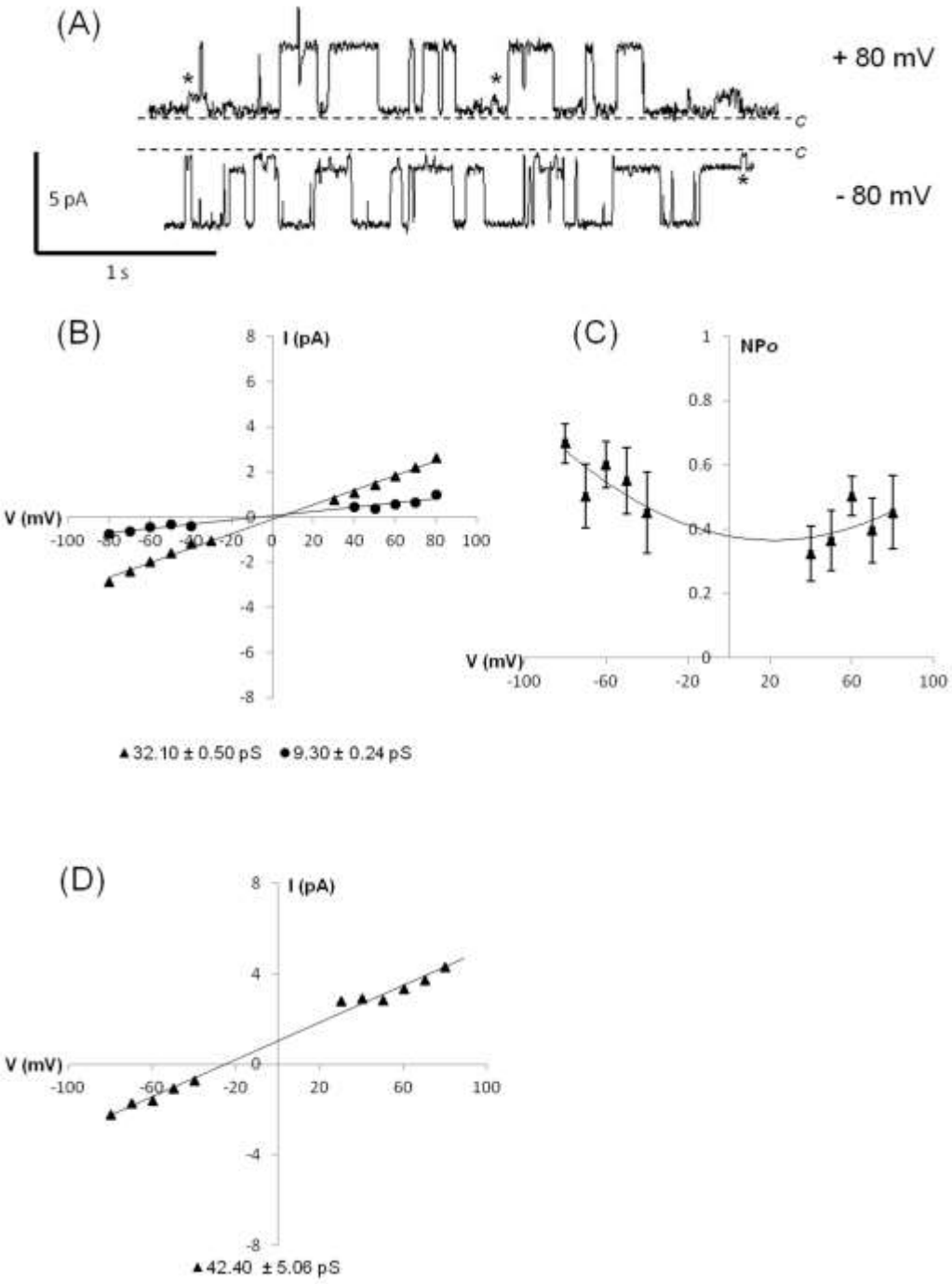

Figure 5. Channels formed by Jbtx C-ter, the 49-residue C-terminal region of Jbtx. (A) Single channel currents observed at + 80 mV and - 80 mV in a typical experiment after Jbtx C-ter

(2.19 µM) addition to the cis side of the bilayer under symmetrical (0.5 M:0.5 M KCl, cis:trans) conditions at pH 7.5. The letter C on the right side of the traces indicates the current level at which all channels are closed. Smaller channel current jumps are marked with asterisks. (B) Current-voltage relations of the channels formed by Jbtx C-ter in PLBs at pH 7.5 under symmetrical 0.5 M KCl conditions. They show the presence of two conductances of 32.10±0.50 pS (♦) and 9.30±0.24 pS (●, conductance corresponding to the current jumps indicated by asterisks in A). The data derived from 5 experiments was pooled together. (C) Open probability of the main channel formed by Jbtx C-ter. The data was derived from 5 experiments under symmetrical conditions as in A. (D) Under asymmetrical conditions (1.25 M:0.5 M KCl, cis:trans) at pH 7.5, the reversal potential was shifted to - 23.15±7.75 mV, which demonstrated the cationic selectivity of the main channel of Jbtx C-ter. The data was obtained in 3 experiments. Straight lines were fitted to the data points by linear regression and the conductances are given under the corresponding graphs (panels B and D). The NPo data points were fitted by a polynomial regression line of order 2 (panel C).

3.5. Channel properties of Jbtx Δ-β

Channels formed by Jbtx Δ-β, the peptide derived after deletion of the β-hairpin region of Jbtx, inserted easily into the bilayers at concentrations comparable to those used with the three other peptides (Figure 6, panel A). Similarly, two conducting states were observed under symmetrical conditions (0.5 M:0.5 M KCl, cis:trans), corresponding to one main channel conductance of 38.95±3.97 pS (n = 4) and a smaller channel conductance of 10.06±0.88 pS (n = 3) (Figure 6, panel B). The channels were not voltage-dependent, with their opening probability remaining at about 60% at any voltage (Figure 6, panel C).

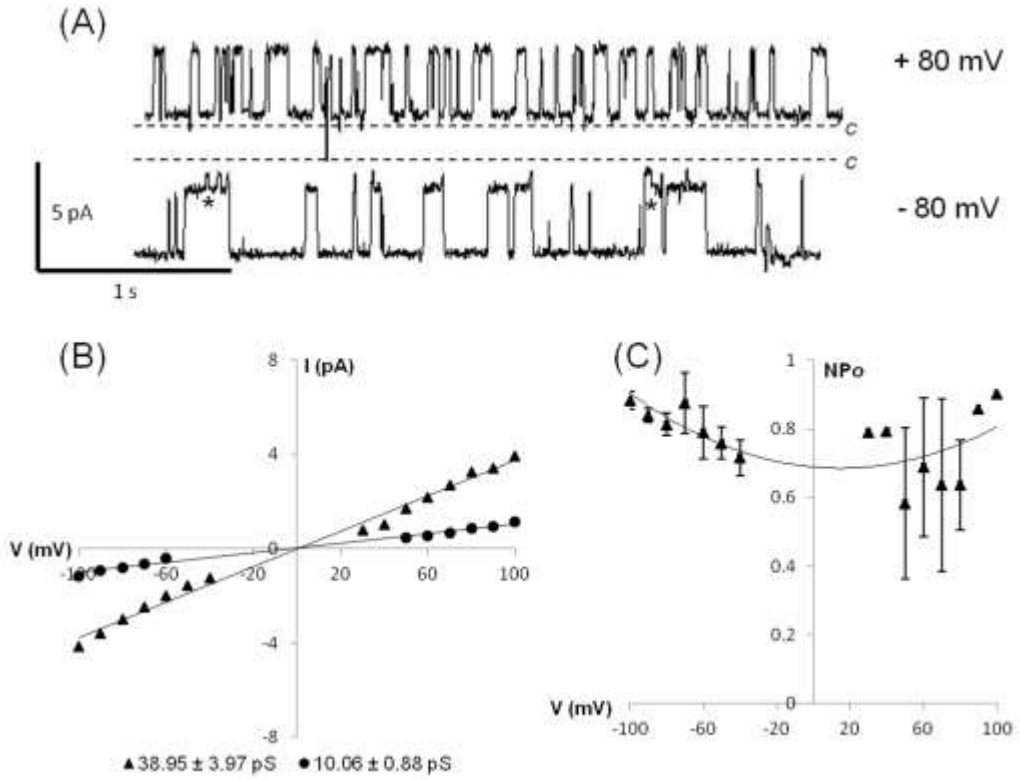

Figure 6. Channels formed by Jbtx Δ-β, the 79-residue peptide derived from Jbtx in which the β-hairpin region was deleted. (A) Single channel currents observed at + 80 mV and - 80 mV in a typical experiment after Jbtx Δ-β (1.53 μM) addition to the cis side of the bilayer under symmetrical (0.5 M:0.5 M KCl, cis:trans) conditions at pH 7.5. The letter C on the right side of the traces indicates the current level at which all channels are closed. Smaller channel current jumps are marked with asterisks. (B) Current-voltage relations of the channels formed by Jbtx Δ-β in PLBs at pH 7.5 under symmetrical 0.5 M KCl conditions. They show the presence of two conductances of 38.95±3.97 pS(♦) and 10.06±0.88 pS (●, conductance corresponding to the current jumps indicated by asterisks in A). The data from 4 experiments was pooled together. (C) Open probability of the main channel formed by Jbtx Δ-β. The data was derived from 4 experiments under symmetrical conditions as in A. The NPo data points were fitted by a polynomial regression line of order 2 (panel C).

4. Discussion

This study demonstrates, for the first time, that a plant urease and its insecticidal domain permeabilize phospholipid bilayers forming well resolved channels in planar lipid bilayers, and provides the initial characterization of the channels' signature (conductance, rectification, selectivity and voltage dependence). Our group has shown that both the wild-type fragment of JBU and the corresponding recombinant peptide Jbtx are functionally similar in terms of insecticidal activity [26, 27]. It is therefore clear that the LE residues and His tags of Jbtx and its mutated versions do not affect the peptide's function. But could they be responsible for channel formation of Jbtx and its mutants? This is unlikely, however, because at the pH at which PLB experiments were conducted, the overall net charge of the peptides remained almost unchanged (theoretical isolectric point of 4.57 without His tag, and 5.14 with His tag) and therefore does not promote their interaction with membranes. This is also supported by studies showing that His tags do not affect membrane permeabilisation [37, 38]. Finally, as demonstrated in our manuscript, the full length urease JBU, which of course has no LE residues and no His tags, also forms channels in PLBs, that share several biophysical properties with those made by Jbtx.

This newly discovered activity of JBU reinforces its "moonlighting" nature [39], i.e., the fact that this protein has more than one function, adding ion channel activity to the other previously reported biological properties unrelated to its urea-hydrolyzing function [8]. The channels formed by JBU, Jbtx and its derived peptides displayed similar biophysical properties. They had two conducting states ranging between around 7 pS to 18 pS (the "smaller channels") and 32 pS to 79 pS (the "main channels"), respectively, and were all highly selective to cations, represented here by potassium ions. The fact that JBU and Jbtx share similar channel properties strongly suggests that this peptide is within the pore-forming domain(s) of the urease. Indeed, structural analysis demonstrates that an extensive region of Jbtx is exposed at the surface of

JBU (Figure 7). Bacillus thuringiensis (Bt) toxin Cry3Aa is a good example of a protein in which the domain 1 region alone is responsible for pore formation in PLBs by the whole protein [40].

The range of conductance measured for JBU, Jbtx and its mutants is common for physiological potassium channels [36] and similar to that of channels formed by 100-500 nM concentrations of the Bt insecticidal protein Cry1Aa in receptor-free PLBs [41]. Small conductance channels were also described for other pore-forming proteins, such as colicin E1 from E. coli, which forms small 30 pS channels, but also large, 480 pS channels [42]. Actually, conductances observed for many pore-forming toxin are usually larger, often in the 300 pS to 1-2 nS range. On the other hand, cation selectivity is shared by several pore-forming toxins, but the pores are usually not very selective [43], as exemplified by Bt toxins [34, 44].

Jack bean urease is not the first insecticidal plant toxin described as capable to form pores. Thionins are small peptides (~ 5 kDa) toxic to fungi, bacteria and mammalian cells. They appear to act directly on membranes [45], either by disruption or by cation-selective ion channel formation [45-47]. Some plant defensins are also membrane-disturbing molecules [48, 49], but despite its 3 cysteine residues, Jbtx shares no sequence identity to these polypeptides. The active doses reported in this work for JBU (18-30 nM) and for Jbtx and derived peptides (0.7 – 2.5 μM) are in the same range of those reported in the literature for plant pore forming proteins [50].

As indicated above, the conductances of JBU and the Jbtx peptides belonged to two classes: those of the main channels and those of the smaller channels. The latter may represent subconducting states of the main channels. The fact that more than one conducting state was observed is far from being unique in the field of pore-forming toxins (PFT)[43, 51]. Whereas in the present study the analysis was restricted only to records corresponding to the activity of

presumably one main channel, multiple levels of currents were observed at higher doses, which may have corresponded to the presence of several identical channels in the membrane, or, alternatively, to the simultaneous activity of oligomers of different sizes. Indeed, the tendency of JBU and Jbtx to oligomerize and how this affected some of their biological properties were previously reported [27, 29, 52]. Iacovache and coworkers [53] suggested that pre-oligomerization was an important step for some pore-forming proteins before inserting into membranes because of the resulting structural rearrangement that would provide the required hydrophobicity. On the other hand, oligomerization could also take place within the membrane after monomer insertion, as has been demonstrated for Bt insecticidal toxins [54, 55]. Barros and co-workers [29] proposed that Jbtx-2Ec was able to interact in a parallel orientation at a polar/non-polar interface or to arrange itself in a transmembrane configuration. As noted in their work, Jbtx-2Ec (as well as Jbtx,[27]) is amphipathic, a feature considered essential for membrane activity of pore-forming peptides [56].

Jbtx formed ion channels in both zwitterionic (PE:PC:Ch) and negatively charged (PE:POPG) membranes. In the latter, insertion of the peptide was easier and the channel conductances were larger. The affinity of Jbtx for negatively charged membranes suggests that anionic lipids may constitute the actual receptors of the toxin in target cells. Previously, we reported the interaction of JBU with negatively charged polysialogangliosides (GD1b and GT1b) and with sialoproteins (mucin, tireoglobulin and fetuin) at the surface of erythrocytes and after absorption onto ELISA microplates [7, 57]. For some pore forming toxins, lipids per se constitute the specific receptors responsible for binding of the toxins as an early step of intoxication. This is the case for cholera toxin, which binds very selectively to GM1gangliosides on the apical membrane of intestinal cells [58, 59] and for the Cry5B Bt toxin, which docks on glycolipids of Caenorhabditis elegans nematodes [60].

Considering the data presented here and all previously available information it is not yet possible to distinguish whether the protein or the peptide modulate pre-existing ion channels in biological membranes or interact directly with the cell membrane by forming ion channels de novo, or both. Further studies lipids or gangliosides, or both, fused into phospholipid membranes, either PLBs or liposomes, will be required to better mimic the conditions found in actual biological membranes. Further work is also needed to investigate how voltage affects the insertion of the molecules into the bilayers and on the strong voltage-dependency of the channels formed by JBU and Jbtx N-ter.

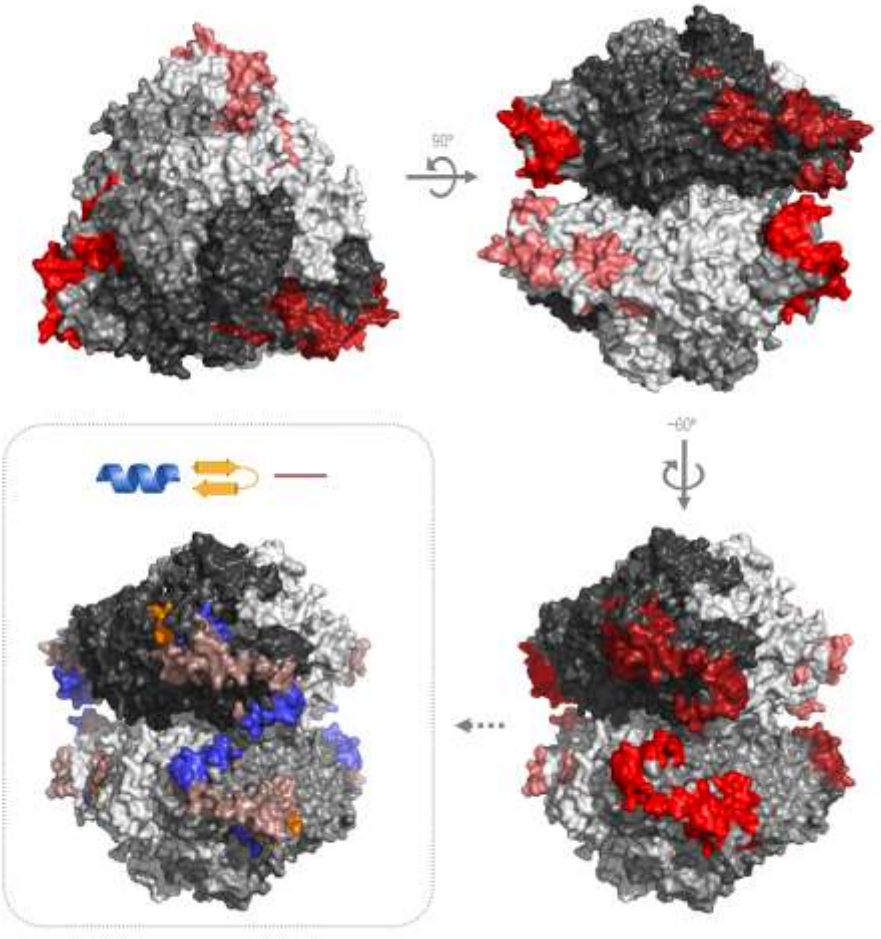

Figure 7: Jbtx residues exposed at the surface of JBU. The region comprising the Jbtx peptide [26] was identified in the native 2.05 Å resolution atomic structure of JBU (PDB ID 3LA4, [32]) using PyMol (Schrödinger, LLC). The molecular surface of the JBU hexamer is shown in

different orientations (two upper panels and right lower panel). Urease monomers are colored in different shades of gray, while the peptide regions are colored in reddish hues. The box (left lower panel showing the hexamer in the same orientation as in the right lower panel) highlights different parts of the secondary structure of the Jbtx moiety (colored according to icons above the structure).

Interestingly, Jbtx Δ-β, the Jbtx mutant lacking the β-hairpin region, formed channels in PLBs like JBU, Jbtx and its two other mutants. This result was quite unexpected. Based on the 2.05 Å resolution atomic structure, molecular modeling and dynamics applied to Jbtx, Balasubramaniam and coworkes [32, 61] proposed that a structural arrangement of the β-hairpin region (which maps similar regions in Jbtx and Jbtx C-ter, i.e., 281DKIRLGDTDLIAEI294, as shown in Figure 1) would be responsible for channel formation through a β-barrel configuration, in which neighboring β-hairpins, each originating from a single monomer, would be associated. However, the present work demonstrating that the deletion from Jbtx of this β-hairpin did not affect its channel forming capability even though some properties of the channels formed were altered, provides a strong argument against the β-hairpin being crucial for membrane permeabilization. Actually, the 3-D structure of JBU [32] shows that the region that maps the Jbtx peptide contains also two short α-helices located on the N-terminal side of the β-hairpin, one of them present in Jbtx N-ter (226EANCKAAMEIVCRR239) and the other in Jbtx C-ter (268REEYANKY275) (Figure 1). Interestingly, two identical α-helices corresponding to the region 226EANCKAAMEIVCRR239 in each molecule are found in close proximity at the surface of the hexameric JBU (Figure 7). This raises the hypothesis of a cooperative behavior of these short helices in the channel forming process and goes along with the fact that it is necessary for more than one of these short helices to cross the bilayer. It is therefore possible that an

oligomeric rearrangement of such helical structures could do so, resulting in channel formation and membrane permeabilization by JBU, Jbtx or the N- and C- terminal halves, an unprecedented feature for a pore-forming protein. Whereas there are many examples of pore-forming toxins that cross biological membranes by means of β-barrel structures, α-helical transmembrane pores constitute an alternate strategy common to bacterial, fungal and plant toxins that permeabilize target cells [43, 53, 62].

Liposome permeabilization and biological activities of Jbtx peptides were also explored by [27]. In that study, the two terminal domains variants of Jbtx and the β-hairpin deleted mutant were shown to behave very similarly in inducing leakage in lipid vesicles. Consistent with a neurotoxic effect, few micrograms of either JBU, Jbtx or its variants, particularly Jbtx N-ter, were able to block neuromuscular junctions when injected into cockroaches in vivo. This activity resembles the effects of neurotoxins which act directly on receptor ion channels [63], among which are pore-forming neurotoxins [64]. However, only Jbtx N-ter and Jbtx Δ-β displayed insecticidal activity while Jbtx C-ter (which contains the β-hairpin) was completely inactive [27]. A possible explanation for this contrasting effect of these peptides is that biological multilayered tissues systems, such as the neuromuscular junction and the whole insect, probably add additional levels of tissue- or cell specificity to the entomotoxic effects of Jbtx-related peptides, rendering Jbtx N-ter biologically active as opposed to Jbtx C-ter [27].

In summary, this study is the first direct demonstration of a cation-selective pore-formation mechanism employed by JBU, a C. ensiformis urease, to permeabilize phospholipid membranes. The region involved in this process is most likely the one that is mapped, at least partially, by the recombinant insecticidal peptide Jbtx. However the β-hairpin region of Jbtx does not appear to constitute a critical structure in the membrane permeabilizing function of the peptide, and therefore, of JBU itself. The diverse biological activities of urease and its

recombinant peptide, including plant defense against insect pests, may well be related to their capacity to form pores in target cell membranes.

Authors contributions

A.R.P and A.H.S.M collected all experimental data. R.L.B. constructed JBU molecular models. Production of Jbtx and its mutated forms was performed in Dr. Carlini's lab, at the Center of Biotecnology, Universidade Federal do Rio Grande do Sul, and the electrophysiological work was conducted in Dr. Schwartz group, at Groupe d'Étude des Protéines Membranaires, Université de Montréal.

Acknowledgements

This work was supported by grants from the Government of Canada (DFAIT-SEP to AP and NSERC Discovery to JLS), the Government of Quebec (FRQ-NT-IIP (Centre SÈVE) to AP and FQRNT-RS/CR to JLS) and the Brazilian agencies Coordenação de Aperfeiçoamento de Pessoal de Nível Superior (CAPES), Conselho Nacional de Desenvolvimento Científico e Tecnológico (CNPq) and Fundação de Amparo à Pesquisa do Estado do Rio Grande do Sul (FAPERGS).

Figure captions

References

[1] N.E. Dixon, T.C. Gazzola, R.L. blakeley, B. Zermer, J Am Chem Soc 97 (1975) 4131-4133.

[2] C. Follmer, Phytochemistry 69 (2008) 18-28.

[3] J.B. Sumner, J Biol Chem 69 (1926) 435-441.

[4] B. Zerner, Bioorg Chem 19 (1991) 116-131.

[5] A. Sirko, R. Brodzik, Acta Biochim Pol 47 (2000) 1189-1195.

[6] B. Krajewska, J Mol Catal B-Enzym 59 (2009) 9-21.

[7] C. Follmer, G.B. Barcellos, R.B. Zingali, O.L. Machado, E.W. Alves, C. Barja-Fidalgo, J.A. Guimaraes, C.R. Carlini, Biochem J 360 (2001) 217-224.

[8] C.R. Carlini, J.C. Polacco, Crop Sci 48 (2008) 1665-1672.

[9] E.W. Alves, A.T. Ferreira, C.T. Ferreira, C.R. Carlini, Toxicon 30 (1992) 1411-1418.

[10] C.R. Carlini, J.A. Guimaraes, J.M. Ribeiro, Br J Pharmacol 84 (1985) 551-560.

[11] F.A. Ghazaleh, I.M. Francischetti, M.E. Gombarovits, C.R. Carlini, Arch Biochem Biophys 339 (1997) 362-367.

[12] D. Olivera-Severo, G.E. Wassermann, C.R. Carlini, Arch Biochem Biophys 452 (2006) 149-155.

[13] G.E. Wassermann, D. Olivera-Severo, A.F. Uberti, C.R. Carlini, J Cell Mol Med 14 (2010) 2025-2034.

[14] C. Follmer, R. Real-Guerra, G.E. Wasserman, D. Olivera-Severo, C.R. Carlini, Eur J Biochem 271 (2004) 1357-1363.

[15] C.F. Benjamin, C.R. Carlini, C. Barja-Fidalgo, Toxicon 30 (1992) 879-885.

[16] A.F. Uberti, D. Olivera-Severo, G.E. Wassermann, A. Scopel-Guerra, J.A. Moraes, P. Barcellos-de-Souza, C. Barja-Fidalgo, C.R. Carlini, Toxicon 69 (2013) 240-249.

[17] F. Staniscuaski, C.R. Carlini, Toxins 4 (2012) 55-67.

[18] A.B. Becker-Ritt, C.R. Carlini, Biopolymers 98 (2012) 367-384.

[19] M. Postal, A.H. Martinelli, A.B. Becker-Ritt, R. Ligabue-Braun, D.R. Demartini, S.F. Ribeiro, G. Pasquali, V.M. Gomes, C.R. Carlini, Peptides 38 (2012) 22-32.

[20] A.B. Becker-Ritt, A.H. Martinelli, S. Mitidieri, V. Feder, G.E. Wassermann, L. Santi, M.H. Vainstein, J.T. Oliveira, L.M. Fiuza, G. Pasquali, C.R. Carlini, Toxicon 50 (2007) 971-983.

[21] C.R. Carlini, A.E. Oliveira, P. Azambuja, J. Xavier-Filho, M.A. Wells, J Econ Entomol 90 (1997) 340-348.

[22] C. Follmer, G.E. Wassermann, C.R. Carlini, Plant Sci 167 (2004) 241-246.

[23] A.R. Piovesan, F. Staniscuaski, J. Marco-Salvadori, R. Real-Guerra, M.S. Defferrari, C.R. Carlini, Insect Biochem Mol Biol 38 (2008) 1023-1032.

[24] M.S. Defferrari, D.R. Demartini, T.B. Marcelino, P.M. Pinto, C.R. Carlini, Insect Biochem Mol Biol 41 (2011) 388-399.

[25] C.T. Ferreira-DaSilva, M.E. Gombarovits, H. Masuda, C.M. Oliveira, C.R. Carlini, Arch Insect Biochem Physiol 44 (2000) 162-171.

[26] F. Mulinari, F. Staniscuaski, L.R. Bertholdo-Vargas, M. Postal, O.B. Oliveira-Neto, D.J. Rigden, M.F. Grossi-de-Sa, C.R. Carlini, Peptides 28 (2007) 2042-2050.

[27] A.H.S. Martinelli, K. Kappaun, M. Postal, A.R. Piovesan, F. Stanisçuaski, D.R. Demartini, R. Ligabue-Braun, H. Verli, C.A. Dal Belo, C.G. Moreira de Almeida, C. Follmer,

C.R. Carlini, G. Pasquali, Biochimica et Biophysica Acta - General Subjects 1840 (2014) 935-944.

[28] F. Staniscuaski, V.T. Brugge, C.R. Carlini, I. Orchard, J Insect Physiol 55 (2009) 255-263.

[29] P.R. Barros, H. Stassen, M.S. Freitas, C.R. Carlini, M.A.C. Nascimento, C. Follmer, Biochim Biophys Acta-Proteins and Proteomics 1794 (2009) 1848-1854.

[30] F. Bontems, B. Gilquin, C. Roumestand, A. Menez, F. Toma, Biochemistry 31 (1992) 7756-7764.

[31] R.L. Fahrner, T. Dieckmann, S.S.L. Harwig, R.I. Lehrer, D. Eisenberg, J. Feigon, Chem Biol 3 (1996) 543-550.

[32] A. Balasubramanian, K. Ponnuraj, J Mol Biol 400 (2010) 274-283.

[33] A.R. Piovesan, Urease de Canavalia ensiformis e peptideos derivados: Interação com membrane lipídica e formação de canais iônicos. , Graduate Program in Cellular and Molecular Biology, Universidade Federal do Rio Grande do Sul, Porto Alegre, RS, Brazil, 2013.

[34] J.L. Schwartz, L. Garneau, D. Savaria, L. Masson, R. Brousseau, E. Rousseau, J Membr Biol 132 (1993) 53-62.

[35] P. Muller, D.O. Rudin, H.T. Tein, W.C. Wescott, J Phys Chem 67 (1963) 534-535.

[36] B. Hille, Ionic Channels of Excitable Membranes, Sinauer Associates, Sunderland, MA, 2001.

[37] C. Zeilinger, M. Steffens, H.A. Kolb, Biochim Biophys Acta 1720 (2005) 35-43.

[38] V. Kruger, M. Deckers, M. Hildenbeutel, M. van der Laan, M. Hellmers, C. Dreker, M. Preuss, J.M. Herrmann, P. Rehling, R. Wagner, M. Meinecke, J Biol Chem 287 (2012) 33314-33326.

[39] C.J. Jeffery, Mol Biosyst 5 (2009) 345-350.

[40] J.L. Schwartz, R. Laprade, in: J.F. Charles, A. Delécluse, C. Nielsen-Leroux (Eds.), Entomopathogenic Bacteria: from Laboratory to Field Application. , Kluwer Associate Publishing, Norwell, MA, USA, 2000, pp. 199-218.

[41] O. Peyronnet, V. Vachon, J.L. Schwartz, R. Laprade, J Membr Biol 184 (2001) 45-54.

[42] A.A. Sobko, T.I. Rokitskaya, E.A. Kotova, Biochim Biophys Acta-Biomembranes 1788 (2009) 1962-1966.

[43] M.W. Parker, S.C. Feil, Prog Biophys Mol Biol 88 (2005) 91-142.

[44] T. Puntheeranurak, P. Uawithya, L. Potvin, C. Angsuthanasombat, J.L. Schwartz, Mol Membr Biol 21 (2004) 67-74.

[45] B. Stec, Cell Mol Life Sci 63 (2006) 1370-1385.

[46] P. Hughes, E. Dennis, M. Whitecross, D. Llewellyn, P. Gage, J Biol Chem 275 (2000) 823-827.

[47] P. Llanos, M. Henriquez, J. Minic, K. Elmorjani, D. Marion, G. Riquelme, J. Molgo, E. Benoit, Eur Biophys J Biophy 33 (2004) 283-284.

[48] A.M. Aerts, I. Francois, B.P.A. Cammue, K. Thevissen, Cell Mol Life Sci 65 (2008) 2069-2079.

[49] E.O. Mello, S.F.F. Ribeiro, A.O. Carvalho, I.S. Santos, M. Da Cunha, C. Santa-Catarina, V.M. Gomes, Curr Microbiol 62 (2011) 1209-1217.

[50] K. Thevissen, F.R.G. Terras, W.F. Broekaert, App Environ Microbiol 65 (1999) 5451-5458.

[51] O. Peyronnet, B. Nieman, F. Genereux, V. Vachon, R. Laprade, J.L. Schwartz, Biochim Biophys Acta-Biomembranes 1567 (2002) 113-122.

[52] C. Follmer, C.R. Carlini, Arch Biochem Biophys 435 (2005) 15-20.

[53] I. Iacovache, M.T. Degiacomi, F.G. van der Goot, Comprehensive Biophysics, Elsevier B. V., Lausanne, Switzerland, 2012, pp. 164-188.

[54] N. Groulx, H. McGuire, R. Laprade, J.-L. Schwartz, R. Blunck, J Biol Chem 286 (2011) 42274-42282.

[55] V. Vachon, R. Laprade, J.-L. Schwartz, J Invertebr Pathol 111 (2012) 1-12.

[56] V. Teixeira, M.J. Feio, M. Bastos, Prog Lipid Res 51 (2012) 149-177.

[57] C.R. Carlini, J.A. Guimaraes, Toxicon 29 (1991) 791-806.

[58] S.L. Griffiths, R.A. Finkelstein, D.R. Critchley, Biochem J 238 (1986) 313-322.

[59] D.E. Saslowsky, Y.M. Welscher, D.J. Chinnapen, J.S. Wagner, J. Wan, E. Kern, W.I. Lencer, J Biol Chem 288 (2013) 25804-25809.

[60] J.S. Griffitts, S.M. Haslam, T.L. Yang, S.F. Garczynski, B. Mulloy, H. Morris, P.S. Cremer, A. Dell, M.J. Adang, R.V. Aroian, Science 307 (2005) 922-925.

[61] A. Balasubramanian, N. Balaji, N. Gautham, K. Ponnuraj, Mol Simul 39 (2012) 357-366.

[62] N. Rojko, K.C. Kristan, G. Viero, E. Zerovnik, P. Macek, M. Dalla Serra, G. Anderluh, Journal of Biological Chemistry 288 (2013) 23704-23715.

[63] G. Corzo, E. Villegas, F. Gomez-Lagunas, L.D. Possani, O.S. Belokoneva, T. Nakajima, J Biol Chem 277 (2002) 23627-23637.

[64] Z.I. Andreeva-Kovalevskaya, A.S. Solonin, E.V. Sineva, V.I. Ternovsky, Biochemistry-Moscow 73 (2008) 1473-+.

[65] T. Schwede, J. Kopp, N. Guex, M.C. Peitsch, Nucleic Acids Res 31 (2003) 3381-3385.

Discussão geral

Neste trabalho foram apresentados resultados que demonstram a interação da JBU, Jbtx e peptídeos derivados com membranas lipídicas, através do uso de dois sistemas amplamente difundidos, os modelos de permeabilização de lipossomos e o modelo de *planar lipid bilayer*.

Estudos prévios já haviam demonstrado que tanto JBU quanto Jbtx atuam sobre membranas de células eucarióticas, de mamíferos, insetos e fungos, levando à uma diversidade de efeitos. Mutantes do Jbtx, com deleção de regiões específicas da molécula, mantiveram a capacidade de interação com lipossomos e outras atividades biológicas apresentadas tanto pelo peptídeo e pela JBU. Este achado sugere que esta região da JBU apresenta mais do que um motivo estrutural que confere atividade biológica, e que estas se sobrepõem (Martinelli et al, 2013) (anexo 1). Evolutivamente, isso seria vantajoso para a planta produtora de urease, dificultando que a proteína perdesse suas funções (pelo menos, inseticida e antifúngica) ao acumular mutações.

A ligação de JBU, Jbtx e derivados em vesículas lipídicas se dá mesmo na ausência de receptores de membrana, indicando que há interação destas proteínas diretamente com os fosfolipídeos, podendo formar poros e canais inônicos. Martinelli e colaboradores apresentaram o perfil de hidrofobicidade de Jbtx, sendo possível verificar que na região N terminal há 22 % de resíduos hidrofóbicos, e na região C terminal, 26 % (Martinelli et al, 2013) (anexo 1). Valores próximos a esses são encontrados em outras toxinas que interagem com membranas, como a neurotoxina botulínica (Kamata et al, 2000) e a toxina epidermolítica (Eriksson et al, 1989), com 33 % e 28 % de seus resíduos compreendendo as suas regiões hidrofóbicas, respectivamente.

A evidência que estas moléculas são capazes de se inserir em membranas lipídicas e ter função de canal iônico, juntamente com dados anteriores mostrando a ação convulsivante e liberadora de neurotransmissores da CNTX (e da JBU, se dada por via endovenosa em camundongos) (Carlini et al, 1984; Barja-Fidalgo et al, 1991), e os efeitos dessas proteínas e do Jbtx em insetos (Mulinari et al, 2007; Stanisçuaski e Carlini, 2012), sugere que estes efeitos neurotóxicos podem ser decorrentes de mecanismos que começaram agora ser esclarecidos. Por exemplo, estudos preliminares com culturas de hipocampo ratos neonatos indicam que, em doses nanomolares, tanto a JBU como o Jbtx induzem um aumento da frequência dos potenciais de ação espontâneos, sugerindo uma modulação da atividade dos canais de sódio.

Além disso, a JBU aumenta consideravelmente o influxo de cálcio nessas células em cultura, por mecanismos que ainda precisam ser esclarecidos (dados não publicados).

A interferência da CNTX nos fluxos e níveis intracelulares de cálcio já havia sido demonstrada anteriormente. Em vesículas de retículo sarcoplasmático de músculo esquelético de coelho, a CNTX induz uma diminuição dose-dependente no transporte de cálcio para o interior das vesículas, através do desacoplamento do transporte de Ca^{2+} pela $Mg^{2+}Ca^{2+}$.ATPase (Alves et al, 1992); a hidrólise de ATP durante o ciclo catalítico da $Mg^{2+}Ca^{2+}$.ATPase promove o aumento das concentrações citoplasmáticas deste íon em vesículas invertidas (inside-out) (Alves et al, 1992). Em plaquetas ativadas por CNTX, ocorre um influxo de cálcio do meio extracelular, por meio de canais voltagem-dependentes, sem haver formação de inositol trifosfato ou mobilização de reservas intracelulares de cálcio (Ghazaleh et al, 1997). Esse fenômeno também foi verificado em plaquetas ativadas por outras ureases (Olivera-Severo et al, 2006, Wassermann et al, 2010). A elevação dos níveis intracelulares de Ca^{2+} , decorrente desse influxo, poderia desencadear a exocitose dos grânulos densos plaquetários promovida por essas proteínas, ou ainda a exocitose de vesículas contendo neurotransmissores, como verificado para a CNTX (Barja-Fidalgo et al, 1991).

Em *R. prolixus*, a neurotoxicidade da JBU e do Jbtx é caracterizada por movimentos descoordenados das antenas e membros e, em doses sub-letais, paralisia-reversível. Observou-se ainda em preparações da junção neuromuscular de baratas que, o Jbtx, induz em doses de microgramas, a redução da tensão de repouso do músculo coxal, bem como da amplitude da força de contração muscular, provavelmente inferindo nos receptores N-metil-D-aspartato (NMDAR) e/ou GABA, prevalentes nas sinápses periféricas de insetos (Dal-Belo et, al 2012). Também há evidências de que o Jbtx interfere na atividade da óxido nítrico sintatase no CNS de insetos, reduzindo drasticamente os níveis de NO nesse tecido, tanto após tratamento *in vivo* como *ex vivo*.

Por outro lado, ainda é necessário determinar de que maneira a JBU e o Jbtx desempenham os fenômenos fisiopatológicos sobre os diferentes sistemas neuronais. Nesse aspecto, sabe-se que, além de provelmente se ligar diretamente à membrana, a JBU (mas não o Jbtx) modula vias de signalização envolvendo eicosanóides, tanto em mamíferos (Carlini e Polacco, 2008) quanto em insetos (Stanisçuaski e Carlini, 2012); já o Jbtx parece infererir com nucleotídeos cíclicos (Stanisçuaski et al, 2009).

Em resumo, a capacidade da JBU, do Jbtx e de seus mutantes em formarem canais, sugere que essa atividade seja uma das etapas concomitantes ao complexo mecanismo de ação dessas proteínas, e que ainda não havia sido identificada, e que pode ser crítica para diversos dos efeitos biológicos descritos para essas moléculas, em particular, a sua neurotoxicidade.

Conclusões

Os resultados apresentados nos Capílulos 1 e 2 dessa tese nos permitiram concluir que:

- A JBU (0.027 μM) é capaz de se ligar a lipossomos feitos de DOPG causando em torno de 40 % de extravasamento de CF, porém em doses tão baixas quanto 0.0086 μM já é possível detectar extravasamento de CF;
- O Jbtx, Jbtx N-ter, Jbtx C-ter e Jbtx Δ-β, em concentrações entre 0,4 e 0,8 μM, interagem com lipossomos compostos por PA, causando mais de 80 % extravasamento de carboxifluorescína.
- A presença de 100 mM de NaCl no tampão do ensaio reduz, mas não abole, a atividade dos peptídeos e da JBU de se ligarem aos lipossomos;
- A desnaturação através de fervura por 10 minutos praticamente anula o efeito de Jbtx N-ter e Jbtx C-ter, mostrando que na ausência de estrutura terciária as moléculas não interagem com os lipossomos. O Jbtx ainda mantém uma atividade residual, mesmo após fervura.
- JBU (9.2 nM) forma canais iônicos em membranas compostas de PE:PC:Ch (7:2:1); apresenta um canal majoritário com propriedades retificadoras cuja condutância em voltagens positivas é de 79.15 ± 8.05 pS e em voltagens negativas é de 43.95 ± 3.10 pS. Forma também dois canais menores com condutâncias lineares, 29.65 ± 5.34 pS e 10.52 ± 0.22 pS, que podem ser considerados sub-estados do canal majoritário. Os canais apresentam seletividade para cátions.
- Em concentrações duas ordens de grandeza maior, o Jbtx (1.32 μM) também forma canais iônicos em membranas compostas de PE:PC:Ch (7:2:1) ou PE:POPG (4:1). Diferentemente de JBU, o canal majoritário possui propriedades lineares, com a mesma condutância em voltagens negativas e positivas. Em membranas neutras, o canal majoritário tem condutância de 38.63 ± 4.48 pS e em negativas, de 45.52 ± 1.91 pS. O Jbtx também forma um canal de menor condutância, com 7.61 ± 1.15 pS em membranas neutras, e 18.2 ± 2.6 pS em membranas negativas. Os canais são altamente seletivos para cátion.
- Jbtx N-ter (2.55 μM) forma canais iônicos em membranas compostas de PE:PC:Ch (7:2:1). O canal majoritário possui propriedades lineares, com a mesma condutância em voltagens negativas e positivas: 35.75 ± 1.15 pS. Também forma um canal de menor condutância, com 8.87 ± 1.27 pS. Os canais são voltagem-dependentes,

mostrando maior probabilidade de abertura em voltagens negativas. Os canais são altamente seletivos para cátion.

- Jbtx C-ter (2.28 μM) também forma canais em membranas compostas de PE:PC:Ch (7:2:1). O canal majoritário possui propriedades lineares com valor de condutância igual a 32.10 ± 0.05 pS. Também forma um canal de menor condutância, com 9.30 ± 0.024 pS. Os canais são seletivos para cátion.
- Jbtx Δ-β (1.56 μM) igualmente formou canais em membrana composta de PE:PC:Ch (7:2:1). O canal majoritário possui propriedades lineares com valor de condutância igual a 38.95 ± 3.97 pS. O canal menor tem condutância igual a 10.06 ± 0.88 pS. Os canais formados por esse mutante também são seletivos para cátion.
- A inserção dos canais formados pela JBU se mostrou mais difícil comparado à dos peptídeos, provavelmente por ser esta uma molécula com aproximadamente 10 vezes a massa molar do Jbtx.

Bibliografia

Alves EW, Ferreira AT, Ferreira CT, Carlini CR. Effects of canatoxin on the Ca(2+)-ATPase of sarcoplasmic reticulum membranes. Toxicon. 1992;30:1411-8.

Amiche M, Galanth C. Dermaseptins as models for the elucidation of membrane-acting helical amphipathic antimicrobial peptides. Current Pharm Biotechnol. 2011;12:1184-93.

Bakás L, Chanturiya A, Herlax V, Zimmerberg J. Paradoxical lipid dependence of pores formed by the *Escherichia coli* alpha-hemolysin in planar phospholipid bilayer membranes. Biophys J. 2006; 91(10): 3748-55.

Balasubramanian A, Balaji N, Gautham N, Ponnuraj K. Molecular dynamics simulation and molecular modelling studies on the insecticidal domain from jack bean urease. Mol Simul. 2012;- 39:357-66.

Balasubramanian A, Ponnuraj K. Crystal structure of the first plant urease from jack bean: 83 years of journey from its first crystal to molecular structure. J Mol Biol. 2010;400:274-83.

Barja-Fidalgo C, Guimaraes JA, Carlini CR. Lipoxygenase-mediated secretory effect of canatoxin, the toxic protein from *Canavalia ensiformis* seeds. Toxicon. 1991a; 29: 453–60.

Barja-Fidalgo, C., Guimarães, J.A., Carlini, C.R. Canatoxin, a plant protein, induces insulin release from isolated pancreatic islets. Endocrinology. 1991b; 128, 675-679.

Barros PR, Stassen H, Freitas MS, Carlini CR, Nascimento MAC, Follmer C. Membrane-disruptive properties of the bioinsecticide Jaburetox-2Ec: Implications to the mechanism of the action of insecticidal peptides derived from ureases. Biochim Biophys Acta-Proteins and Proteomics. 2009;1794:1848-54.

Becker-Ritt AB, Carlini CR. Fungitoxic and insecticidal plant polypeptides. Biopolymers. 2012;98:367-84.

Becker-Ritt AB, Martinelli AH, Mitidieri S, Feder V, Wassermann GE, Santi L, et al. Antifungal activity of plant and bacterial ureases. Toxicon. 2007;50:971-83.

Benini S, Rypniewski WR, Wilson KS, Miletti S, Ciurli S, Mangani S. A new proposal for urease mechanism based on the crystal structures of the native and inhibited enzyme from *Bacillus pasteurii*: why urea hydrolysis costs two nickels. Structure. 1999; 7(2): 205-16.

Benjamin CF, Carlini CR, Barja-Fidalgo C. Pharmacological characterization of rat paw edema induced by canatoxin, the toxic protein from *Canavalia ensiformis* (jack bean) seeds. Toxicon. 1992;30:879-85.

Bischofberger M, Iacovache I, van der Goot FG. Pathogenic pore-forming proteins: function and host response. Cell Host Microbe. 2012; 12(3): 266-75.

Bohlmann H, Clausen S, Behnke S, Giese H, Hiller C, Reimannphilipp U, et al. Leaf-specific thionins of barley - a novel class of cell-wall proteins toxic to plant-pathogenic fungi and possibly involved in the defense-mechanism of plants. Embo J. 1988;7:1559-65.

Bontems F, Gilquin B, Roumestand C, Menez A, Toma F. Analysis of side-chain organization on a refined model of charybdotoxin - structural and functional implications. Biochemistry. 1992;31:7756-64.

Bradford M.M.. A rapid and sensitive method for the quantitation of microgram quantities of protein utilizing the principle of protein-dye binding. Anal Biochem. 1976; 72: 248–254

Butko P. Cytolytic toxin Cyt1A and its mechanism of membrane damage: data and hypotheses. Appl. Environ. Microbiol. 2003; 69(5): 2415.

Callahan, B.P., Y. Yuan, and R. Wolfenden. The burden borne by urease. J. Am. Chem. Soc. 2005; 127: 10828–10829.

Campos MM, Carlini CR, Guimarães JA, Marques-Silva VM, Rumjanek VM. Effect of canatoxin on cell cultures. Cell Biol Int Rep. 1991; 15(7): 581-94.

Carlini CR and Grossi-de-Sa MF. Plant toxic proteins with insecticidal properties. A review on their potentialities as bioinsecticides. Toxicon. 2002; 40: 1515–1539.

Carlini CR and Guimaraes JA. Isolation and characterization of a toxic protein from *Canavalia ensiformis* (jack bean) seeds, distinct from concanavalin A. Toxicon. 1981; 19: 667–75.

Carlini CR and Guimarães JA. Plant and microbial toxic proteins as hemilectins: emphasis on canatoxin. Toxicon 1991; 29: 791-806.

Carlini CR and Polacco JC. Toxic properties of urease. Crop Sci 2008; 48: 1665–72.

Carlini CR, Gomes CB, Guimarães JA, Markus RP, Sato H, Trolin G. Central nervous effects of the convulsant protein Canatoxin. Acta pharmacologica et toxicological**.** 1984; 54: 161-166.

Carlini CR, Guimaraes JA, Ribeiro JM. Platelet release reaction and aggregation induced by canatoxin, a convulsant protein: evidence for the involvement of the platelet lipoxygenase pathway. Br J Pharmacol. 1985;84:551-60.

Carlini CR, Guimaraes JA. Plant and microbial toxic proteins as hemilectins: emphasis on canatoxin. Toxicon. 1991;29:791-806.

Carlini CR, Oliveira AE, Azambuja P, Xavier-Filho J, Wells MA. Biological effects of canatoxin in different insect models: evidence for a proteolytic activation of the toxin by insect cathepsinlike enzymes. J Econ Entomol. 1997;90:340-8.

Carlini CR, Polacco JC. Toxic properties of urease. Crop Sci. 2008;48:1665-72.

Cascales E, Buchanan SK, Duché D, Kleanthous C, Lloubès R, Postle K, Riley M, Slatin S, Cavard D. Colicin biology. Microbiol Mol Biol Rev. 2007; 71(1): 158-229.

Castro-Faria-Neto HC, Cordeiro RS, Martins MA, Correia-Da-Silva AC, Bozza PT, Sousa MV, Morhy L. Enterolobin induces rat paw oedema independently of PAF-acether. Mem Inst Oswaldo Cruz. 1991; 86 Suppl 2: 129-31.

Chen RF and Knutson JR. Mechanism of fluorescence concentration quenching of carboxyfluorescein in liposomes: energy transfer to nonfluorescent dimers. Analytical Biochemistry. 1988; 72: 61-77

Christensen B, Fink J, Merrifield RB, Mauzerall D. Channel-forming properties of cecropins and related model compounds incorporated into planar lipid-membranes. P Natl Acad Sci USA. 1988;85:5072-76.

Ciardiello MA, Meleleo D, Saviano G, Crescenzo R, Carratore V, Camardella L, et al. Kissper, a kiwi fruit peptide with channel-like activity: Structural and functional features. J Pept Sci. 2008;14:742-54.

Clarke D, Griffin S, Beales L, Gelais CS, Burgess S, Harris M, Rowlands D. Evidence for the formation of a heptameric ion channel complex by the hepatitis C virus p7 protein in vitro. J Biol Chem. 2006; 281(48): 37057-68.

Dal Belo CA, Reder GM, Moreira de Almeida CG, Pinto PM, Carlini CR. Neuromuscular blockade induced by Jaburetox (a recombinant peptide derived from *Canavalia ensiformis* urease) at in vivo cockroach nerve-muscle preparations. In: Harvey A, Rowan E, editors. 1st Oxford World Symposium on Venoms 2012. p. Abstract.

Dasanayake D, Richaud M, Cyr N, Caballero-Franco C, Pittroff S, Finn RM, Ausió J, Luo W, Donnenberg MS, Jardim A. The N-terminal amphipathic region of the *Escherichia coli* type III secretion system protein EspD is required for membrane insertion and function. Mol Microbiol. 2011; 81(3): 734-50.

D'Avanzo N, McCusker EC, Powl AM, Miles AJ, Nichols CG, Wallace BA. Differential lipid dependence of the function of bacterial sodium channels. PLoS One. 2013; 8(4): 612-16.

Day PJ, Pinheiro TJ, Roberts LM, Lord JM. Binding of ricin A-chain to negatively charged phospholipid vesicles leads to protein structural changes and destabilizes the lipid bilayer. Biochemistry. 2002; 41(8): 2836-43.

Defferrari MS, Demartini DR, Marcelino TB, Pinto PM, Carlini CR. Insecticidal effect of *Canavalia ensiformis* major urease on nymphs of the milkweed bug *Oncopeltus fasciatus* and characterization of digestive peptidases. Insect Biochem Mol Biol. 2011;41:388-99.

Dernick G, Toledo GA, and Lindau M. The Patch Amperometry Technique: Design of a Method to Study Exocytosis of Single Vesicles. Electrochemical Methods for Neuroscience. 2007

Dixon NE, Gazzola TC, blakeley RL, Zermer B. Letter: Jack bean urease (EC 3.5.1.5). A metalloenzyme. A simple biological role for nickel? J Am Chem Soc. 1975;97:4131-3.

Dixon NE, Riddles PW, Gazzola C, Blakeley RL, Zerner B. Jack bean urease (EC 3.5.1.5). II. The relationship between nickel, enzymatic activity, and the “abnormal” ultraviolet spectrum. The nickel content of jack beans. Can. J. Biochem. 1980; 58: 474–480.

Eriksson KO, Naidu AS, Kilar F, Wadstrom T, Hjerten S, Surface hydrophobicity and lectrophoretic mobilities of *Staphylococcal* exotoxins with special reference to toxic shock syndrome toxin-1. APMIS. 1989; 97: 1081-1087.

Fahrner RL, Dieckmann T, Harwig SSL, Lehrer RI, Eisenberg D, Feigon J. Solution structure of protegrin-1, a broad-spectrum antimicrobial peptide from porcine leukocytes. Chem Biol. 1996;3:543-50.

Félétou M, Vanhoutte PM. EDHF: an update. Clin Sci (Lond). 2009; 117(4): 139-55

Ferreira-DaSilva CT, Gombarovits ME, Masuda H, Oliveira CM, Carlini CR. Proteolytic activation of canatoxin, a plant toxic protein, by insect cathepsin-like enzymes. Arch Insect Biochem Physiol. 2000;44:162-71.

Follmer C and Carlini CR. Effect of chemical modification of histidines on the copper-induced oligomerization of jack bean urease (EC 3.5.1.5). Arch Biochem Biophys. 2005; 435(1): 15–20

Follmer C, Barcellos GB, Zingali RB, Machado OL, Alves EW, Barja-Fidalgo C, et al. Canatoxin, a toxic protein from jack beans (*Canavalia ensiformis*), is a variant form of urease (EC 3.5.1.5): biological effects of urease independent of its ureolytic activity. Biochem J. 2001;360:217-24.

Follmer C, Carlini CR. Effect of chemical modification of histidines on the copper-induced oligomerization of jack bean urease (EC 3.5.1.5). Arch Biochem Biophys. 2005;435:15-20.

Follmer C, Real-Guerra R, Wasserman GE, Olivera-Severo D, Carlini CR. Jackbean, soybean and *Bacillus pasteurii* ureases: biological effects unrelated to ureolytic activity. Eur J Biochem. 2004a;271:1357-63.

Follmer C, Wassermann GE, Carlini CR. Separation of jack bean (*Canavalia ensiformis*) urease isoforms by immobilized metal affinity chromatography and characterization of insecticidal properties unrelated to ureolytic activity. Plant Sci. 2004b;167:241-46.

Follmer C. Insights into the role and structure of plant ureases. Phytochemistry. 2008;69:18-28.

Fontes W, Sousa MV, Aragao JB, Morhy L. Determination of the amino acid sequence of the plant cytolysin enterolobin. Arch Biochem Biophys. 1997;347:201-07.

Ghazaleh FA, Francischetti IM, Gombarovits ME, Carlini CR. Stimulation of calcium influx and platelet activation by canatoxin: methoxyverapamil inhibition and downregulation by cGMP. Arch Biochem Biophys. 1997;339:362-7.

Gidalevitz D, Ishitsuka YJ, Muresan AS, Konovalov O, Waring AJ, Lehrer RI, et al. Interaction of antimicrobial peptide protegrin with biomembranes. P Natl Acad Sci USA. 2003;100:6302-07.

Gombarovits MC. Peptídeos Entomotóxicos gerados a partir da CNTX: obtenção, isolamento, propriedades biológicas e caracterização físico-química. 1999. Dissertação de Mestrado. Universidade Federal do Rio de Janeiro, Brasil

Grassi-Kassisse DM, Ribeiro-DaSilva G. Canatoxin triggers histamine secretion from rat peritoneal mast cells. Agents Actions. 1992; 37(3-4): 204-9.

Gratia A**.** Sur un remarquable exemple d'antagonisme entre deux souches de colibacille. C. R. Soc. Biol. (Paris) 1925; 93**:** 1040-1041.

Griffiths SL, Finkelstein RA, Critchley DR. Characterization of the receptor for cholera-toxin and *Escherichia-coli* heat-labile toxin in rabbit intestinal brush-borders. Biochem J. 1986;238:313-22.

Griffitts JS, Haslam SM, Yang TL, Garczynski SF, Mulloy B, Morris H, et al. Glycolipids as receptors for *Bacillus thuringiensi*s crystal toxin. Science. 2005;307:922-25.

Grochulski P, Masson L, Borisova S, Pusztaicarey M, Schwartz JL, Brousseau R, et al. *Bacillus-thuringiensis* Cryla(a) insecticidal toxin - crystal-structure and channel formation. J Mol Biol. 1995;254:447-64.

Groulx N, McGuire H, Laprade R, Schwartz J-L, Blunck R. Single molecule fluorescence study of the *Bacillus thuringiensis* toxin Cry1Aa reveals tetramerization. J Biol Chem. 2011;286:42274-82.

Heiss EH, Schilder YD, Dirsch VM. Chronic treatment with resveratrol induces redox stress- and ataxia telangiectasia-mutated (ATM)-dependent senescence in p53-positive cancer cells. J Biol Chem. 2007; 282(37): 26759-66.

Hille B. Ionic Channels of Excitable Membranes. Sunderland, MA: Sinauer Associates; 2001.

Hope MJ, Bally MB, Webb G, Cullis PR, Production of large unilamellar vesicles by a rapid extrusion procedure. Characterization of size distribution, trapped volume and ability to maintain a membrane potential, Biochim. Biophys. Acta. 1985; 812: 55–65.

Hughes P, Dennis E, Whitecross M, Llewellyn D, Gage P. The cytotoxic plant protein, beta-purothionin, forms ion channels in lipid membranes. J Biol Chem. 2000;275:823-27.

Hyland C, Vuillard L, Hughes C, Koronakis V. Membrane interaction of *Escherichia coli* hemolysin: flotation and insertion-dependent labeling by phospholipid vesicles. J Bacteriol. 2001; 183(18): 5364-70.

Iacovache I, Degiacomi MT, van der Goot FG. Pore forming toxins. Comprehensive Biophysics. Lausanne, Switzerland: Elsevier B. V.; 2012. p. 164-88.

Jang H, Ma B, Woolf TB, Nussinov R. Interaction of protegrin-1 with lipid bilayers: Membrane thinning effect. Biophys J. 2006;91:2848-59.

Jeffery CJ. Moonlighting proteins-an update. Mol Biosyst. 2009;5:345-50.

Kamata Y, Tahara R, Kozaki S. Difference in hydrophobicity between botulinum type B activated and non-activated, Toxicon. 2000; 38: 1247-1251.

Kendall DA, MacDonald RC. A fluorescence assay to monitor vesicle fusion and lysis, J. Biol. Chem. 1982; 257: 13892–13895.

Ketchem RR, Hu W, Cross TA. High-resolution conformation of gramicidin A in a lipid bilayer by solid-state NMR. Science. 1993; 261(5127): 1457-60.

Krajewska B. Ureases I. Functional, catalytic and kinetic properties: A review. J Mol Catal B-Enzym. 2009;59:9-21.

Ligabue-Braun R, Andreis FC, Verli H, Carlini CR. 3-to-1: unraveling structural transitions in ureases. Naturwissenschaften. 2013; 100: 459-67

Llanos P, Henriquez M, Minic J, Elmorjani K, Marion D, Riquelme G, et al. Neuronal and muscular alterations caused by two wheat endosperm proteins, puroindoline-a and alpha1-purothionin, are due to ion pore formation. Eur Biophys J. 2004;33:283-84.

Lopez CF, Nielsen SO, Ensing B, Moore PB, and Klein ML. Structure and dynamics of model pore insertion into a membrane. Biophys J. 2005; 88(5): 3083–3094.

Lorence A, Darszon A, Díaz C, Liévano A, Quintero R, Bravo A. d- Endotoxins induce cation channels in *Spodoptera frugiperda* brush border membranes in suspension and in planar lipid bilayers. FEBS Lett. 1995; 360: 217–222.

Ludtke SJ, He K, Heller WT, Harroun TA, Yang L, Huang HW. Membrane pores induced by magainin. Biochemistry. 1996; 35(43): 13723-8.

Martinell AHS. Jaburetox, Peptídeo Tóxico Derivado da Urease: Estudos de Estrutura e Função. [thesis] Porto Alegre, RS, Brazil: Universidade Federal do Rio Grande do Sul; 2012.

Martinelli AHS, Kappaun K, Postal M, Piovesan AR, Stanisçuaski F, Demartini DR, et al. Structure-function studies on Jaburetox, a recombinant insecticidal and antifungal peptide derived from jack bean (*Canavalia ensiformis*) urease. Unpublished results.

Martinelli AHS, Piovesan A, Kappaun K, Follmer C, Schwartz JL, Carlini CR. Membrane-disturbing properties of urease and derived recombinant peptides. Toxicon. 2012;60:178-78.

Menegassi A, Wassermann GE, Olivera-Severo D, Becker-Ritt AB, Martinelli AHS, Feder V, Carlini CR. Urease from cotton (*Gossypium hirsutum*) seeds: Isolation, physicochemical characterization, and antifungal properties of the protein. J. Agric. Food Chem. 2008; 56: 4399–4405.

Micheletto YMS, Moro CF, Carlini CR, da Silveira NP. Study of influence of jack bean urease in the dimensions of human platelet mimetic liposomes. FBPOL 3rd French Brazilian Meeting on Polymers. 2011. (Abstract)

Miyazaki Y, Aoki M, Yano Y, Matsuzaki K. Interaction of antimicrobial peptide magainin 2 with gangliosides as a target for human cell binding. Biochemistry. 2012; 51(51): 10229-35.

Mobley HL, Island MD, Hausinger RP. Molecular biology of microbial ureases. Microbiol Rev. 1995; 59(3): 451-80.

Mobley HLT & Hausinger R P. Microbial ureases: significance, regulation and molecular characterization. Microbiol. Rev. 1989; 53: 85–103.

Mor A, Nicolas P. The NH2-terminal alpha-helical domain 1-18 of dermaseptin is responsible for antimicrobial activity. J Biol Chem. 1994;269:1934-39.

Moro CF. Comportamento do peptídeo entomotóxico Jaburetox-2Ec em solução e a sua interação com lipossomas miméticos de plaquetas humanas. [dissertation]. Porto Alegre, RS, Brazil: Universidade Federal do Rio Grande do Sul; 2010.

Moro, C. F. (2007). Influence of chemical variables on the aggregation of the peptide insecticide derived from the urease from Jack bean (*Canavalia ensiformis*) for spectroscopy of light scattering. Porto Alegre: UFRGS, Conclusion Course (BS Chemistry), Institute Chemistry, Federal University of Rio Grande do Sul.

Mosmann T. Rapid colorimetric assay for cellular growth and survival: application to proliferation and cytotoxicity assays. J Immunol Methods. 1983; 65(1-2): 55-63.

Mueller M, Grauschopf U, Maier T, Glockshuber R, Ban N. The structure of a cytolytic alpha-helical toxin pore reveals its assembly mechanism. Nature. 2009 Jun 4;459(7247):726-30.

Mulinari F, Staniscuaski F, Bertholdo-Vargas LR, Postal M, Oliveira-Neto OB, Rigden DJ, et al. Jaburetox-2Ec: an insecticidal peptide derived from an isoform of urease from the plant *Canavalia ensiformis*. Peptides. 2007;28:2042-50.

Nguyen TH, Rao NZ, Schroeder WM, Moore PB. Coarse-grained molecular dynamics of tetrameric transmembrane peptide bundles within a lipid bilayer. Chem Phys Lipids. 2010; 163(6): 530-7.

O'Connell AM, Koeppe RE 2nd, Andersen OS. Kinetics of gramicidin channel formation in lipid bilayers: transmembrane monomer association. Science. 1990; 250(4985): 1256-9.

Oliveira AE, Gomes VM, Sales MP, Fernandes KVS, Carlini CR, Xavier-Filho J. The toxicity of Jack bean [*Canavalia ensiformis* (L.) DC.] Canatoxin to plant pathogenic fungi. Rev. Bras. Biol. 1999; 59: 59–62.

Olivera-Severo D, Wassermann GE, Carlini CR. *Bacillus pasteurii* urease shares with plant ureases the ability to induce aggregation of blood platelets. Arch Biochem Biophys. 2006;452:149-55.

Oscarsson J, Mizunoe Y, Li L, Lai XH, Wieslander A, Uhlin BE. Molecular analysis of the cytolytic protein ClyA (SheA) from *Escherichia coli*. Mol Microbiol. 1999; 32(6): 1226-38.

Parker MW, Feil SC. Pore-forming protein toxins: from structure to function. Prog Biophys Mol Biol. 2005;88:91-142.

Peyronnet O, Nieman B, Genereux F, Vachon V, Laprade R, Schwartz JL. Estimation of the radius of the pores formed by the *Bacillus thuringiensis* Cry1C delta-endotoxin in planar lipid bilayers. Biochim Biophys Acta-Biomembranes. 2002;1567:113-22.

Peyronnet O, Vachon V, Schwartz JL, Laprade R. Ion channels induced in planar lipid bilayers by the *Bacillus thuringiensis* toxin Cry1Aa in the presence of gypsy moth (*Lymantria dispar*) brush border membrane. J Membr Biol. 2001;184:45-54.

Piovesan AR, Staniscuaski F, Marco-Salvadori J, Real-Guerra R, Defferrari MS, Carlini CR. Stage-specific gut proteinases of the cotton stainer bug *Dysdercus peruvianus*: role in the release of entomotoxic peptides from *Canavalia ensiformis* urease. Insect Biochem Mol Biol. 2008;38:1023-32.

Piovesan AR. Urease de *Canavalia ensiformis*: processamento diferencial por ninfas e adultos de Dysdercus peruvianus e formação de canal in vitro. [dissertation] Porto Alegre, RS: Universidade Federal do Rio Grande do Sul; 2009.

Postal M, Martinelli AH, Becker-Ritt AB, Ligabue-Braun R, Demartini DR, Ribeiro SF, et al. Antifungal properties of *Canavalia ensiformis* urease and derived peptides. Peptides. 2012;38:22-32.

Puntheeranurak T, Uawithya P, Potvin L, Angsuthanasombat C, Schwartz JL. Ion channels formed in planar lipid bilayers by the dipteran-specific Cry4B *Bacillus thuringiensis* toxin and its alpha 1-alpha 5 fragment. Mol Membr Biol. 2004;21:67-74.

Real-Guerra, R, Carlini, CR, Stanisçuaski, F. Role of lysine and acidic amino acid residues on the insecticidal activity of Jackbean urease. Toxicon. 2013; 71: 1–8

Rojko N, Kristan KC, Viero G, Zerovnik E, Macek P, Dalla Serra M, et al. Membrane damage by an α-helical pore forming protein equinatoxin ii proceeds through succesion of ordered steps. J Biol Chem. 2013;[Epub ahead of print], Jun 26.

Saslowsky DE, Welscher YM, Chinnapen DJ, Wagner JS, Wan J, Kern E, et al. Ganglioside GM1-mediated transcytosis of cholera toxin bypasses the retrograde pathway and depends on the structure of the ceramide domain. J Biol Chem. 2013;[Epub ahead of print] Jul 24.

Schwartz JL, Garneau L, Savaria D, Masson L, Brousseau R, Rousseau E. Lepidopteran-specific crystal toxins from *Bacillus-thuringiensis* form cation-selective and anion-selective channels in planar lipid bilayers. J Membr Biol. 1993;132:53-62.

Schwartz JL, Laprade R. Membrane permeabilisation by Bacillus thuringiensis toxins: protein insertion and pore formation. In: Charles JF, Delécluse A, Nielsen-Leroux C, editors. Entomopathogenic bacteria: from laboratory to field application Norwell, MA, USA: Kluwer Associate Publishing; 2000. p. 199-218.

Schwartz JL, Lu YJ, Söhnlein P, Brousseau R, Laprade R, Masson L, Adang MJ. Ion channels formed in planar lipid bilayers by *Bacillus thuringiensis* toxins in the presence of *Manduca sexta* midgut receptors. FEBS Lett. 1997; 412(2): 270-6.

Schwede T, Kopp J, Guex N, Peitsch MC. SWISS-MODEL: an automated protein homology-modeling server. Nucleic Acids Res. 2003;31:3381-85.

Shenkarev ZO, Balandin SV, Trunov KI, Paramonov AS, Sukhanov SV, Barsukov LI, et al. Molecular mechanism of action of beta-hairpin antimicrobial peptide arenicin: oligomeric structure in dodecylphosphocholine micelles and pore formation in planar lipid bilayers. Biochemistry. 2011;50:6255-65.

Silvestro L, Axelsen PH. Membrane-induced folding of cecropin A. Biophys J. 2000;79:1465-77.

Silvestro L, Axelsen PH. The structure of cecropin A bound to monolayer and bilayer membranes by infrared analysis: A model of peptide adsorption and insertion. Biophys J. 1999;76:A64-A64.

Silvestro L, Gupta K, Weiser JN, Axelsen PH. The concentration-dependent membrane activity of cecropin A. Biochemistry. 1999; 38(12): 3850.

Sirko A, Brodzik R. Plant ureases: Roles and regulation. Acta Biochim Pol. 2000;47:1189-95.

Sitaram N, Nagaraj R. Interaction of antimicrobial peptides with biological and model membranes: structural and charge requirements for activity. Biochim Biophys Acta-Biomembranes. 1999;1462:29-54.

Sobko AA, Rokitskaya TI, Kotova EA. Histidine 440 controls the opening of colicin E1 channels in a lipid-dependent manner. Biochim Biophys Acta-Biomembranes. 2009;1788:1962-66.

Sousa MV, Richardson M, Fontes W, Morhy L. Homology between the seed cytolysin enterolobin and bacterial aerolysins. J Protein Chem. 1994; 13(8): 659-67.

Staniscuaski F, Brugge VT, Carlini CR, Orchard I. In vitro effect of *Canavalia ensiformis* urease and the derived peptide Jaburetox-2Ec on Rhodnius prolixus Malpighian tubules. J Insect Physiol. 2009;55:255-63.

Staniscuaski F, Carlini CR. Plant ureases and related peptides: understanding their entomotoxic properties. Toxins. 2012;4:55-67.

Stanisçuaski F, Ferreira-Dasilva CT, Mulinari F, Pires-Alves M, Carlini CR. Insecticidal effects of canatoxin on the cotton stainer bug Dysdercus peruvianus (Hemiptera: Pyrrhocoridae). Toxicon. 2005; 45(6): 753-60.

Stec B. Plant thionins - the structural perspective. Cell Mol Life Sci. 2006;63:1370-85.

Steiner H, Hultmark D, Engström A, Bennich H, Boman HG. Sequence and specificity of two antibacterial proteins involved in insect immunity. Nature. 1981; 292(5820): 246-8.

Sumner JB. The isolation and crystallization of the enzyme urease. J Biol Chem. 1926;69:435-41.

Tamburrini M, Cerasuolo I, Carratore V, Stanziola AA, Zofra S, Romano L, et al. Kiwellin, a novel protein from kiwi fruit. Purification, biochemical characterization and identification as an allergen. Protein J. 2005;24:423-29.

Tang M, Hong M. Structure and mechanism of beta-hairpin antimicrobial peptides in lipid bilayers from solid-state NMR spectroscopy. Mol Biosyst. 2009; 5(4): 317-22.

Taveecharoenkool T, Angsuthanasombat C, Kanchanawarin C. Combined molecular dynamics and continuum solvent studies of the pre-pore Cry4Aa trimer suggest its stability in solution and how it may form pore. PMC Biophys. 2010; 3(1):10

Teixeira V, Feio MJ, Bastos M. Role of lipids in the interaction of antimicrobial peptides with membranes. Prog Lipid Res. 2012;51:149-77.

Teorell T. Transport processes and electrical phenomena in ionic membranes. Prog Biophys Biophys Chem. 1953;3:305-69.

Thevissen K, Terras FRG, Broekaert WF. Permeabilization of fungal membranes by plant defensins inhibits fungal growth. App Environ Microbiol. 1999;65:5451-58.

Uberti AF, Olivera-Severo D, Wassermann GE, Scopel-Guerra A, Moraes JA, Barcellos-de-Souza P, et al. Pro-inflammatory properties and neutrophil activation by *Helicobacter pylori* urease. Toxicon. 2013;69:240-9.

Vachon V, Laprade R, Schwartz J-L. Current models of the mode of action of *Bacillus thuringiensis* insecticidal crystal proteins: A critical review. J Invertebr Pathol. 2012;111:1-12.

Wassermann GE, Olivera-Severo D, Uberti AF, Carlini CR. *Helicobacter pylori* urease activates blood platelets through a lipoxygenase-mediated pathway. J Cell Mol Med. 2010;14:2025-34.

Wieloch W, Boguś MI, Ligęza M, Koszela-Piotrowska I, Szewczyk A. Coronatin-1 isolated from entomopathogenic fungus *Conidiobolus coronatus* kills *Galleria mellonella* hemocytes *in vitro* and forms potassium channels in planar lipid membrane. Toxicon. 2011; 58: 369–379

Wilmes M, Cammue BPA, Sahl H-G, Thevissen K. Antibiotic activities of host defense peptides: more to it than lipid bilayer perturbation. Nat Prod Rep. 2011;28:1350-58.

Yoneyama F, Shioya K, Zendo T, Nakayama J, Sonomoto K. Effect of a negatively charged lipid on membrane-lacticin Q interaction and resulting pore formation. Biosci Biotechnol Biochem. 2010; 74(1): 218-21.

Zerner B. Recent advances in the chemistry of an old enzyme, urease. Bioorg Chem. 1991;19:116-31.

ANEXOS

ANEXO 1 – Manuscrito: “Structure-function studies on Jaburetox, a recombinant insecticidal and antifungal peptide derived from jack bean (*Canavalia ensiformis*) urease”

Biochimica et Biophysica Acta 1840 (2014) 935–944

Contents lists available at ScienceDirect

Biochimica et Biophysica Acta

journal homepage: www.elsevier.com/locate/bbagen

Structure–function studies on jaburetox, a recombinant insecticidal peptide derived from jack bean (*Canavalia ensiformis*) urease

Anne H.S. Martinelli [a,b], Karine Kappaun [a], Rodrigo Ligabue-Braun [a], Marina S. Defferrari [a], Angela R. Piovesan [a], Fernanda Stanisçuaski [a,c], Diogo R. Demartini [a], Chariston A. Dal Belo [d], Carlos G.M. Almeida [d], Cristian Follmer [e], Hugo Verli [a,c], Celia R. Carlini [a,b,f,*,1], Giancarlo Pasquali [a,c,**,1]

[a] Graduate Program in Cellular and Molecular Biology, Center of Biotechnology, Universidade Federal do Rio Grande do Sul (UFRGS), Porto Alegre, RS, Brazil
[b] Department of Biophysics, Institute of Biosciences, UFRGS, Brazil
[c] Department of Molecular Biology and Biotechnology, UFRGS, Porto Alegre, RS, Brazil
[d] Interdisciplinary Centre of Biotechnological Research, Universidade Federal do Pampa, UNIPAMPA, São Gabriel, RS, Brazil
[e] Department Physical Chemistry, Institute of Chemistry, Universidade Federal do Rio de Janeiro, RJ, Brazil
[f] Instituto do Cérebro (InsCer), Pontifícia Universidade Católica do Rio Grande do Sul, Porto Alegre, RS, Brazil

ARTICLE INFO

Article history:
Received 12 May 2013
Received in revised form 2 November 2013
Accepted 6 November 2013
Available online 14 November 2013

Keywords:
Site-directed mutagenesis
β-hairpin
Urease-derived peptide
Molecular modeling
Membrane-disturbing
Insect

ABSTRACT

Background: Ureases are metalloenzymes involved in defense mechanisms in plants. The insecticidal activity of *Canavalia ensiformis* (jack bean) ureases relies partially on an internal 10 kDa peptide generated by enzymatic hydrolysis of the protein within susceptible insects. A recombinant version of this peptide, jaburetox, exhibits insecticidal, antifungal and membrane-disruptive properties. Molecular modeling of jaburetox revealed a prominent β-hairpin motif consistent with either neurotoxicity or pore formation.
Methods: Aiming to identify structural motifs involved in its effects, mutated versions of jaburetox were built: 1) a peptide lacking the β-hairpin motif (residues 61–74), JbtxΔ-β; 2) a peptide corresponding the N-terminal half (residues 1–44), Jbtx N-ter, and 3) a peptide corresponding the C-terminal half (residues 45–93), Jbtx C-ter.
Results: 1) JbtxΔ-β disrupts liposomes, and exhibited entomotoxic effects similar to the whole peptide, suggesting that the β-hairpin motif is not a determinant of these biological activities; 2) both Jbtx C-ter and Jbtx N-ter disrupted liposomes, the C-terminal peptide being the most active; and 3) while Jbtx N-ter persisted to be biologically active, Jbtx C-ter was less active when tested on different insect preparations. Molecular modeling and dynamics were applied to the urease-derived peptides to complement the structure–function analysis.
Major conclusions: The N-terminal portion of the Jbtx carries the most important entomotoxic domain which is fully active in the absence of the β-hairpin motif. Although the β-hairpin contributes to some extent, probably by interaction with insect membranes, it is not essential for the entomotoxic properties of Jbtx.
General significance: Jbtx represents a new type of insecticidal and membrane-active peptide.

1. Introduction

Ureases (EC 3.5.1.5, urea amidohydrolase), are nickel dependent enzymes that catalyze urea hydrolysis into ammonia and carbon dioxide. Evolutionarily conserved [1], these proteins have been isolated from a wide variety of organisms including plants, fungi and bacteria. In plants, ureases contribute to the bioavailability of nitrogen and in defense mechanisms [2,3]. Ureases represent an unexplored group of plant proteins with potential use for insect control [3,4] and as antifungal agents [5]. Studies have shown that ureases from *Canavalia ensiformis* (jack bean) and *Glycine max* (soybean) display insecticidal activity (reviewed in [6]) and antifungal properties, inhibiting growth and affecting membrane integrity of filamentous fungi [7] as well as of yeasts [8] in the 10^{-7} M range. The urease from pigeon pea (*Cajanus cajan*) was recently described to exhibit insecticidal and antifungal properties at similar dose ranges [9].

The molecular basis of the insecticidal mechanism of action of plant ureases is not yet completely understood [6]. It has been demonstrated that the entomotoxic effect of canatoxin [10], an isoform of *C. ensiformis* (jack bean) urease [11], is partially due to an internal 10 kDa peptide

Abbreviations: Jbtx, jaburetox; JbtxΔ-β, β-hairpin deleted version of Jbtx; Jbtx N-ter, N-terminal domain of Jbtx; Jbtx C-ter, C-terminal domain of Jbtx; Jbtx-2Ec, a version of Jbtx containing a V5 epitope; LUV, large unilamellar vesicle; MD, molecular dynamics; RMSD, root mean square deviation; CD, circular dichroism

* Correspondence to: C. R. Carlini, Center of Biotechnology and Department of Biophysics, Universidade Federal do Rio Grande do Sul, Av. Bento Gonçalves, 9500, Predio 43.431, Porto Alegre, RS, CEP 91501-970, Brazil. Tel.: +55 51 3308 7606.
** Correspondence to: G. Pasquali, Department of Molecular Biology and Biotechnology, Universidade Federal do Rio Grande do Sul, Av. Bento Gonçalves, 9500, Predio 43.432, Porto Alegre, RS, CEP 91501-970, Brazil.
E-mail addresses: ccarlini@ufrgs.br, celia.carlini@pq.cnpq.br (C.R. Carlini), pasquali@cbiot.ufrgs.br (G. Pasquali).
[1] These authors share senior authorship.

0304-4165/$ – see front matter © 2013 Elsevier B.V. All rights reserved.
http://dx.doi.org/10.1016/j.bbagen.2013.11.010

(pepcanatox), that is released from the protein upon hydrolysis by insect cathepsin-like digestive enzymes [12–16]. Jaburetox-2Ec (Jbtx-2Ec), a recombinant peptide analog to pepcanatox, exhibited a potent insecticidal effect on two economically important crop pests: *Spodoptera frugiperda* (fall armyworm) and *Dysdercus peruvianus* (cotton stainer bug) [17,18]. Jbtx-2Ec was also shown to both permeabilize large unilamellar liposomes (LUVs) [19] and to affect transmembrane potential of insect Malpighian tubules, causing inhibition of diuresis [20]. A β-hairpin motif in the modeled structure of Jbtx-2Ec has been proposed [17,19] and its presence has been confirmed in the crystallographic structures of jack bean [21] and pigeon pea [9] ureases. This motif is present also in one class of pore-forming peptides and neurotoxic peptides [22] such as charybdotoxin, which affect ion channels [23]. A variant form of Jbtx-2Ec lacking the fused V5-antigen, here called simply Jbtx, also exhibited antifungal activity [8].

Aiming to identify motifs possibly involved in the different biological activities of Jbtx, here we described the cloning and expression of mutated versions of the Jbtx-encoding cDNA. Truncated versions of the peptide, with deletions of the regions of the β-hairpin motif, the N-terminal or the C-terminal halves of the molecule, were tested on LUV permeabilization, for insecticidal and other entomotoxic effects. Structural analyses of the truncated peptides were also carried out.

2. Materials and methods

2.1. Jbtx cDNA constructs

Jaburetox-2Ec, the first version of the recombinant urease-derived peptide cloned in [17], harbored a V5-antigen with 18 amino acids derived from the pET101/D-TOPO plasmid. In order to eliminate this foreign sequence, the jack bean urease truncated cDNA encoding 93 amino acids, called simply jaburetox (Jbtx), was cloned and expressed in *Escherichia coli* via pET-23a vector (Novagen), as described in [8]. This sequence was used as template for site-directed mutagenesis and PCR amplifications of the mutant forms as described below.

2.2. Jbtx lacking the internal β-hairpin (JbtxΔ-β)

In order to delete the β-hairpin motif (residues 61–74) of the Jbtx peptide, site-directed mutagenesis was performed using the QuickChange Site-directed Mutagenesis Kit (Stratagene). As this method is often used to generate a few nucleotide deletions, some modifications in the primers' design were made, as described by [24]. Pairs of complementary primers were designed (Table 1), and site-directed mutagenesis was performed according to the kit manufacturer's instructions. The deleted gene version was confirmed by sequencing on an ABI Prism 3100 automated sequencer (Applied Biosystems) platform (ACTGene Ltd, Center of Biotechnology, UFRGS). Sequence comparisons were performed using the BLASTx software [25], available at (http://www.ncbi.nlm.nih.gov). The resulting peptide was called JbtxΔ-β.

Table 1
Primers used in this study.

Primer	Size	Sequence
5′ Del_β-hairpin	40-Mer	AGTATGGTCCGACTATTGGTGAAAAGGATTTTGCCCT TTA
3′ Del_ β-hairpin	40-Mer	TAAAGGGCAAAATCCTTTTCACCAATAGTCGGACCAT ACT
5′ Del_ α-helix	40-Mer	CTTTCACCAAAGCCATTCCTTATGGTCCGACTATTGGTGA
3′ Del_ α-helix	40-Mer	TCACCAATAGTCGGACCATAAGGAATGGCTTTGGTGA AAG
5′ N-terminal	25-Mer	CCAACATATGGGTCCAGTTAAATGA
3′ N-terminal	25-Mer	CCCCCTCGAGGGTGAAAGGACAATC
5′ C-terminal	25-Mer	CCAACATATGAAAGCCATTCCTCGT
3′ C-terminal	25-Mer	CCCCCTCGAGTATAACTTTTCCACC

2.3. Jbtx N-terminal (Jbtx N-ter) and C-terminal (Jbtx C-ter) domain versions

The Jbtx gene regions corresponding to the N-terminal (residues 1–44) and C-terminal (residues 45–93) halves of the peptide were amplified by PCR with specifically designed primers (Table 1) and products were cloned into pET23a (Novagen). PCRs were performed in a final volume of 50 μL containing 50 ng of the template plasmid DNA, 200 ng of each primer, 200 μM each dNTPs, 2.5 U *Pfu* taq DNA polymerase (Fermentas) and 1× *Pfu* reaction buffer. Amplification was carried out under the following conditions: denaturation at 95 °C for 3 min, annealing at 55 °C for 30 s and elongation at 72 °C for 2 min. After a total of 35 cycles, the final products were digested with *Nde*I and *Xho*I (Fermentas), dephosphorylated with thermosensitive alkaline phosphatase (Promega) and ligated into the expression vector pET23a (Novagen). The inserts of the recombinant plasmids were fully sequenced in order to confirm their sequences essentially as described above. The resulting peptides were called Jbtx N-terminal (Jbtx N-ter) and Jbtx C-terminal (Jbtx C-ter). A schematic representation of all Jbtx-related peptides is shown in Fig. 1.

2.4. Expression and purification of Jbtx recombinant peptides

Recombinant pET23a plasmids were transformed into *E. coli* BL21-CodonPlus (DE3)-RIL cells (Stratagene) for Jbtx gene expressions following the provider's instructions. For the purification of the original Jbtx peptide and its mutated forms, 200 mL of Luria Bertani medium containing 100 μg/mL ampicillin and 40 μg/mL chloramphenicol were separately inoculated with 2 mL overnight cultures of each *E. coli* strain. Cells were grown for approximately 2 h at 37 °C under shaking until an optical density of 0.7 was reached. At this point, IPTG was added to cultures to a final concentration of 0.5 mM. After 3 h of additional culture, cells were harvested by centrifugation and suspended in 10 mL of lysis buffer (50 mM Tris buffer, pH 7.5, 500 mM NaCl, 5 mM imidazole), sonicated and centrifuged (14,000 *g*, 30 min). The supernatant was loaded onto a Ni^{+2} loaded Chelating Sepharose (GE Healthcare) column, previously equilibrated with the lysis buffer. After 30 min, the column was washed with 50 mL of the same buffer containing 50 mM imidazole. Bound protein was eluted with 200 mM imidazole in the lysis buffer. Samples were then dialyzed against buffer A (50 mM phosphate buffer, pH 7.5, 1 mM EDTA, 5 mM β-mercaptoethanol) in order to remove the imidazole. Protein concentration was measured by Bradford assay [26]. Predicted molecular mass of the peptides was obtained by submitting the deduced sequences to the ProtScale tool [27] available at the Expasy site (http://web.expasy.org/protscale).

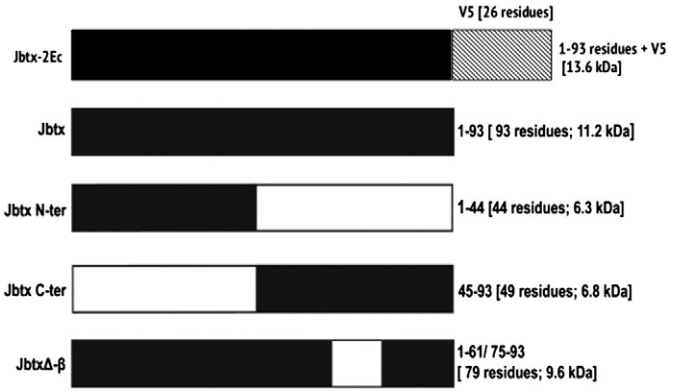

Fig. 1. Schematic representation of the sequences of jaburetox and mutants. The number of amino acid residues of each molecule (shown in black) is indicated on the right side.

Molar concentrations of peptides were calculated assuming a monomeric form in solution. Hydropathicity analysis of the peptides was carried out according to [28].

2.5. Tandem mass spectrometry (MS/MS)

In gel digestion of Jbtx peptides was performed for all samples analyzed, except for the positive control (C+), which was submitted to in solution digestion. For in gel digestion the protocol in [29] was followed, using 50 mM ammonium bicarbonate (AB) unless otherwise explained. Briefly, the bands on the gel were distained with 50 mM AB in 40% acetonitrile (ACN). Following, gel pieces were dehydrated with 100% ACN and lyophilized. Reduction was performed with 50 mM dithiothreitol (DTT) in 50 mM AB, for 30 min at 56 °C, in the dark, followed by the alkylation performed with 50 mM iodoacetamide (IAA) in 50 mM AB for 30 min, at room temperature, also in the dark. The gel pieces were washed with 50 mM AB + 40% ACN for 15 min, and a second dehydration step was done. Proteins in the gel were digested for 3 h (Jbtx N-ter and Jbtx C-ter) or 16 h (Jbtx and JbtxΔ-β) in 500 μL of 100 mM AB solution containing 100 ng of sequencing grade trypsin (Promega) at 37 °C. After digestion, supernatants were transferred to microcentrifuge tubes and gel pieces were washed with 1% formic acid in 60% ACN, and the supernatants were combined accordingly. Digested peptides were lyophilized and submitted to tandem mass spectrometry analyses. In the case of in solution digestion, sample of Jbtx peptide (30 μg in 20 mM sodium phosphate, 5 mM β-mercaptoethanol, 1 mM EDTA, pH 7.5) was reduced with 50 mM DTT and alkylated with 50 mM IAA (30 min each, at room temperature). Then, DTT to a final concentration of 10 mM was added for 15 min at room temperature. Digestion was performed in this case with 0.6 mg of trypsin (Promega) for 3 h at 37 °C. After the digestion process, the samples were desalted with ZipTip™ (Millipore®) according to the manufacturer's instructions. The eluted peptides were lyophilized and analyzed by tandem mass spectrometry.

The lyophilized digested peptides were suspended in 0.1% formic acid (10 μL) and 5 μL of each solution was subjected to reversed phase chromatography (NanoAcquity UltraPerformance LC-UPLC® chromatograph (Waters) using a Nanoease C18, 75 μm ID at 35 °C. The column was equilibrated with 0.1% trifluoroacetic acid (TFA) and the peptides were eluted in a 20 min gradient, ramping from 0 to 60% acetonitrile in 0.1% TFA at 0.6 nL/min constant flow. Eluted peptides were subjected to electrospray ionization and analyzed by mass spectrometry using a Q-TOF Micro™ spectrometer (Micromass). The voltage applied to the cone for the ionization step was 35 V. The three most intense ions in the range of m/z 200–2000 and +2 or +3 charges were selected for fragmentation. The acquired MS/MS spectra were processed using the Proteinlynx v.2.0 software (Waters) and the generated .mgf files were used to perform database searches using the MASCOT software version 2.4.00 (Matrix Science) against the NCBI database, and taxid was restricted to Viridiplantae (taxid:33090). Results were analyzed manually.

2.6. Electrophoresis

The peptide fractions of Jbtx and its mutant forms were visualized in SDS-Tricine gels [30]. The gels were stained with colloidal Coomassie G-250 (Sigma Chem. Co) according to [31].

2.7. Western blot

Western blots were performed according to [32]. Briefly, peptides were electrophoresed, transferred to PVDF membranes (Millipore) and immersed in a blocking buffer consisting of 5% nonfat dry milk in phosphate-buffered saline (PBS, 137 mM NaCl, 2.7 mM KCl and 4.3 mM $Na_2HPO_4 \cdot 7H_2O$, pH 7.3). After washing, the membrane was incubated with rabbit anti-jaburetox-2Ec polyclonal antibodies (1:7500 dilution) for 2 h at room temperature, followed by a 2 h incubation with anti-rabbit IgG (1:20,000 dilution) alkaline phosphatase conjugate (Sigma Chem. Co.). Colorimetric detection was carried out using 5-bromo-4-chloro-3-indolyl-phosphate p-toluidine salt and nitro-blue tetrazolium chloride.

2.8. Leakage experiment

Large unilamellar vesicles (LUVs) were produced and the leakage experiment was conducted as described previously [19]. LUVs were prepared using 10 mg of L-α-phosphatidic acid (egg chicken, Avant Polar Lipids), at a concentration of 20 mg/mL. The leakage promoted by Jbtx and its mutated forms at a final concentration of 5 μg/mL in 25 mM Tris, pH 7.0, was evaluated by the carboxyfluorescein release assay [19]. The concentration of LUVs in the experiment was estimated based on the absorbance of the fluorescent probe at 490 nm, and adjusted to a value of 0.1. In the leakage assays, fluorescence intensity of the reaction mixture (LUVs plus peptide or buffer) was recorded as a function of time. The samples were excited at 490 nm and the fluorescence was acquired at 518 nm. It was assumed that the absence of leakage (0%) corresponded to the fluorescence of the vesicles at time zero; 100% leakage was taken as the value of fluorescence intensity obtained after the addition of 1% (v/v) Triton X-100. All measurements were carried out in a Cary Eclipse fluorescence spectrophotometer (Varian).

2.9. Insecticidal activity

Fifth-instar *Rhodnius prolixus* were kindly provided by Dr. Hatisaburo Masuda and Dr. Pedro L. Oliveira (Institute of Medical Biochemistry, Universidade Federal do Rio de Janeiro, RJ, Brazil) and by Dr. Denise Feder (Universidade Federal Fluminense, RJ, Brazil). The phytophagous milkweed bugs (*Oncopeltus fasciatus*) were reared in our laboratory as previously described [15].

2.9.1. Injection assays

Fifth instars of *O. fasciatus* or *R. prolixus* were injected into the hemocoel using a Hamilton Microliter 900 series syringe (Hamilton). Group of 10 insects (*O. fasciatus*) or 5 insects (*R. prolixus*) were injected with 20 mM sodium phosphate buffer (pH 7.5) containing peptides at a final dose of 0.015 μg (*O. fasciatus*) or 0.05 μg (*R. prolixus*) per mg of insect body weight. Control insects received injections of buffer alone. Mortality rate within each group was recorded after 48 or 96 h. Two independent bioassays were carried out for each peptide on each insect model. Results shown are means ± standard errors.

2.9.2. Feeding assays

Fifth instars *R. prolixus* were fed on *R. prolixus* saline solution (150 mM NaCl, 8.6 mM KCl, 2.0 mM $CaCl_2$, 8.5 mM $MgCl_2$, 4.0 mM $NaHCO_3$, 34.0 mM glucose, 5.0 mM HEPES, pH 7.0) containing 1 mM ATP and enough peptide (tested individually) to give final doses of 0.1 μg per mg of body weight. Groups of 5 insects for each peptide were fed for approximately 30 min, at 37 °C, by placing their mouth apparatus inside glass capillaries containing the test solutions. Control insects fed solely on *R. prolixus* saline solution containing 1 mM ATP, under the same conditions. Mortality rate within each group was recorded after 24 h. One triplicated bioassay was carried out for each peptide. The results shown are means and standard errors.

2.10. Measurement of fluid secretion by Rhodnius prolixus Malpighian tubules

The assay was performed essentially as described in [20], using *R. prolixus* serotonin-stimulated Malpighian tubules. Secretion rate was expressed as the percentage of fluid secretion measured after the addition of Jbtx or mutated peptides as compared to serotonin (2.5×10^{-8} M) alone (control). For each peptide and dose, 5–6 replicates were done. The results shown are means ± standard error.

2.11. In vivo cockroach metathoracic coxal-adductor nerve–muscle preparation

The *in vivo* cockroach metathoracic coxal-adductor muscle preparation was used [33] to characterize further the entomotoxic activity of Jbtx and its mutated versions. Male adult *Phoetalia pallida* (3–4 months after molting) were reared in our laboratory at controlled temperature (22–25 °C) on a 12 h:12 h light:dark cycle. Animals were immobilized by chilling and mounted, ventral side up, in a Lucite holder covered with 1 cm soft rubber that restrained the body and provided a platform to which the metathoracic coxae could be firmly attached using entomologic needles. The left leg was then tied at the medial joint with a dentistry suture line connected to a 1 *g* force transducer (AVS Instruments, São Carlos, SP, Brazil). The transducer was mounted in a micromanipulator to allow adjustment of muscle length. The exoskeleton was removed from over the appropriated thoracic ganglion. Nerve 5, which includes the motor axon to the muscle, was exposed and a bipolar electrode was inserted to provide electrical stimulation. The nerve was covered with mineral oil to prevent dryness and stimulated at 0.5 Hz, 5 ms, with twice the threshold, during 120 min. Twitch tension was digitalized, recorded and retrieved using a computer based software AQCAD (AVS Instruments, São Carlos, SP, Brazil). Data were further analyzed using the software ANCAD (AVS Instruments, São Carlos, SP, Brazil). Jbtx and peptides were dissolved in insect physiological solution (214 mM NaCl, 3.1 mM KCl, 9 mM $CaCl_2$, 0.1 mM $MgSO_4$, and 5 mM HEPES, pH 7.2 [34]). The test solutions were prepared daily and 20 μL were injected into the insect's third abdominal segment using a Hamilton syringe.

2.12. Molecular modeling and simulation

The three-dimensional model for Jbtx was built by comparative modeling with MODELLER9v10 [35] employing the structure of the *C. ensiformis* major urease isoform (PDB ID: 3LA4), [21] as template. Ten models were built, stereochemically evaluated and theoretically validated for their three-dimensional profiles with PROCHECK [36] and Verify3D [37], respectively. The best scored model was then selected. The amino-terminal Met residue and the carboxy-terminal LEHHHHHH segment were added with SwissPDBviewer [38]. The Jbtx peptide was then subjected to molecular dynamics (MD) simulations with GROMACS 4.5 suite [39] using GROMOS96 53a6 force field [40] for 500 ns. The systems were solvated in triclinic boxes using periodic boundary conditions and SPC water models [41]. Counterions (Na^+) were added to neutralize the systems. The Lincs method [42] was applied to constrain covalent bond lengths, allowing an integration step of 2 fs after an initial energy minimization using Steepest Descents algorithm. Electrostatic interactions were calculated with Particle Mesh Ewald method [43]. Temperature and pressure were kept constant by coupling proteins, ions, and solvent to external temperature and pressure baths with coupling constants of $\tau = 0.1$ and 0.5 ps [44], respectively. The dielectric constant was treated as $\varepsilon = 1$, and the reference temperature was adjusted to 300 K. The system was slowly heated from 50 to 300 K, in steps of 5 ps, each step increasing the reference temperature by 50 K, allowing a progressive thermalization of the molecular system. The simulation was performed to 500 ns, with no restraint, considering a reference value of 3.5 Å between heavy atoms for a hydrogen-bond, and a cutoff angle of 30° between hydrogen-donor–acceptor [39].

2.13. Statistical analysis

Data were evaluated by ANOVA followed by the Bonferroni's or Student *t* test using GraphPad Prism software (Version 5.0 for Windows). See legends to figures for more details. A $p < 0.05$ was considered statistically significant.

3. Results

3.1. MD simulation of Jbtx

It has been previously suggested that a prominent β-hairpin in the predicted model of the urease-derived peptide Jbtx could be responsible at least in part for its membrane-disturbing activity and some of its biological properties [17,19]. The presence of this β-hairpin was confirmed by x-ray crystallographic data of jack bean urease [21], and short simulations of the crystal-derived peptide were performed [45].

In order to establish if this β-hairpin would still be present in the peptide once it has been released from the urease molecule, a 3D-model of Jbtx was constructed using the crystal structure of jack bean urease as template and subjected to molecular dynamics for 500 ns (Fig. 2, panels A and B). The MD simulation indicated that Jbtx becomes more globular when in aqueous solution (Fig. 2, panel B), changing its conformation along the simulation with an increase of RMSD, as compared to the initial crystal-derived structure (Supplementary Fig. 1). The secondary structure of Jbtx changed in solution, with loss of many helix turns and formation of a minute beta sheet. The β-hairpin at Jbtx's C-terminal half was conserved despite the increase in coil content (Fig. 2, panels B and D).

3.2. Expression of recombinant jaburetox (Jbtx) and mutated forms

Aiming to identify motifs probably involved in the biological activities of Jbtx, mutated forms of the peptide lacking the internal β-hairpin (JbtxΔ-β), the N-terminal half (Jbtx C-ter) or the C-terminal half (Jbtx N-ter) domains were constructed. A schematic representation of these peptides is shown in Fig. 1.

All the His-tagged peptides were purified and analyzed by SDS-PAGE (Fig. 3A and B). The predicted molecular masses of the peptides based on their deduced amino acid sequences are 11,193 Da for Jbtx, 9625.6 Da for JbtxΔ-β, 6325.8 Da for Jbtx N-ter and 6772.5 Da for Jbtx C-ter. As it can be observed from the SDS-PAGE results, all the recombinant peptides showed the expected mass, except for the Jbtx N-ter peptide which behaved as a dimer with an estimated molecular mass of approximately 12 kDa (Fig. 3B).

Anti-Jbtx-2Ec polyclonal antibodies recognized equally Jbtx-2Ec, Jbtx and JbtxΔ-β (result not shown) and although with a weaker reactivity, also interacted with the two half-peptides (Fig. 3C).

All bands seen in the lanes corresponding to each peptide were excised from the SDS-PAGE gels, digested with trypsin and submitted to MS/MS analysis. The identities of the peptides Jbtx, JbtxΔ-β, and Jbtx C-ter (and aggregated forms of the peptides) were confirmed by MS/MS analysis as shown in Fig. 3D. On the other hand, the peptide Jbtx N-ter was not identified in the MS/MS assay. The band corresponding to the dimer of the peptide Jbtx N-ter in the SDS-PAGE (Fig. 3B) reacted positively with the anti-Jbtx antibodies (Fig. 3C), thus confirming its identity. The tendency to form aggregates previously described for jaburetox-2Ec [19,46] persisted in Jbtx, as well as in all the mutated forms of this peptide, as confirmed by the MS/MS analysis. After a few days in aqueous solution, all the peptides formed insoluble precipitates. These aggregates did not revert to the monomeric state under a number of tested conditions [19]. High ionic strength accelerates the aggregation of Jbtx (data not shown), suggesting hydrophobic interactions as a driving force for the oligomerization process. Because it was not possible to ascertain the oligomeric state of each peptide in solution, their monomeric states were considered when expressing molar concentrations in the subsequent assays.

Since all mutated peptides retained considerable antigenicity towards anti-Jbtx-2Ec polyclonal antibodies, they probably kept their tridimensional structures, resembling the corresponding portions in Jbtx. The CD spectrum of Jbtx (not shown) indicated the presence mainly of irregular structures, with a minor contribution of β-sheets and helices. This type of CD spectrum has been observed for Chab I,

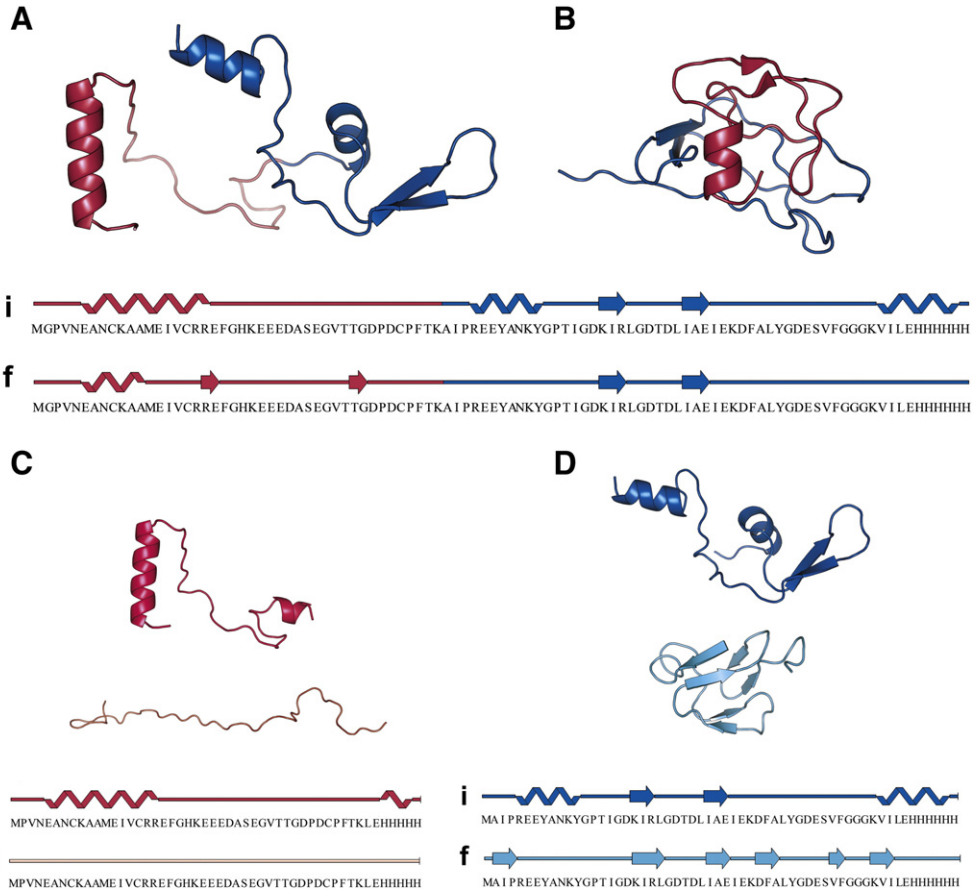

Fig. 2. Structural changes in jaburetox and its mutated versions after MD simulation of 500 ns. Three-dimensional representations of the full Jbtx peptide (A) initial and (B) final structures, with the N-terminal domain (residues 1–44) depicted in pink and the C-terminal domain in blue; (C) Jbtx N-ter (amino-terminal mutant): top, initial state; bottom, final state; (D) Jbtx C-ter (carboxy-terminal mutant): top, initial state; bottom, final state; Schematic representations of the secondary structure content of the (i) initial and (f) final structures are colored according to their three-dimensional counterparts. The corresponding amino acid sequences are also shown.

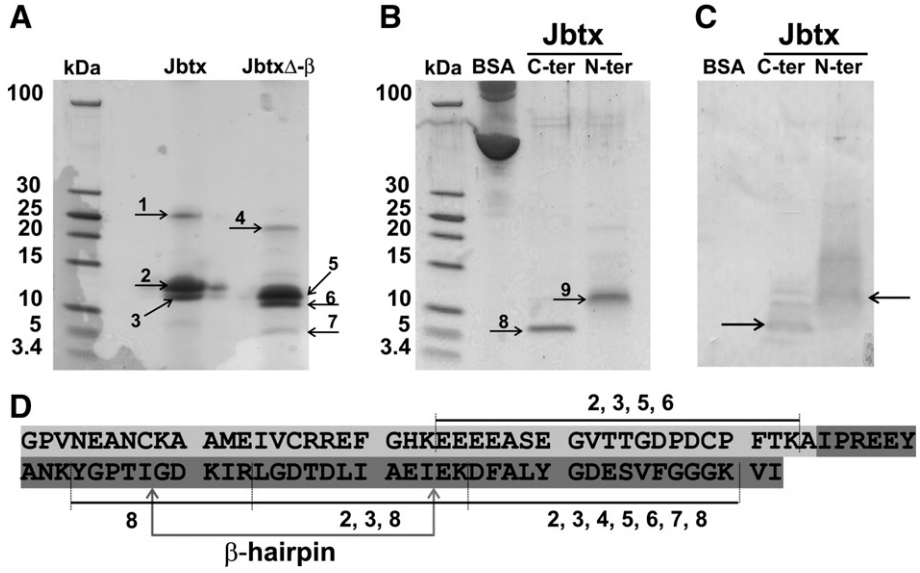

Fig. 3. (A and B) SDS-Tricine PAGE of jaburetox and their derived peptides. Numbered arrows indicate the bands that were excised and analyzed by mass spectrometry. *Lanes*: Jbtx, jaburetox; JbtxΔ-β, jaburetox with deleted β-hairpin motif; BSA, bovine serum albumin; C-ter, carboxy-terminal region of jaburetox; N-ter, amino-terminal region of jaburetox. (C) Western blot analysis with polyclonal anti-jaburetox antibodies. *Lanes*: BSA, bovine serum albumin as negative control; C-ter, carboxy-terminal region of jaburetox; N-ter, amino-terminal region of jaburetox; (D) amino acid sequence of jaburetox. The numbered lines above and below the sequence correspond to the arrows in panels A and B, showing parts of the jaburetox sequence identified by mass spectrometry. The sequence of Jbtx N-ter mutant is shown in light gray and that of the Jbtx C-ter in dark gray. The region corresponding to the β-hairpin is also indicated.

a charybdotoxin analog [47], and also for the acid unfolded state of equine β-lactoglobulin, which has residual helices and β-hairpins [48,49].

Simulations were carried out to establish the putative structures in solution of the mutated peptides representing the two half domains of Jbtx. The N-terminal mutant (residues 1 to 44) became completely unfolded after simulation (Fig. 2, panel C), while the C-terminal mutant (residues 45 to 93) showed propensity towards stabilization of a newly-formed β-sheet (Fig. 2, panel D).

3.3. Vesicle leakage promoted by Jbtx peptides

We employed LUVs composed by L-α-phosphatidic acid [19] as a membrane model to evaluate which part of the Jbtx molecule interacts with phospholipid membranes and induces vesicle leakage. Fig. 4 shows typical results. Vesicle leakage was more prominent when LUVs were treated with either Jbtx C-ter or Jbtx (5 μg/mL), although all peptides produced at least 80% of leakage at the end of the 10 min incubation period. Taken together, these findings showed that the β-hairpin is not essential for the membrane-disruptive activity of Jbtx. Moreover, the data indicated that all Jbtx-related peptides are able to induce LUV leakage, while the C-terminal region of the peptide seems to contribute the greatest effect. In fact, hydropathicity plots indicated the presence of prominent hydrophobic regions in both, the N-terminal and the C-terminal domains of Jbtx (Supplementary Fig. 2).

3.4. Insecticidal effect of Jbtx peptides

In order to compare the insecticidal activity of Jbtx to that previously described for Jbtx-2Ec [6,18], we tested the entomotoxic effect of Jbtx upon injection into *R. prolixus* nymphs. Employing a dose of 0.05 μg/mg of insect weight, 100% mortality was observed 48 h after injection (result not shown), indicating that the absence of the V5 epitope in Jbtx did not affect its insecticidal property. When the insecticidal activity of the β-hairpin deleted form (JbtxΔ-β) was assayed in *R. prolixus* nymphs, it produced an entomotoxic (mortality) effect equivalent to that of the original Jbtx, either by injection (Fig. 5A) or by feeding (Fig. 5B). Four days after injection into fifth instars *R. prolixus*, we have observed that the Jbtx N-term induced up to 60% mortality, while Jbtx C-ter caused less than 10% mortality

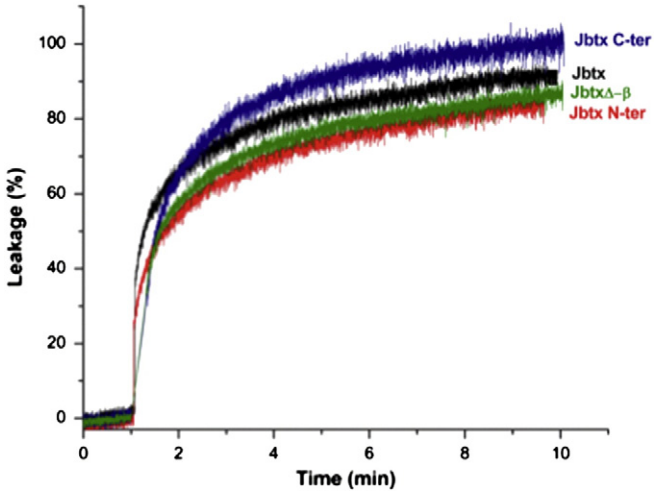

Fig. 4. Effect of jaburetox and derived mutants on LUVs composed by L-α-phospatidic acid. The carboxyfluorescein release assay was performed for each peptide at a final concentration of 5 μg/mL (Jbtx, 0.44 μM; JbtxΔ-β, 0.51 μM; Jbtx N-ter, 0.79 μM; and Jbtx C-ter, 0.73 μM) in 25 mM Tris, pH 7.0. The absence of leakage (0%) corresponds to the fluorescence of the vesicles at time zero; 100% leakage was taken as the value of fluorescence intensity obtained after addition of 1% (v/v) Triton X-100. The experiments were performed at 25 °C. The figure shows superimposed tracings of a typical result for each peptide to facilitate comparison.

(Fig. 5A). On the other hand, 24 h after feeding, both Jbtx N-ter and Jbtx C-ter had similar lethal effects on *R. prolixus* nymphs, ranging from 60 to 80% mortality (Fig. 5B).

Fifth instars *O. fasciatus* were also injected with Jbtx and its mutant variants. Similarly to what was observed for *R. prolixus* upon injections, Jbtx N-ter (Fig. 6A) and JbtxΔ-β (Fig. 6B) displayed lethal effects comparable to that of Jbtx, while Jbtx C-ter was near to inactive (Fig. 6A), suggesting that the N-terminal portion of the Jbtx carries its insecticidal domain.

3.5. Antidiuretic effect of Jbtx-related peptides on Malpighian tubules

We have previously described that, in the dose range of 10^{-16} to 10^{-15} M, Jbtx 2-Ec inhibited the serotonin-stimulated fluid secretion in *R. prolixus* Malpighian tubules [20]. Fig. 7 shows that Jbtx and all its variants, at a concentration of 1×10^{-15} M, were able to inhibit fluid secretion in the tubules producing similar antidiuretic effect.

3.6. In vivo neuromuscular blockade of cockroach nerve–muscle preparations induced by Jbtx-related peptides

The injection of Jbtx or its mutant versions (32 μg/g of animal weight) produced a time-dependent blockade of the cockroach nerve–muscle preparation (Fig. 8). Jbtx was the most effective and induced a complete neuromuscular paralysis at 35 ± 10 min followed by Jbtx N-ter at 80 ± 2 min (Fig. 8B). In contrast, the neuromuscular blockades induced by Jbtx Δ-β or Jbtx C-ter were only partial at the end of the 120 min recording time. The administration of insect saline alone did not interfere with normal neuromuscular responses during 120 min recordings (Fig. 8A). Thus, similar to what was observed in the case of the insecticidal activity (upon injection), these data suggest that the N-terminal half of Jbtx carries its entomotoxic domain. In this type of assay, however, there is a contribution of the β-hairpin to the effect.

4. Discussion

In this study we evaluated the jack bean urease-derived peptide Jbtx and three domain-deleted variants in order to identify the regions of the molecule that are critical for its entomotoxic activities. A previous version of Jbtx, harboring a large V5-antigen derived from the pET101/D-TOPO plasmid and called jaburetox-2Ec (Jbtx-2Ec), was shown to be lethal to *R. prolixus* by oral route and hemocoel injection [50,51] and to permeabilize vesicles composed of charged lipids [19]. Jbtx has the same 93 amino acid urease-derived sequence and the polyhistidine tail found in Jbtx-2Ec, but lacks the V5 epitope present in the later. Here we demonstrated that Jbtx displays insecticidal activity equivalent to that described for Jbtx-2Ec, evidencing that the epitope V5 is not implied in its entomotoxicity.

Comparing the structure obtained here for Jbtx with the model of jaburetox-2Ec generated by comparative modeling [19] (prior to the first description of the crystal structure of a plant urease [21]), important conformational similarities can be seen in the region correspondent to the short helix as well as in the large content of random coil conformation, even though jaburetox-2Ec exhibited a more well-defined β-hairpin than Jbtx. The differences in the models generated for these peptides might be attributed in part to the distinct initial structures used in the MD simulation, as *H. pylori* urease and jack bean urease served as template in the comparative modeling for jaburetox-2Ec [19] and Jbtx (this work), respectively.

Balasubramanian and Ponnuraj [21] were the first to report in 2010 the crystal structure of a plant (*C. ensiformis*, jack bean) urease at 2.05 Å of resolution. These authors confirmed the presence of an internal β-hairpin motif in the jack bean urease, previously suggested by our group to be present in the structure of jaburetox-2Ec [17,19], and proposed to be involved in the insecticidal activity of both urease and its derived entomotoxic peptide. The same group described insecticidal

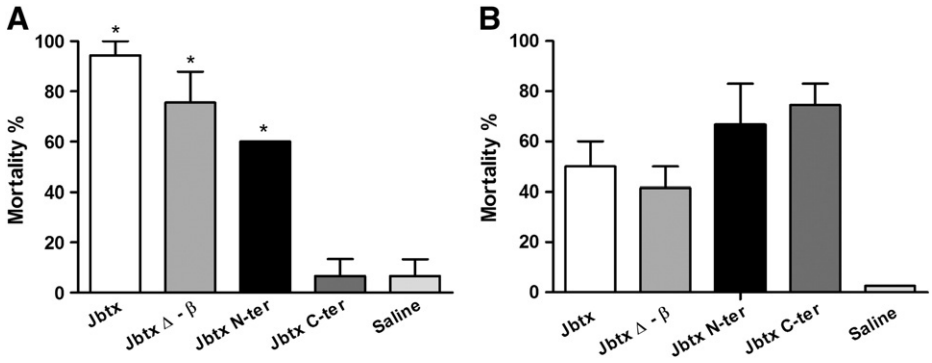

Fig. 5. Insecticidal effect of Jbtx and derived peptides on fifth instar *Rhodnius prolixus*. (A) Groups of 5 insects were injected with each peptide separately at final doses of 0.05 μg per mg of body weight. Control insects were injected with *Rhodnius* saline. The mortality was recorded after 96 h. Two independent bioassays were carried out for each peptide. Results shown are means and standard error. (B) Groups of 5 insects were fed on *R. prolixus* saline plus 1 mM ATP and the peptides separately at final doses of 0.1 μg per mg of body weight. Control insects were fed solely on *R. prolixus* saline plus 1 mM ATP. Mortality rate within each group was recorded after 24 h. Results shown are means and standard error.

and antifungal properties of the pigeon pea (*Cajanus cajan*) urease and reported the presence of a similar β-hairpin motif in the crystal structure of this urease [9]. Moreover, Balasubramanian and coworkers, using molecular modeling studies and short (5 ns) molecular dynamics simulations of Jbtx, suggested that its β-hairpin could self-associated into a β-barrel able to anchor into a membrane-like environment, and hypothesized an insecticidal mode of action of Jbtx based on pore formation [45].

Also present in bacterial ureases, the microbial β-hairpin motif is formed with contributions from the α- and the β urease chains while its counterpart in the single chain of plant ureases is formed exclusively by amino acids located in a region corresponding to the bacterial α-chain [21]. Our group reported that, contrasting to plant ureases, *Bacillus pasteurii* urease has no insecticidal activity against *Dysdercus peruvianus* [52]. Since the β-hairpin motif is present in the *B. pasteurii* urease as well [21], a plausible explanation for this could be the fact that part of the sequence corresponding to the N-terminal half of Jbtx is missing in bacterial ureases.

Here we demonstrated that Jbtx and JbtxΔ-β, its β-hairpin deleted version, behaved almost indistinguishably regarding LUV leakage, antidiuretic effect and insecticidal activity upon injection. These results strongly suggested that the β-hairpin motif is not involved in membrane-disturbing activity or in these biological properties of the peptide.

At that point we had no clues to any other possible motif in the Jbtx molecule that could be responsible for its biological properties, so we decided to produce two half-peptides, corresponding to the N-terminal and C-terminal half versions of Jbtx (Jbtx N-ter and Jbtx C-ter, respectively). The mutated peptides Jbtx N-ter and Jbtx C-ter were then tested for LUV leakage and for different types of entomotoxic activities. Two distinct groups of results were obtained depending on the assay: (i) Jbtx, JbtxΔ-β and Jbtx N-ter were equally active while and Jbtx C-ter was inactive or significantly less active; and (ii) all the peptides produced similar effects.

When tested for insecticidal activity upon injection into *R. prolixus* (Fig. 5A) or *O. fasciatus* (Fig. 6) nymphs, Jbtx, Jbtx Δ-β and Jbtx N-ter caused significant mortality after 96 h, while the survival rate of insects injected with Jbtx C-ter was equivalent to that of control group. It thus became clear from these experiments that the N-terminal half of Jbtx (Jbtx N-ter) has the insecticidal domain of Jbtx. This conclusion agrees with the fact that the deletion of the β-hairpin, which is present in the Jbtx C-ter, did not interfere on the entomotoxicity.

On the other hand, all the peptides were able to induce blockade of the cockroach neuromuscular junction *in vivo* (Fig. 8). The neuromuscular blockade induced by Jbtx resembles the effect of neurotoxins which act directly on receptor ion channels [53], among which are pore-forming neurotoxins [54]. In this work we did not attempt to elucidate the pharmacological interactions of Jbtx and related peptides at specific sites of insect neuromuscular junctions. The Jbtx N-ter peptide had an effect comparable to that of the intact peptide producing almost complete neuromuscular blockade after 40 min of recordings while JbtxΔ-β and Jbtx C-ter were clearly less active. The activity loss of JbtxΔ-β in this bioassay may reflect some critical alteration of the peptide 3D-structure affecting also its N-terminal domain, which alone is capable of producing full effect in the absence of the β-hairpin.

Upon feeding to *R. prolixus* (Fig. 5B) all the peptides were lethal, even Jbtx C-ter, contrasting with its lack of activity when injected into the hemolymph. This fact points to the presence of two active domains in the Jbtx molecule, with the amphipatic β-hairpin in the C-terminal domain probably interacting with insect's gut membranes as predicted,

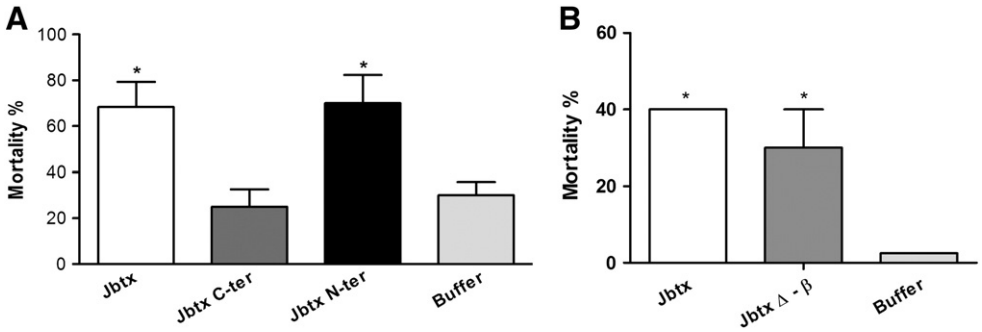

Fig. 6. Insecticidal effect of Jbtx and derived peptides on fifth instars *Oncopeltus fasciatus*. (A) Groups of 10 nymphs were injected with 1.5 μL of Jbtx, Jbtx N-ter or Jbtx C-ter into the hemocoel (dose of 0.015 μg/mg of insect body weight) or 20 mM phosphate buffer, pH 7.5 (control group). (B) Groups of 5 nymphs were injected with 1.5 μL of Jbtx or JbtxΔ-β peptides into the hemocoel (dose of 0.015 μg/mg of insect body weight) or 20 mM phosphate buffer, pH 7.5 (control group). The mortality rate was recorded after 96 h. Results are means ± standard error of triplicates of two independent experiments. (*) indicates statistically significant difference ($p \leq 0.05$) from the control group.

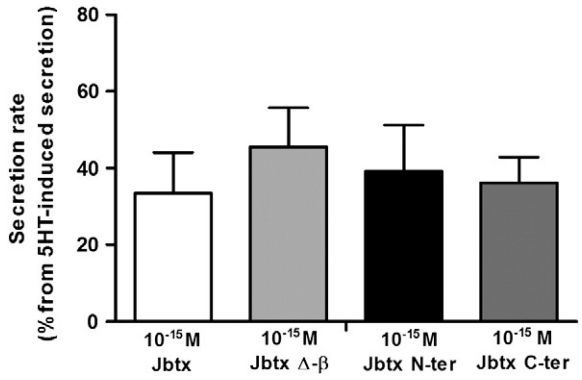

Fig. 7. Effect of jaburetox and mutants on secretion of *Rhodnius prolixus* Malpighian tubules. The assay was performed as described by Staniscuaski et al. [20]. Tubules were incubated with 2.5×10^{-8} M serotonin (5-hydroxy-tryptamine, 5-HT) for 20 min to record the maximal secretion. After washing, the tubules were incubated with the peptides (1×10^{-15} M) in the presence of serotonin for another 20 min. The secretion rate was expressed as a percentage from the control (serotonin without peptides). Results shown are means ± standard deviation of 5–6 replicates for each peptide.

when given by oral route. This conclusion could also be drawn from the facts that all the peptides had equivalent antidiuretic effects (Fig. 7) and that both terminal domains of Jbtx were able to induce leakage of vesicles (Fig. 4). The preliminary results using Planar Lipid Bilayers another artificial membrane composed only of lipids, also showed that all mutant versions of Jbtx form ion channels displaying membrane-disturbing properties (Piovesan A., unpublished data). On the other hand, Jbtx C-ter showed significantly lower activity than Jbtx or Jbtx N-ter, when its first contact within the insect was with the hemolymph probably due to a "saturating" effect of the lipid-rich medium on its membrane-disrupting ability.

All the peptides, including Jbtx C-ter, produced antidiuresis or were lethal given by oral route, circumstances where their first interaction happened with single cell layered tissues such as the Malpighian tubules [55] or the gut [56]. One hypothesis to explain the lack of specificity of these assays to discriminate the different Jbtx variants could be that biological multilayered tissue systems, such as the neuromuscular junction [57] and the whole insect (by injection, skipping the first contact with the gut), probably add additional levels of tissue- or cell specificity to the entomotoxic effects of Jbtx-related peptides. Altogether, our data indicate that the main entomotoxic domain of the urease-derived peptide Jbtx is located in its N-terminal half. However, depending on the bioassay, the C-terminal domain and/or its β-hairpin motif could also contribute part of the biological activity of Jbtx.

From the molecular dynamics simulation, it seems that the monomeric Jbtx peptide is mostly formed by coils (Fig. 2). Our simulation results confirm and expand previous theoretical observations [19], such as the compaction of the peptide in solution. Simulations of the half-peptides indicated that after 500 ns Jbtx N-ter adopts a random coil conformation while Jbtx C-ter acquires a newly-formed β-sheet (Fig. 2). These data may explain why Jbtx is highly prone to aggregation [19], and the instability of Jbtx N-ter in aqueous solution (unpublished results), possibly a consequence of the unfolding of the highly hydrophobic N-terminal of Jbtx that would require protein–protein (or protein–membrane) contact to stabilize.

Presently, to the best of our knowledge, it is not possible to compare the MD simulated structure of Jbtx to that of any other known insecticidal or membrane-disrupting peptide. The high level of coils, especially in the N-terminus, may be related to the peptide toxicity,

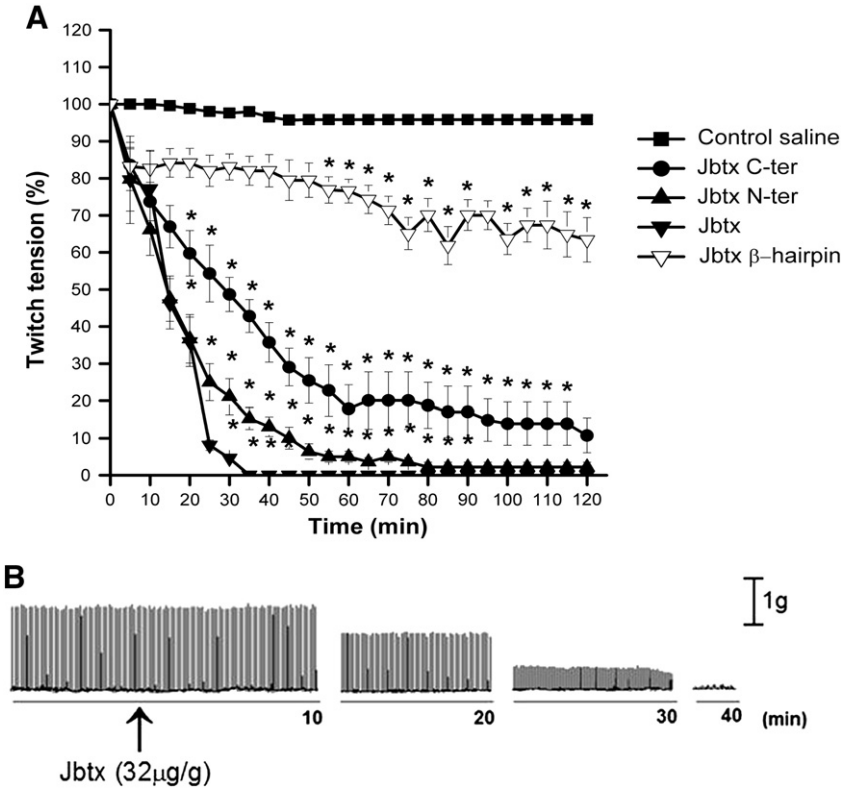

Fig. 8. Neuromuscular paralysis induced by Jbtx and peptides on *in vivo* cockroach coxal-adductor methatoracic nerve–muscle preparation. (A) Time course of the blockade of the neuromuscular activity in the presence of 32 μg/g of each version of Jbtx peptides against control insects treated only with saline (means ± standard error, n = 12). Note that Jbtx and Jbtx N-ter were able to induce complete paralysis. * indicates $p \leq 0.05$ in comparison to control saline, with ANOVA two way and Student *t* test. (B) Representative myographic 120 min recording of the coxal-adductor methatoracic nerve–muscle preparation of a Jbtx-treated cockroach.

since some toxins employ these unfolded states as recognition motifs. One example of such toxins is colicin, from *E. coli* [58]. These unfolded recognition domains may be advantageous for the toxins that carry them, since they allow these proteins to overcome steric restrictions while providing large average interaction surfaces per residue [58–60]. There are many reports in the literature of folding and oligomerization of proteins and peptides that acquire their biologically active state upon interaction with lipids or membranes. Examples are cecropin A, a 37-residue insect antimicrobial peptide [61,62], the Cyt1Aa toxin produced by *Bacillus thuringiensis* [63], anticancer β-hairpin peptides [64], antimicrobial, cell-penetrating peptides and fusion peptides such as the HIV fusion peptide FP23 [65], to cite a few.

The tendency to oligomerize and to interact with lipids exhibited by Jbtx brings the question whether the active form of the peptide (or its N-ter and C-ter versions) is an oligomer rather than a monomer. The oligomerization/aggregation phenomenon was also observed for Jbtx-2Ec, causing an enormous impact of the membrane-disruptive ability of the peptide [19].

Jbtx has promising biotechnological potential as a biopesticide. We are currently testing transgenic Jbtx expressing sugar cane (*Saccharum officinarum*) plants, and so far we have observed an increase of resistance to several species of lepidopterans in greenhouse conditions (Becker-Ritt et al., unpublished data). These data indicate the effectiveness of the peptide as an environment friendly insecticide with practical application, reducing crop losses while avoiding the use of chemical toxic agents.

We conclude that the urease-derived peptide Jbtx probably represents a new example of membrane-active peptide with insecticidal and fungitoxic activities. Its insecticidal activity was tracked down mostly to its N-terminal region and does not require the prominent β-hairpin present in the C-terminal region, although this part of the molecule probably contributes to its overall entomotoxic properties. Understanding the complex behavior of these peptides in solution as well as in the presence of lipids and biological membranes is a critical step towards unraveling their mechanisms of action and exploiting their potential as insecticidal agents.

Supplementary data to this article can be found online at http://dx.doi.org/10.1016/j.bbagen.2013.11.010.

Authors' contributions

A.H.S.M. and K.K. constructed the mutated peptides, M.S.D. helped in the insect bioassays, A.R.P. and C.F. carried out LUVs leakage assay, F.S. run the Malpighian tubules assay, D.R.D. performed MS assays, R.L-B. and H.V. conducted molecular modeling and simulations, C.A.D.B. and C.G.M.A. tested the peptides on the cockroach neuromuscular junction, C.R.C. wrote the paper and together with G.P., conceived and supervised all the work.

Acknowledgements

The authors wish to thank the Centro Nacional de Supercomputação at Universidade Federal do Rio Grande do Sul, for the assistance and access to the supercomputer; Dr. Yraima Cordeiro, Inst. Biophysiscs Carlos Chagas Filho, Universidade Federal do Rio Grande do Sul, for preliminary circular dichroism analyses of the peptides and B.Sc. Marinês de Avila Heberle, Unipampa, for helping collecting data on the cockroach preparation. This work was supported by grants from the Brazilian agencies: Coordenação de Aperfeiçoamento de Pessoal de Nível Superior (CAPES)—Edital de Toxinologia [proj 54/2011]; Conselho Nacional de Desenvolvimento Científico e Tecnológico (CNPq)—Edital Universal [proj. 47.0785/2011-47.5908/2012]; Fundação de Amparo à Pesquisa do Estado do Rio Grande do Sul (FAPERGS)—PRONEX [proj. 10/0014-2]. The authors declare no conflicts of interest related to this work.

References

[1] R. Ligabue-Braun, F.C. Andreis, H. Verli, C.R. Carlini, 3-to-1: unraveling structural transitions in ureases, Naturwissenschaften 100 (2013) 459–467.
[2] J.C. Polacco, M.A. Holland, Roles of urease in plant cells, Int. Rev. Cytol. 145 (1993) 65–103.
[3] C.R. Carlini, J.C. Polacco, Toxic properties of urease, Crop Sci. 48 (2008) 1665–1672.
[4] C.R. Carlini, M.F. Grossi-de-Sa, Plant toxic proteins with insecticidal properties. A review on their potentialities as bioinsecticides, Toxicon 40 (2002) 1515–1539.
[5] A.B. Becker-Ritt, C.R. Carlini, Fungitoxic and insecticidal plant polypeptides, Biopolymers 38 (2012) 367–384.
[6] F. Staniscuaski, C.R. Carlini, Plant ureases and related peptides: understanding their entomotoxic properties, Toxins 4 (2012) 55–67.
[7] A.B. Becker-Ritt, A.H. Martinelli, S. Mitidieri, V. Feder, G.E. Wassermann, L. Santi, M.H. Vainstein, J.T. Oliveira, L.M. Fiuza, G. Pasquali, C.R. Carlini, Antifungal activity of plant and bacterial ureases, Toxicon 50 (2007) 971–983.
[8] M. Postal, A.H.S. Martinelli, A.B. Becker-Ritt, R. Ligabue-Braun, D.R. Demartini, S.F.F. Ribeiro, G. Pasquali, V.M. Gomes, C.R. Carlini, Antifungal properties of Canavalia ensiformis urease and derived peptides, Peptides 38 (2012) 22–32.
[9] A. Balasubramanian, V. Durairajpandian, S. Elumalai, N. Mathivanan, A.K. Munirajan, K. Ponnuraj, Structural and functional studies on urease from pigeon pea (*Cajanus cajan*), Int. J. Biol. Macromol. 58 (2013) 301–309.
[10] C.R. Carlini, J.A. Guimaraes, Isolation and characterization of a toxic protein from *Canavalia ensiformis* (jack bean) seeds, distinct from concanavalin A, Toxicon 19 (1981) 667–675.
[11] C. Follmer, G.B. Barcellos, R.B. Zingali, O.L. Machado, E.W. Alves, C. Barja-Fidalgo, J.A. Guimaraes, C.R. Carlini, Canatoxin, a toxic protein from jack beans (*Canavalia ensiformis*), is a variant form of urease (EC 3.5.1.5): biological effects of urease independent of its ureolytic activity, Biochem. J. 360 (2001) 217–224.
[12] C.R. Carlini, A.E. Oliveira, P. Azambuja, J. Xavier-Filho, M.A. Wells, Biological effects of canatoxin in different insect models: evidence for a proteolytic activation of the toxin by insect cathepsinlike enzymes, J. Econ. Entomol. 90 (1997) 340–348.
[13] C.T. Ferreira-DaSilva, M.E. Gombarovits, H. Masuda, C.M. Oliveira, C.R. Carlini, Proteolytic activation of canatoxin, a plant toxic protein, by insect cathepsin-like enzymes, Arch. Insect Biochem. Physiol. 44 (2000) 162–171.
[14] A.R. Piovesan, F. Staniscuaski, J. Marco-Salvadori, R. Real-Guerra, M.S. Defferrari, C.R. Carlini, Stage-specific gut proteinases of the cotton stainer bug *Dysdercus peruvianus*: role in the release of entomotoxic peptides from *Canavalia ensiformis* urease, Insect Biochem. Mol. Biol. 38 (2008) 1023–1032.
[15] M.S. Defferrari, D.R. Demartini, T.B. Marcelino, P.M. Pinto, C.R. Carlini, Insecticidal effect of *Canavalia ensiformis* major urease on nymphs of the milkweed bug *Oncopeltus fasciatus* and characterization of digestive peptidases, Insect Biochem. Mol. Biol. 41 (2011) 388–399.
[16] R. Real-Guerra, C.R. Carlini, F. Staniscuaski, Role of lysine and acidic amino acid residues on the insecticidal activity of jackbean urease, Toxicon 71 (2013) 76–83.
[17] F. Mulinari, F. Staniscuaski, L.R. Bertholdo-Vargas, M. Postal, O.B. Oliveira-Neto, D.J. Rigden, M.F. Grossi-de-Sa, C.R. Carlini, Jaburetox-2Ec: an insecticidal peptide derived from an isoform of urease from the plant *Canavalia ensiformis*, Peptides 28 (2007) 2042–2050.
[18] F. Staniscuaski, C.T. Ferreira-Dasilva, F. Mulinari, M. Pires-Alves, C.R. Carlini, Insecticidal effects of canatoxin on the cotton stainer bug *Dysdercus peruvianus* (Hemiptera: Pyrrhocoridae), Toxicon 45 (2005) 753–760.
[19] P.R. Barros, H. Stassen, M.S. Freitas, C.R. Carlini, M.A.C. Nascimento, C. Follmer, Membrane-disruptive properties of the bioinsecticide Jaburetox-2Ec: implications to the mechanism of the action of insecticidal peptides derived from ureases, Biochim. Biophys. Acta, Proteins Proteomics 1794 (2009) 1848–1854.
[20] F. Staniscuaski, V.T. Brugge, C.R. Carlini, I. Orchard, In vitro effect of *Canavalia ensiformis* urease and the derived peptide Jaburetox-2Ec on *Rhodnius prolixus* Malpighian tubules, J. Insect Physiol. 55 (2009) 255–263.
[21] A. Balasubramanian, K. Ponnuraj, Crystal structure of the first plant urease from jack bean: 83 years of journey from its first crystal to molecular structure, J. Mol. Biol. 400 (2010) 274–283.
[22] A. Menez, Functional architectures of animal toxins: a clue to drug design? Toxicon 36 (1998) 1557–1572.
[23] A. Nikouee, M. Khabiri, S. Grissmer, R. Ettrich, Charybdotoxin and margatoxin acting on the human voltage-gated potassium channel hKv1.3 and its H399N mutant: an experimental and computational comparison, J. Phys. Chem. B 116 (2012) 5132–5140.
[24] X.D. Li, Y.F. Qiu, Y. Shen, C. Ding, P.H. Liu, J.P. Zhou, Z.Y. Ma, Splicing together different regions of a gene by modified polymerase chain reaction-based site-directed mutagenesis, Anal. Biochem. 373 (2008) 398–400.
[25] S.F. Altschul, D.J. Lipman, Protein database searches for multiple alignments, Proc. Natl. Acad. Sci. U. S. A. 87 (1990) 5509–5513.
[26] M.M. Bradford, A rapid and sensitive method for the quantitation of microgram quantities of protein utilizing the principle of protein-dye binding, Anal. Biochem. 72 (1976) 248–254.
[27] E. Gasteiger, C. Hoogland, A. Gattiker, S. Duvaud, M.R. Wilkins, R.D. Appel, A. Bairoch, Protein identification and analysis tools on the ExPASy server, in: J.M. Walker (Ed.), The Proteomics Protocols Handbook, Humana Press, 2005, pp. 571–607.
[28] J. Kyte, R.F. Doolittle, A simple method for displaying the hydropathic character of a protein, J. Mol. Biol. 157 (1982) 105–132.
[29] D.R. Demartini, C.R. Carlini, J.J. Thelen, Global and targeted proteomics in developing jack bean (*Canavalia ensiformis*) seedlings: an investigation of urease isoforms mobilization in early stages of development, Plant Mol. Biol. 75 (2011) 53–65.

[30] H. Schagger, G. Vonjagow, Tricine sodium dodecyl-sulfate polyacrylamide-gel electrophoresis for the separation of proteins in the range from 1-kDa to 100-kDa, Anal. Biochem. 166 (1987) 368–379.
[31] N. Dyballa, S. Metzger, Fast and sensitive colloidal Coomassie G-250 staining for proteins in polyacrylamide gels, J. Vis. Exp. 30 (2009).
[32] H. Towbin, T. Staehelin, J. Gordon, Electrophoretic transfer of proteins form polyacrylamide gels to nitrocellulose sheets. Procedure and some applications, Proc. Natl. Acad. Sci. U. S. A. 76 (1979) 4350–4354.
[33] R.J. Full, D.R. Stokes, A.N. Ahn, R.K. Josephson, Energy absorption during running by leg muscles in a cockroach, J. Exp. Biol. 201 (1998) 997–1012.
[34] K.A. Wafford, D.B. Sattelle, Effects of amino acid neurotransmitter candidates on an identified insect motoneurone, Neurosci. Lett. 63 (1986) 135–140.
[35] R. Sánchez, A. Šali, Comparative protein structure modeling: introduction and practical examples with Modeller, Methods Mol. Biol. 143 (2000) 97–129.
[36] R.A. Laskowski, M.W. Macarthur, D.S. Moss, J.M. Thornton, PROCHECK—a program to check the stereochemical quality of protein structures, J. Appl. Crystallogr. 26 (1993) 283–291.
[37] R. Luthy, J.U. Bowie, D. Eisenberg, Assessment of protein models with 3-dimensional profiles, Nature 356 (1992) 83–85.
[38] N. Guex, M.C. Peitsch, SWISS-MODEL and the Swiss-PdbViewer: an environment for comparative protein modeling, Electrophoresis 18 (1997) 2714–2723.
[39] B. Hess, C. Kutzner, D. van der Spoel, E. Lindahl, GROMACS 4: algorithms for highly efficient, load-balanced, and scalable molecular simulation, J. Chem. Theory Comput. 4 (2008) 435–447.
[40] C. Oostenbrink, A. Villa, A.E. Mark, W.F. Van Gunsteren, A biomolecular force field based on the free enthalpy of hydration and solvation: the GROMOS force-field parameter sets 53A5 and 53A6, J. Comput. Chem. 25 (2004) 1656–1676.
[41] H.J.C. Berendsen, J.R. Grigera, T.P. Straatsma, The missing term in effective pair potentials, J. Phys. Chem. 91 (1987) 6269–6271.
[42] B. Hess, H. Bekker, H.J.C. Berendsen, J. Fraaije, LINCS: a linear constraint solver for molecular simulations, J. Comput. Chem. 18 (1997) 1463–1472.
[43] T. Darden, D. York, L. Pedersen, Particle Mesh Ewald—an N. Log(N) method for Ewald sums in large systems, J. Chem. Phys. 98 (1993) 10089–10092.
[44] H.J.C. Berendsen, J.P.M. Postma, W.F. Vangunsteren, A. Dinola, J.R. Haak, Molecular dynamics coupling to an external bath, J. Chem. Phys. 81 (1984) 3684–3690.
[45] A. Balasubramanian, N. Balaji, N. Gautham, K. Ponnuraj, Molecular dynamics simulation and molecular modelling studies on the insecticidal domain from jack bean urease, Mol. Simul. 39 (2012) 357–366.
[46] K. Kappaun, Estudos com o Jaburetox: efeito tóxico de *E. coli* liofilizadas carregadas com o peptídeo e análise da influencia do epitopo V5 na formação de agregados, (M.Sc. dissertation) Cellular and Molecular Biology, Universidade Federal do Rio Grande do Sul, Porto Alegre, Brazil, 2012.
[47] E. Drakopoulou, J. Vizzavona, J. Neyton, V. Aniort, F. Bouet, H. Virelizier, A. Menez, C. Vita, Consequence of the removal of evolutionary conserved disulfide bridges on the structure and function of charybdotoxin and evidence that particular cysteine spacings govern specific disulfide bond formation, Biochemistry 37 (1998) 1292–1301.
[48] K. Nakagawa, A. Tokushima, K. Fujiwara, M. Ikeguchi, Proline scanning mutagenesis reveals non-native fold in the molten globule state of equine beta-lactoglobulin, Biochemistry 45 (2006) 15468–15473.
[49] M. Yamamoto, K. Nakagawa, M. Ikeguchi, Importance of polypeptide chain length for the correct local folding of a beta-sheet protein, Biophys. Chem. 168 (2012) 40–47.
[50] G. Tomazetto, F. Mulinari, F. Staniscuaski, B. Settembrini, C.R. Carlini, M.A.Z. Ayub, Expression kinetics and plasmid stability of recombinant *E-coli* encoding urease-derived peptide with bioinsecticide activity, Enzyme Microb. Technol. 41 (2007) 821–827.
[51] F. Staniscuaski, V.T. Brugge, C.R. Carlini, I. Orchard, Jack bean urease alters serotonin-induced effects on *Rhodnius prolixus* anterior midgut, J. Insect Physiol. 56 (2010) 1078–1086.
[52] C. Follmer, R. Real-Guerra, G.E. Wasserman, D. Olivera-Severo, C.R. Carlini, Jackbean, soybean and *Bacillus pasteurii* ureases: biological effects unrelated to ureolytic activity, Eur. J. Biochem. 271 (2004) 1357–1363.
[53] G. Corzo, E. Villegas, F. Gomez-Lagunas, L.D. Possani, O.S. Belokoneva, T. Nakajima, Oxyopinins, large amphipathic peptides isolated from the venom of the wolf spider Oxyopes kitabensis with cytolytic properties and positive insecticidal cooperativity with spider neurotoxins, J. Biol. Chem. 277 (2002) 23627–23637.
[54] Z. Andreeva-Kovalevskaya, A.S. Solonin, E.V. Sineva, V.I. Ternovsky, Pore-forming proteins and adaptation of living organisms to environmental conditions, Biochem. Mosc. 73 (2008) 1473–1492.
[55] S.H.P. Maddrell, Secretion by the Malpighian tubules of Rhodnius. The movements of ions and water, J. Exp. Biol. 51 (1969) 71–97.
[56] W.R. Terra, Evolution of digestive systems of insects, Annu. Rev. Entomol. 35 (1990) 181–200.
[57] G.A. Edwards, H. Ruska, E. de Harven, Neuromuscular junctions in flight and tymbal muscles of the Cicada, J. Biochem. Biophys. Cytol. 4 (1958) 251–256.
[58] G. Anderluh, Q. Hong, R. Boetzel, C. MacDonald, G.R. Moore, R. Virden, J.H. Lakey, Concerted folding and binding of a flexible colicin domain to its periplasmic receptor TolA, J. Biol. Chem. 278 (2003) 21860–21868.
[59] A.K. Dunker, J.D. Lawson, C.J. Brown, R.M. Williams, P. Romero, J.S. Oh, C.J. Oldfield, A.M. Campen, C.R. Ratliff, K.W. Hipps, J. Ausio, M.S. Nissen, R. Reeves, C.H. Kang, C.R. Kissinger, R.W. Bailey, M.D. Griswold, M. Chiu, E.C. Garner, Z. Obradovic, Intrinsically disordered protein, J. Mol. Graph. Model. 19 (2001) 26–59.
[60] V.N. Uversky, Natively unfolded proteins: a point where biology waits for physics, Protein Sci. 11 (2002) 739–756.
[61] L. Silvestro, P.H. Axelsen, Membrane-induced folding of cecropin A, Biophys. J. 79 (2000) 1465–1477.
[62] L. Otvos, Antibacterial peptides isolated from insects, J. Pept. Sci. 6 (2000) 497–511.
[63] C. Rodriguez-Almazan, I. Ruiz de Escudero, P. Emiliano Canton, C. Munoz-Garay, C. Perez, S.S. Gill, M. Soberon, A. Bravo, The amino- and carboxyl-terminal fragments of the Bacillus thuringensis Cyt1Aa toxin have differential roles in toxin oligomerization and pore formation, Biochemistry 50 (2011) 388–396.
[64] C. Sinthuvanich, A.S. Veiga, K. Gupta, D. Gaspar, R. Blumenthal, J.P. Schneider, Anticancer beta-hairpin peptides: membrane-induced folding triggers activity, J. Am. Chem. Soc. 134 (2012) 6210–6217.
[65] P. Wadhwani, J. Reichert, J. Bürck, A.S. Ulrich, Antimicrobial and cell-penetrating peptides induce lipid vesicle fusion by folding and aggregation, Eur. Biophys. J. 41 (2012) 177–187.

Registro intracelular

Experimento realizado em colaboração com a Prof[a]. Dr[a]. Eloísa da Silveira Loss do Departamento de Fisiologia, Instituto de Ciências Básicas da Saúde - UFRGS. Para esta técnica foram utilizados ratos Wistar machos imaturos de 10 a 15 dias, provenientes do Biotério do Intituto de Ciências Básicas da Saúde desta universidade. Para cada experimento, os testículos foram decapsulados e cuidadosamente estirados com o auxílio de duas pinças de ponta fina, expondo de 3 a 10 túbulos seminíferos. Eles foram então fixados no fundo de uma câmara de perfusão com uma grade produzida com fio ortodôntico (Fig. 1b). A câmara foi preenchida com 1 mL de solução Krebs-Ringer (KRb) glicosado e levado para perfusão. As características eletrofisiológicas de células de Sertoli imaturas foram analizadas usando túbulos seminíferos inteiros, sem células de Leydig. Os túbulos foram perfundidos com fluxo de 1 mL/min de KRb glicosado (5 mM), 36 °C, pH 7.4, gaseificado e equilibrado com carbogênio - O_2:CO_2 (95:5; v/v). O potencial de membrana das células de Sertoli foi registrado com microeletrodos de borosilicato preenchidos com KCl 3M com resistência entre 15 e 25 MΩ. Essa resistência de ponta é apropriada para o empalamento de células de tamanho similar às células de Sertoli (Fig. 2b) e o diâmetro ajuda a eliminar o empalamento de células estreitas como as células peritubulares (von Ledebur et al, 2002). O sinal do registro intracelular foi amplificado usando um amplificador intracelular Intra 767 WPI (World Precision Instruments Inc., USA) e monitorado por um osciloscópio (Tektronik, 2 Channel Digital Oscilloscope TDS 210). Os traços observados no osciloscópio foram adquiridos e armazenados em computador através de uma placa e um programa de interface (Wavestar Lite Version 1.0.10). Pulsos de corrente (0.5 nA, 0.5 Hz e 200 ms) foram aplicados através do eletrodo de registro por um estimulador de pulso de corrente (S48K Astromed, Grass Instruments) para avaliar a resistência da membrana. Soluções contendo JBU ou Jbtx foram aplicadas topicamente ao banho após a estabilização do potencial de repouso da célula por pelo menos 5 minutos. Solução de Krebs-Ringer bicarbonato (KRb): NaCl (146 mM), KCl (4.7 mM), KH_2PO_4 (1.2 mM), $NaHCO_3$ (25 mM), $MgSO_4 \cdot 7\ H_2O$ (1.2 mM), $CaCl_2 \cdot 2\ H_2O$ (2.5 mM), e glicose (5.5 mM).

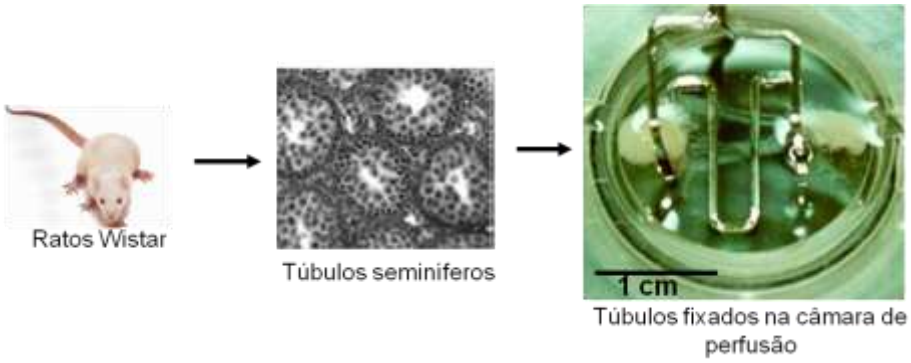

Figura 1b: Esquema da preparação da técnica de registro intracelular. Túbulos seminíferos são dissecados de ratos Wistar imaturos para serem fixados numa câmara de perfusão.

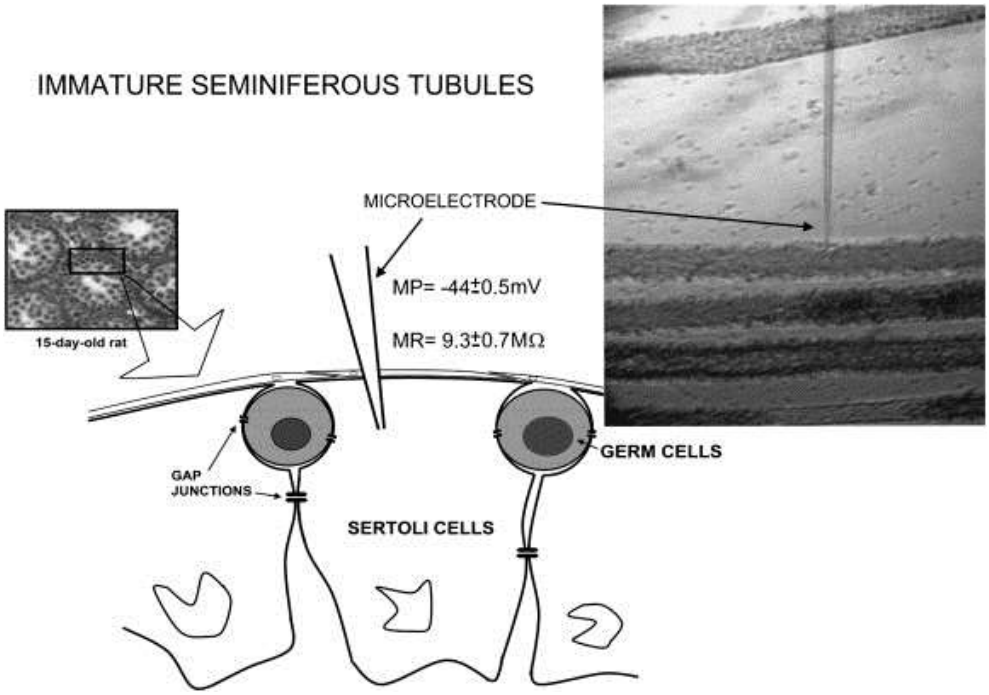

Figura 2b: Detalhe da técnica de registro intracelular. A célula de Sertoli é empalada usando um microeletrodo; sabe-se que é ela através do potencial de membrana de repouso, em torno de -44 mV. Figura extraída de Loss et al 2011.

Ação eletrofisiológica de JBU e Jbtx sobre o potencial de membrana de células de Sertoli

Nesta técnica é avaliado o efeito da aplicação de drogas sobre túbulos seminiferos de ratos Wistar imaturos. Assim é possivel observar e avaliar alterações no potencial de membrana das células de Sertoli, que tem um potencial de repouso estimado em − 44 mV ± 0.5 (n = 48), variando de -35 mV até -60 mV, segundo Wassermann et al, 1992b. Após filtrar e gaseificar o tampão com carbogênio as células foram observadas e empaladas cuidadosamente. A célula empalada foi mantida em perfusão na solução de Krebs-Ringer pH 7.4 por no mínimo cinco minutos para equilibrar o potencial de repouso (~ 46 mV) e então aplicar as toxinas. O primeiro teste foi aplicando o tampão em que JBU ou Jbtx são solubilizados (NaPB 20 mM, EDTA 1 mM e β-Mercaptoetanol 5 mM, pH 7.5) e o observado foi uma intensa despolarização, atingindo -30 mV. Já quando JBU 9.2 nM (5 μg/mL) ou Jbtx 0.45 μM (5 μg/mL) foram aplicados a célula tanto não despolarizou como ainda causou uma leve hiperpolarização, deixando mais negativo ainda o potencial de membrana da célula, como é visto no gráfico da figura 10. Para excluir possíveis alterações e perturbações no potencial de membrana causado especialmente pela JBU (540 kDa) devido ao seu tamanho, tireoglobulina, uma proteína com 660 kDa foi utilizado como controle negativo, ilustrado também no gráfico abaixo. Também são mostrados na figura 11 traçados típicos de um experimento, quando JBU ou Jbtx são topicamente aplicados. O potencial de membrana após alguns minutos voltou para valores próximos ao típico de repouso, indicando que o efeito das proteínas é reversível. No entanto, interessantemente, depois de tratar com JBU e esperar retornar a valores de repouso, quando o tampão foi novamente aplicado não houve a mesma despolarização observada quando somente ele é usado diretamente nos túbulos, sugerindo uma dessensibilização dos possíveis receptores nos quais a proteína pode estar atuando e/ou modulando.

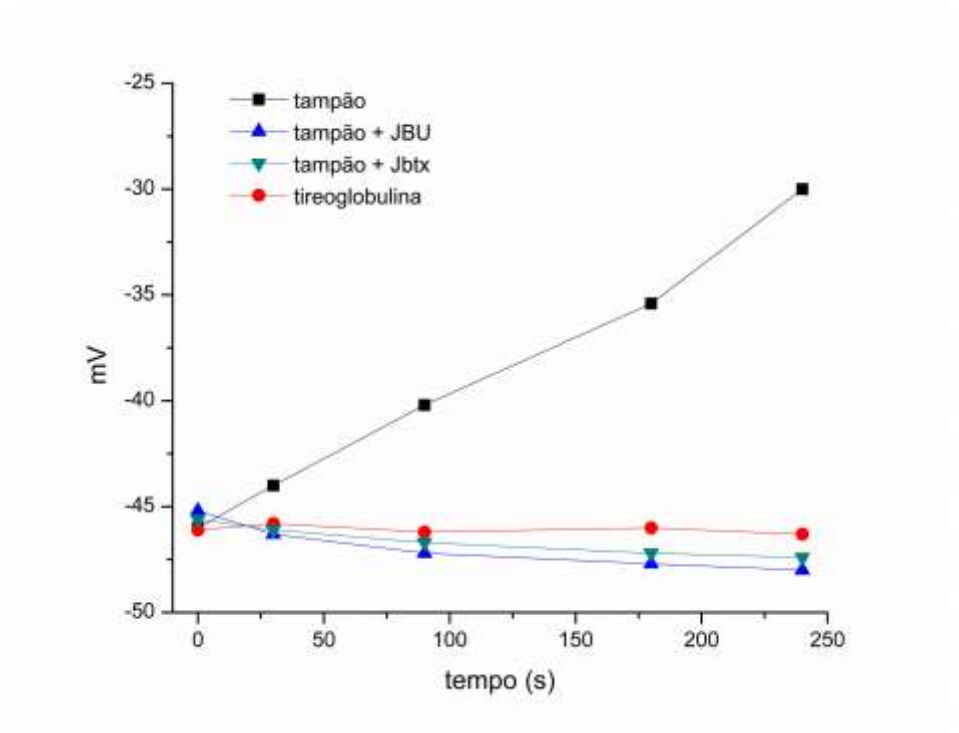

Efeito de JBU e Jaburetox sobre o potencial de membrana de células de Sertoli. A concentração usada foi de 5 µg/mL, o que corresponde a 9.2 nM para JBU (▲, traço azul) e 0.45 µM para Jbtx (▼, traço verde). O traço vermelho corresponde ao controle negativo representado por tireoglobulina (●). O traço preto é o efeito do tampão usado para armazenar JBU e Jbtx (■).

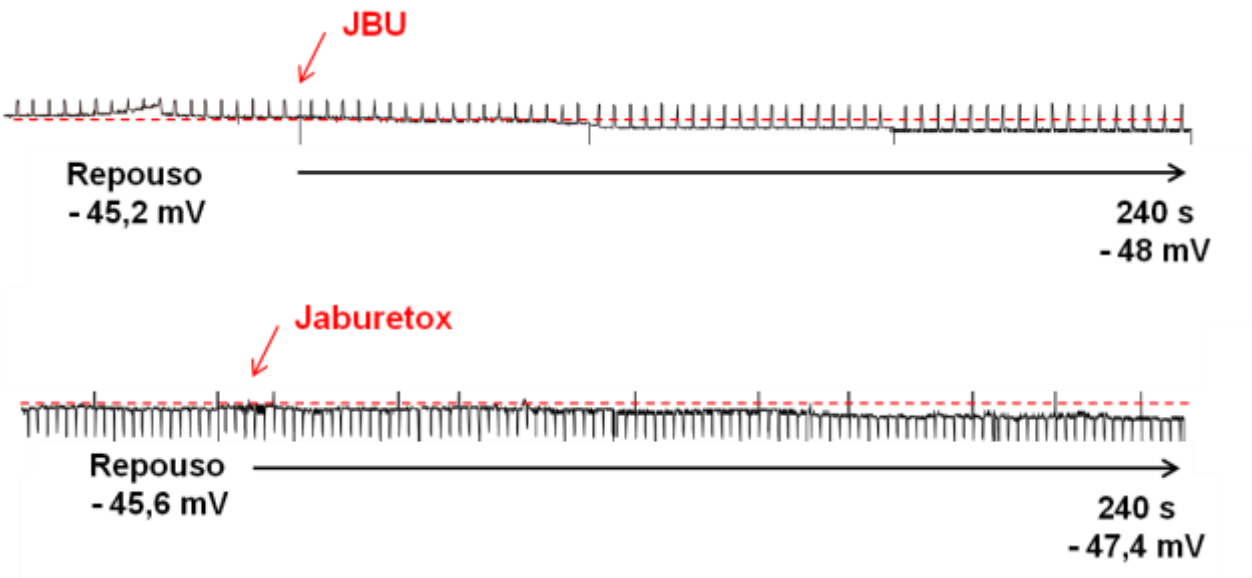

Traçados típicos de um experimento em que o potencial de membrana de células de Sertoli foi afetado pela aplicação de JBU ou Jbtx, mostrando uma hiperpolarização de 2.8 mV para JBU e 1.8 mV para Jbtx, n=3

A intensidade da hiperpolarização causada por JBU e Jbtx é semelhante àquela causada pelo hormônio FSH (hormônio estimulador de folículo) e forscolina ("*forskolin*", ativador de adenilato ciclase e biosíntese de AMP cíclico) (Jacobus et al, 2010) mostrando que apesar de parecer uma hiperpolarização leve, é fisiologicamente relevante. Para os compostos citados, os canais envolvidos na resposta de hiperpolarização são os K^+_{ATP} cuja atividade foi bloqueada por tolbutamida, um clássico inibidor. De fato, canais de potássio são os mais ativados quando o potencial de membrana sofre hiperpolarização por algum tipo de fármaco, como reportado em diversos trabalhos (Soder et al, 2013; Félétou and Vanhoutte 2009; Jacobus et al, 2005; Nakashima and Vanhoutte 1995) sugerindo que JBU e Jbtx possa estar modulando a ativação de canais de K^+

e/ou agindo diretamente sobre a membrana e atuando como canais iônicos que transportam K^+ para fora da célula, o que levaria à hiperpolarização.

Bibliografia

Félétou M, Vanhoutte PM. EDHF: an update. Clin Sci (Lond). 2009; 117(4): 139-55.

Jacobus AP, Rodrigues DO, Borba PF, Loss ES, Wassermann GF. Isoproterenol opens K+(ATP) channels via a beta2-adrenoceptor-linked mechanism in Sertoli cells from immature rats. Horm Metab Res. 2005; 37(4): 198-204.

Jacobus AP, Loss ES, Wassermann GF. Pertussis toxin nullifies the depolarization of the membrane potential and the stimulation of the rapid phase of Ca entry through L-type calcium channels that are produced by follicle stimulating hormone in 10- to 12-day-old rat Sertoli cells. Front Physiol. 2010; 21;1: 138.

Loss ES, Jacobus AP, Wassermann GF. Rapid signaling responses in Sertoli cell membranes induced by follicle stimulating hormone and testosterone: calcium inflow and electrophysiological changes. Life Sci. 2011; 89: 577–583.

Nakashima M, Vanhoutte PM. Isoproterenol causes hyperpolarization through opening of ATP-sensitive potassium channels in vascular smooth muscle of the canine saphenous vein. J Pharmacol Exp Ther. 1995; 272(1): 379-84.

Soder RP, Parajuli SP, Hristov KL, Rovner ES, Petkov GV. SK channel-selective opening by SKA-31 induces hyperpolarization and decreases contractility in human urinary bladder smooth muscle. Am J Physiol Regul Integr Comp Physiol. 2013; 304(2): 155-63.

Von Ledebur EI, Almeida JP, Loss ES, Wassermann GF. Rapid effect of testosterone on rat Sertoli cell membrane potential. Relationship with K + ATP channels. Horm Metab Res. 2002; 34: 550–555.

ANEXO 3

Angela Regina Piovesan
Curriculum Vitae

Angela Regina Piovesan
Curriculum Vitae

Dados pessoais

Nome Angela Regina Piovesan
Nascimento 09/09/1984 - Santa Cruz do Sul/RS - Brasil

Endereço eletrônico
angela.piovesan@ufrgs.br
angelapiovesan@yahoo.com.br

Formação acadêmica/titulação

2009 Doutorado em Biologia Celular e Molecular.
Universidade Federal do Rio Grande do Sul, UFRGS, Porto Alegre, Brasil
Título: Efeitos da urease de Canavalia ensiformis e Jaburetox-2Ec em células isoladas de mamíferos e insetos e em membranas lipídicas artificiais._
Orientador: Célia Carlini
Bolsista do(a): Coordenação de Aperfeiçoamento de Pessoal de Nível Superior

2008 - 2009 Mestrado em Biologia Celular e Molecular.
Universidade Federal do Rio Grande do Sul, UFRGS, Porto Alegre, Brasil
Título: Urease de Canavalia ensiformis: processamento diferencial por ninfas e adultos de Dysdercus peruvianus e formação de canal in vitro., Ano de obtenção: 2009
Orientador: Célia Regina Carlini
Bolsista do(a): Conselho Nacional de Desenvolvimento Científico e Tecnológico

2003 - 2007 Graduação em Ciências Biológicas.
Universidade Federal do Rio Grande do Sul, UFRGS, Porto Alegre, Brasil
Título: Processamento de urease de Canavalia ensiformis por
Orientador: Célia R. Carlini

Formação complementar

2013 - 2013 Curso de curta duração em Protein NMR.
Universidade Federal do Rio Grande do Sul, UFRGS, Porto Alegre, Brasil

2012 - 2012 Curso de curta duração em Qualificação em Coletas em Laboratório Clínico.
Faculdade Factum, FACTUM, Porto Alegre, Brasil

2012 - 2012 Doutorado (intercâmbio) - Centre SÈVE.
Université de Montréal, UDEM, Canadá

2011 - 2011 Doutorado (intercâmbio).
Université de Montreal, UdeM, Montreal, Canadá

2008 - 2009 Mestrado (intercâmbio).
Université de Montreal, UdeM, Montreal, Canadá
Bolsista do(a): Université de Montréal

2007 - 2007 Curso de curta duração em Técnicas moleculares aplicadas a análise proteômic.
Empresa Brasileira de Pesquisa Agropecuária, EMBRAPA, Brasília, Brasil

2007 - 2007 Extensão universitária em Tecnicas Histologicas.
Universidade Federal do Rio Grande do Sul, UFRGS, Porto Alegre, Brasil

2006 - 2006 Curso de curta duração em Minicurso Biologia Molecular Aplicada à Saúde.
Universidade de Caxias do Sul, UCS, Caxias Do Sul, Brasil

2006 - 2006 Curso de curta duração em 1º Curso de Verão em Bioquímica e Biologia Molecul.
Universidade de São Paulo, USP, Sao Paulo, Brasil

2006 - 2006 Curso de curta duração em Curso de História e Filosofia da Ciência.
Universidade Federal do Rio Grande do Sul, UFRGS, Porto Alegre, Brasil

2006 - 2006 Curso de curta duração em Genética na UFRGS: Pesquisa e Ensino ao Alcance de.
Universidade Federal do Rio Grande do Sul, UFRGS, Porto Alegre, Brasil

2006 - 2006 Curso de curta duração em Curso de Direito Ambiental.
Universidade Federal do Rio Grande do Sul, UFRGS, Porto Alegre, Brasil

2006 - 2006 Curso de curta duração em Curso de Bioética.
Universidade Federal do Rio Grande do Sul, UFRGS, Porto Alegre, Brasil

2004 - 2004 Extensão universitária em I Jornada Acadêmica de Biologia da UFRGS.
Universidade Federal do Rio Grande do Sul, UFRGS, Porto Alegre, Brasil

2004 - 2004 Extensão universitária em Bases Neurológicas da Formação e Expressão da Memó.
Universidade Federal do Rio Grande do Sul, UFRGS, Porto Alegre, Brasil

---

Atuação profissional

1. Universidade Federal do Rio Grande do Sul - UFRGS

Vínculo institucional

2009 - Atual Vínculo: Aluno de pós-graduação , Enquadramento funcional: Doutorado , Carga horária: 40, Regime: Dedicação exclusiva

2008 - 2009 Vínculo: Aluno de pós-graduação , Enquadramento funcional: Mestrado , Carga horária: 40, Regime: Dedicação exclusiva

2004 - 2007 Vínculo: Aluno de graduação , Enquadramento funcional: Iniciação Científica , Carga horária: 20, Regime: Parcial

Atividades

10/2004 - Atual Pesquisa e Desenvolvimento, Centro de Biotecnologia
Linhas de pesquisa:
Ureases: aspectos moleculares, mecanismos de ação e potencial biotecnologico.

Áreas de atuação

1. Eletrofisiologia
2. Bioquímica
3. Biofísica
4. Biologia Molecular

Idiomas

Inglês Compreende Bem , Fala Bem , Escreve Bem , Lê Bem

Francês Compreende Bem , Fala Bem , Escreve Razoavelmente , Lê Bem

Italiano Compreende Bem , Fala Razoavelmente , Escreve Razoavelmente , Lê Bem

Producão

Produção bibliográfica

Artigos completos publicados em periódicos

1. PIOVESAN, AR ; MARTINELLI, A. H. S. ; LIGABUE-BRAUN, R. ; SCHWARTZ, JL ; CARLINI, C. R. . Canavalia ensiformis urease, Jaburetox and derived peptides form ion channels in planar lipid bilayers. Archives of Biochemistry and Biophysics., v. 547, p. 6-17, 2014.

2. MARTINELLI, A. H. S. ; KAPPAUN, K. ; LIGABUE-BRAUN, R. ; DEFFERRARI, M. S. ; PIOVESAN, AR ; STANISÇUASKI, F ; DEMARTINI, D. R. ; VERLI, H. ; DAL-BELO, C. A. ; ALMEIDA, C. G. ; FOLLMER, C. ; CARLINI, C. R. ; PASQUALI, G. . Structure-function studies on Jaburetox, a recombinant insecticidal and antifungal peptide derived from jack bean (Canavalia ensiformis) urease. Biochimica et Biophysica Acta. G, General Subjects., v. 1840, p. 935-944, 2013.

3. BALDISSERA, R., BACH, E., LIMA, R. P., MENEGASSI, A., **PIOVESAN, AR**, FONSECA, G. C.
Distribution of understorey web building spiders along an interface area of araucaria forest and pinus plantation in southern Brazil. Neotropical Biology and Conservation. , v.3, p.3 - 8, 2008.

4. PIOVESAN, AR, STANISCUASKI, F, MARCOSALVADORI, J, REALGUERRA, R, DEFFERRARI, M, CARLINI, C
Stage-specific gut proteinases of the cotton stainer bug Dysdercus peruvianus: Role in the release of entomotoxic peptides from Canavalia ensiformis urease. Insect Biochemistry and Molecular Biology. , v.38, p.1023 - 1032, 2008.

Trabalhos publicados em anais de eventos (resumo)

1. **PIOVESAN, AR**, MARTINELLI, A. H. S., VILLODRE, E. S., LENZ, G., SCHWARTZ, JL, CARLINI, C. R.
JBU e Jaburetox: estudos em membranas lipídicas e cultura de células In: XIV Reunião Anual do Programa de Pós-Graduação em Biologia Celular e Molecular, 2012, Porto Alegre, RS.
Livro de Resumos. , 2012. p.18 - 18

2. **PIOVESAN, AR**, SCHWARTZ, JL, CARLINI, C. R.
Interação de JBU e peptídeo derivado com membranas lipídicas artificiais In: XIII Reunião Anual do Programa de Pós-Graduação em Biologia Celular e Molecular, 2011, Porto Alegre, RS.
Livro de Resumos. , 2011. p.15 - 15

3. **PIOVESAN, AR**, CARLINI, C. R., JUTEAU, M., SCHWARTZ, JL
_Jack bean urease and Jaburetox-2Ec: electrophysiological studies in planar lipid bilayer In: XXXIX Reunião Anual da Sociedade Brasileira de Bioquímica e Biologia Molecular - SBBq, 2010, Foz do Iguaçu.
Jack bean urease and Jaburetox-2Ec: electrophysiological studies in planar lipid bilayer. , 2010.

4. **PIOVESAN, AR**, LOSS, E. S., SCHWARTZ, JL, CARLINI, C. R.
Jack Bean Urease and Jaburetox-2Ec: Electrophysiological Studies in Planar Lipid Bilayer and Intracelular Measurements In: Mini-Simposium Urease Multifuncionality, 2010, Porto Alegre.
Urease Multifuncionality. , 2010.

5. **PIOVESAN, AR**, STANISCUASKI, F, CARLINI, C
Processing of Canavalia ensiformis urease in nymphs and adults of Dysdercus peruvianus (Hemiptera:Pyrrhocoridae) In: XXXVII Annual Meeting of the Brazilian Society for Biochemistry and Molecular Biology (SBBq) and XI Congress of the Pan American Association for Biocemistry and Molecular Biology (PABMB), 2008, Águas de Liondóia, SP.
Livro de Resumos da XXXVII Reunião Anual da SBBq. , 2008.

6. **PIOVESAN, AR**, STANISCUASKI, F, CARLINI, C. R.
Diferenças do processamento proteolítico de urease vegetal entre ninfas e adultos de Dysdercus peruvianus (Hemiptera:Pyrrhocoridae) In: XXII Reunião Anual da Federação De Sociedades de Biologia Experimental, 2007, Águas de Liondóia, SP.
XXII Reunião Anual da FESBE. , 2007.

7. **PIOVESAN, AR**, STANISCUASKI, F, CARLINI, C. R.
Diferenças do processamento proteolítico de urease vegetal entre ninfas e adultos de Dysdercus peruvianus (Hemiptera:Pyrrhocoridae) In: XVIII Salão de Iniciação Científica - UFRGS, 2006, Porto Alegre, RS.
Livro de Resumos. , 2006. p.353 - 353

8. PIOVESAN, AR, Stanisçuaski, F, CARLINI, C. R.
Differences in the proteolytic processing of plant urease in adults and nymphs of Dysdercus peruvianus (Hemiptera; Pyrrhocoridae). In: XXXV Reunião Anual da SBBq, 2006, Águas de Lindóia.
Livro de resumos da XXXV Reunião Anual da SBBq. , 2006.

9. **PIOVESAN, AR**, STANISCUASKI, F, Salvadori, J., CARLINI, C. R.
Diferenças do processamento de urease vegetal entre ninfas e adultos de Dysdercus peruvianus In: XVII Salão de Iniciação Científica - UFRGS, 2005, Porto Alegre, RS.
Livro de Resumos. , 2005. p.437 - 437

10. PIOVESAN, AR, Stanisçuaski, F, CARLINI, C. R.
Differences in the proteolytic processing of plant urease in adults and nymphs of Dysdercus peruvianus (Hemiptera; Pyrrhocoridae). In: XXXIV Reunião Anual da SBBq, 2005, Águas de Lindóia.
Livro de Resumos da XXXIV Reunião Anual da SBBq. , 2005.

Trabalhos publicados em anais de eventos (resumo expandido)

1. **PIOVESAN, AR**, MARTINELLI, A. H. S., KAPPAUN, K., FOLLMER, C., SCHWARTZ, JL, CARLINI, C. R.
Membrane-disturbing properties of urease and derived recombinant peptides In: 17th World Congress of the Internatioal Society on Toxinology & Venom Week, 2012, Honolulu,USA.
Toxicon (Oxford). Elsevier, 2012. v.60. p.178 - 178